Energy and AI 18 (2024) 100424

Contents lists available at ScienceDirect

Energy and AI

journal homepage: www.sciencedirect.com/journal/energy-and-ai

Application of artificial intelligence in the materials science, with a special focus on fuel cells and electrolyzers

Mariah Batool [a,b,1], Oluwafemi Sanumi [a,c,1], Jasna Jankovic [a,b,c,*]

[a] Center for Clean Energy Engineering (C2E2), Center for Clean Energy Engineering (C2E2), 44 Weaver Road, Unit 5233, University of Connecticut, Storrs, CT, 06269-5233, United States
[b] Institute of Materials Science (IMS), 25 King Hill Road, Unit 3136, University of Connecticut, Storrs, CT, 06269-3136, United States
[c] Department of Materials Science & Engineering (MSE), 25 King Hill Road, Unit 3136, University of Connecticut, Storrs, CT, 06269-3136, United States

HIGHLIGHTS

- Transformation of global technological developments by artificial intelligence (AI).
- Overview of AI fundamentals to enhance foundational understanding.
- Scope and status of AI research in materials science from discovery to optimization.
- Role of AI to characterize, fabricate, test and analyze fuel cells and electrolyzers.
- Challenges and future perspectives of AI in advancing clean energy technologies.

ARTICLE INFO

Keywords:
Artificial Intelligence (AI)
Machine Learning (ML)
Materials science
Electrochemical systems
Fuel cells
Electrolyzers
Proton Exchange Membrane Fuel Cells (PEMFCs)

ABSTRACT

Artificial Intelligence (AI) has revolutionized technological development globally, delivering relatively more accurate and reliable solutions to critical challenges across various research domains. This impact is particularly notable within the field of materials science and engineering, where artificial intelligence has catalyzed the discovery of new materials, enhanced design simulations, influenced process controls, and facilitated operational analysis and predictions of material properties and behaviors. Consequently, these advancements have streamlined the synthesis, simulation, and processing procedures, leading to material optimization for diverse applications. A key area of interest within materials science is the development of hydrogen-based electrochemical systems, such as fuel cells and electrolyzers, as clean energy solutions, known for their promising high energy density and zero-emission operations. While artificial intelligence shows great potential in studying both fuel cells and electrolyzers, existing literature often separates them, with a clear gap in comprehensive studies on electrolyzers despite their similarities. This review aims to bridge that gap by providing an integrated overview of artificial intelligence's role in both technologies. This review begins by explaining the fundamental concepts of artificial intelligence and introducing commonly used artificial intelligence-based algorithms in a simplified and clearly comprehensible way, establishing a foundational knowledge base for further discussion. Subsequently, it explores the role of artificial intelligence in materials science, highlighting the critical applications and drawing on examples from recent literature to build on the discussion. The paper then examines how artificial intelligence has propelled significant advancements in studying various types of fuel cells and electrolyzers, specifically emphasizing proton exchange membrane (PEM) based systems. It thoroughly explores the artificial intelligence tools and techniques for characterizing, manufacturing, testing, analyzing, and optimizing these systems. Additionally, the review critically evaluates the current research landscape, pinpointing progress and prevailing challenges. Through this thorough analysis, the review underscores the fundamental role of artificial intelligence in advancing the generation and utilization of clean energy, illustrating its transformative potential in this area of research.

* Corresponding author.
E-mail address: jasna.jankovic@uconn.edu (J. Jankovic).
[1] Both these authors contributed equally to this paper.

https://doi.org/10.1016/j.egyai.2024.100424

Available online 17 September 2024

1. Introduction

Technological advancement in the fields of science and engineering nowadays is accompanied by the collection, handling, and analysis of ever larger, more sophisticated, and complex data [1–3]. Such complicated datasets are oftentimes too difficult or even impossible to process manually or using conventional data processing approaches [4,5]. To aid this process, artificial intelligence can be implemented. Artificial intelligence (also referred to as AI) originates from the notion of imparting the capability of "human-like thinking/intelligence" to computers permitting them to analyze critical information and take appropriate problem-solving steps while evaluating their output with the objective to learn from the process [6,7].

AI was initially theorized through fictional works during the first half of the 20th century and the concept was later adopted and formally recognized by scientists and mathematicians in the 1950s [8]. However, from the conception to the actual implementation of the concept, it faced many obstacles concerning social acceptance, financial feasibility, technological capacity, and metacognitive accuracy [9,10]. However, with the rapid progression in the field of computer sciences leading to modern-day operating systems with improved problem-solving algorithms, AI flourished [11,12].

In general, AI is divided into four different types based on its functionality i.e., reactive, limited memory, theory of mind, and self-aware, as shown in Fig. 1 [13].

Reactive AI is programmed to acquire a predictable outcome, generating the same response to an identical situation each time, while Limited Memory AI possesses the ability to learn from experience, continually improving over time like neurons in the human brain. Reactive and Limited Memory AI are the types that are most researched these days, and most AI models available today are based on these two types. Theory of Mind AI is still in the development stage and refers to machines acquiring the capability of decision-making and emotional intelligence like humans. The most advanced form of AI, which is to be explored yet, is Self-awareness AI defined as machines achieving the capability to not only judge and understand the mental and emotional states of others, but also their own [14].

Nowadays, AI is broadly referred to as two important subsets: machine learning and deep learning [15]. Machine learning (ML) focuses on performing specific tasks by utilizing available data through continuous algorithmic optimization, while deep learning (DL) is a type of advanced ML that consists of multiple layers of neural networks to perform more complex tasks, reaching a logical conclusion on tasks involving unstructured data and does not always require labeled data, although labeled data is still commonly used for training [16]. The association between AI and its subsets, ML and DL, can be explained using the representation in Fig. 2 [17,18,19].

To realize AI in more depth, it is crucial to discuss some of the most utilized AI techniques these days under the sub-classes of ML and DL. The sub-classification of the most important types and algorithms in AI is given in Fig. 3 [21,22]. Traditional ML can be broadly divided into four basic types, which are supervised, unsupervised, semi-supervised, and reinforcement learning. However, DL encompassing advanced techniques applicable across supervised, unsupervised, or hybrid learning frameworks, is sometimes recognized as a distinct type of ML [23].

1.1. Supervised learning

Supervised learning utilizes labeled datasets to train algorithms that can be used for either data classification or prediction of results. These models involve a cross-validation step to adjust the weight of the input until an appropriate fitting is completed [24]. Supervised learning models are based on mainly two sub-types: classification and regression [25].

Classification is the type of supervised learning which categorizes the input dataset into different classes based on the recognition of specific characteristics of the dataset [26]. The most frequently used classification algorithms include logistic regression, support vector machines (SVM), decision trees, etc.

- Logistic regression is used to predict the probability of an event occurring, providing results in a binary format. It is commonly employed for binary classification problems [27].
- SVM algorithm is used to locate a hyperplane to categorize data points in an n-dimensional space where 'n' refers to the number of features [28].
- Decision trees use different nodes where data is continuously split according to certain parameters to predict the classification outcome for a given input dataset. A collection of uncorrelated decision trees referred to as random forest algorithm can also be used to generate more accurate predictions with reduced variance [29,30].

The other type of supervised learning is regression, which involves statistical approaches to identify the relationship between a dependent target variable and one or more independent predictor variables. The most common regression algorithms are linear regression and polynomial regression [31].

- The linear regression model is based on predicting the best linear fitting between a dependent and an independent variable [32].
- The polynomial regression algorithm involves modeling the relationship between a dependent target variable and an independent predictor variable as an n^{th} degree polynomial [33].

1.2. Unsupervised learning

Unsupervised learning utilizes unlabeled datasets for identifying patterns or data groups without any human intervention [34]. Unsupervised learning models are based on three main types: clustering,

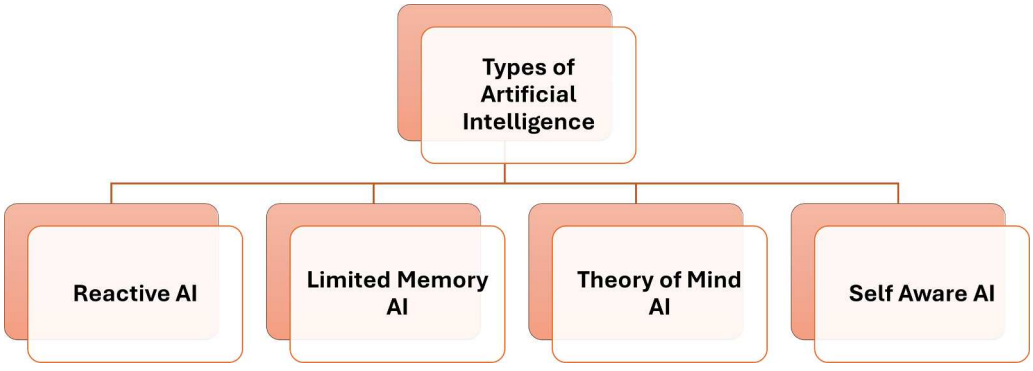

Fig. 1. Types of AI depending upon functionalities. Reproduced with permission. Copyright 2020, Published by MDPI [13].

dimensionality reduction, and anomaly detection [35].

Clustering is the type of unsupervised learning that groups unlabeled data according to their similarities or differences [36]. The most used algorithms of clustering are K-means and hierarchical clustering [37].

- K-means clustering categorizes 'n' observations into 'k' different clusters and computes centroids by data averaging while performing iterative calculations until optimal centroid stabilization has been reached [38].
- Hierarchical clustering either uses agglomerative clustering i.e., repetitive iteration of initially isolated data points based on similarity till a single cluster is achieved, or divisive clustering i.e., division of a data cluster based on the differences between data points [39].

Dimensionality reduction is another type of unsupervised learning which is specifically used when there are numerous features or dimensions associated with the input dataset and lowers the number of data inputs while maintaining the dataset's integrity [40]. The most used dimensionality reduction algorithms include principal component analysis (PCA) and independent component analysis (ICA) [41].

- The PCA algorithm generates a new representation of data identifying the set of principal components through linear transformation and is used to compress huge datasets through the extraction of features [42].
- The ICA algorithm creates a new data representation by identifying statistically independent components through linear transformation and is employed to uncover hidden patterns, components, or sources within complex datasets [43].

Anomaly detection is a separate type of unsupervised learning which involves the identification of those data points or observations in the input dataset that do not agree with the normal data patterns [44].

1.3. Semi-supervised learning

Semi-supervised learning utilizes both labeled data as well as unlabeled data for training models. Though, the amount of labeled data involved is usually much less than the unlabeled data [45]. The semi-supervised learning approach offers the advantages of both supervised and unsupervised learning and is usually of two basic types: Self-training models and low-density separation models.

Self-training models are initially trained with labeled data following the supply of unlabeled data. The model then uses the labeled data to categorize unlabeled data and iterates through the same steps until the whole dataset is labeled while low-density separation models involve finding a decision boundary separating different classes of labeled data based on low and high-density regions [46,47].

1.4. Reinforcement learning

The reinforcement learning approach refers to the training of ML models to reach the best possible outcome through an extended trial-and-error method without the use of any labeled input [48]. Some commonly utilized reinforcement algorithms include dynamic programming and Monte Carlo methods.

Dynamic programming algorithm involves finding the optimal solution for complex problems by subdividing them into smaller problems while the Monte Carlo method involves learning only through repetitive experiences and interactions with the environment [49,50].

1.5. Deep learning

DL is a subset of ML which is based on a network of more complex algorithms called neural networks imitating the network of neurons in the human brain [51]. DL can be both supervised and unsupervised as well as a combination of both (hybrid). To ensure clarity and acknowledge the unique architecture, attributes and capabilities of deep learning, it is delineated as a distinct category in the machine learning classification as presented in Fig. 3 [52,53].

The three common types of DL algorithms are convolutional neural networks (CNNs), artificial neural networks (ANNs), and recurrent neural networks (RNNs) [54].

CNNs utilize several artificial neuron layers involving mathematical

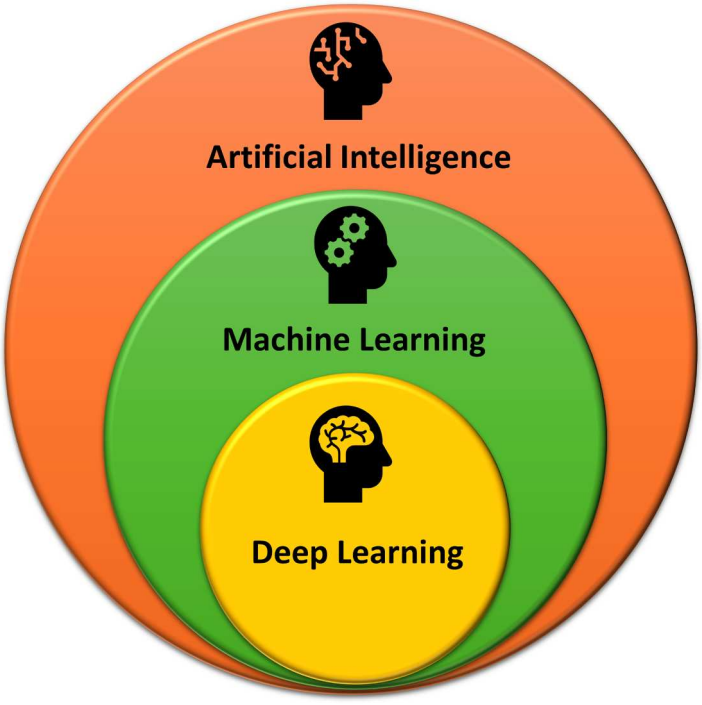

Fig.. 2. The different subsets of AI. Reproduced with permission, Copyright 2021, Published by MDPI [17–20].

functions to process multiple inputs and produce output values which are then fed to the next neuron layer as input until a decisive outcome is achieved [55]. On the other hand, ANNs are used to distinguish the class of new observations on the training data basis, processing the observations one by one and learning by comparing their processed classification to the definite known classification while RNNs only vary from CNNs in the way that they can employ output from any preceding layer of the neural network for sequential interpretation and optimization of outcome [51].

2. Applications of AI in materials science

Such remarkable prospects of AI encouraged scientists to discover and recognize many different avenues and aspects of research to which AI could be applied to yield favorable results. In recent years, AI has been successfully implemented in a plethora of applications across many different sectors such as education, security, agriculture, technology, healthcare, navigation, marketing, entertainment, research, etc. [56–64]. In fact, research and development in various technologies and engineering disciplines these days are contingent upon the continuous evolution and implementation of innovative AI-based algorithms and methodologies [65].

Likewise, materials development and optimization are the backbones of all modern-day systems, which compelled researchers to explore and utilize AI in the field of material science and engineering [66] [67],. In general, materials scientists and engineers investigate and analyze correlations between structure, processes, and properties at the micro- and the nano-metric scale using a combination of high throughput experimental and computational data. Therefore, the current bottleneck to progress is not only limited by the processing of a wide range of information and large datasets, but also by the automatic assessment and critical problem-solving approach, which can aid in autonomous experiment selection [68–70],. Therefore, as opposed to manual and statistical data analysis, AI-based methods offer the advantage of not only exponentially reducing the analysis time but also averting bias during the decision-making process, leading to revolutionary progress in materials discovery and optimization, which was previously not possible [71–74].

Nowadays, ML is the branch of AI that is being explored and applied for innovative research in materials science and engineering the most [75]. Moreover, in the past few years, some promising DL models, mainly for atomistic-level materials research, have also been introduced [76]. A thorough literature survey on the utilization of AI, including ML and DL, within the scope of materials science using Scopus, led to more than 35,000 research publications during the past 20 years. As shown in Fig. 4, AI in materials research has become very active in the past 6 years or so. Whereas Fig. 5 shows different applications to which ML- and DL-based models have been applied in materials science. They are discussed in more detail below.

The development of innovative materials with the required characteristics is a vital process for the development of advanced technologies [77–81]Fig. 6.

The conventional methods of materials discovery and design i.e., experimental measurement and computational simulation, both involve the requirement for a wide range of different high-performance equipment, resources, experimental environments, and expertise, and hence are very challenging and time-consuming procedures. However, with the introduction of the Materials Genome Initiative (MGI), a huge materials dataset has been collected and shared to facilitate swifter materials discovery and design process [83]. Thus, ML with its superb capability of handling and processing high dimensional data, such as that accessible via MGI, can thereby be employed with success [76,78,79]. Some of the examples of materials discovery using ML in conjunction with MGI include materials discovery for thermoelectric materials, metallic glasses, photocatalysts, prediction of staining cell ability of dyes, and functional defect discovery for quantum information, to name a few [84–88]. Some of the most common aspects of the use of AI in material science for materials discovery are discussed below.

2.1. Materials prediction

Materials prediction refers to using ML models to forecast the properties and behaviors of new materials based on their features, compositions, structures, or any other characteristics. Materials prediction helps in forecasting how a material might perform under different conditions or different applications [89,90]. Numerous ML models have been successfully employed for the discovery and prediction of materials with distinctive properties [91,92]. One example of such unique materials is ionic liquids (ILs), which are being explored due to their promising properties of low vapor pressure, low flammability, and recyclability as cleaner alternatives to conventional volatile organic solvents [85]. However, the discovery of suitable ILs requires chemical structure optimization for compatibility with desired applications. An important class of ILs is guanidinium salts-based ILs, which were researched by Carrera et al. [93], who employed an ML-based model investigating quantitative structure-property relationships (QSPR) for the prediction of new guanidinium ILs belonging to four different ionic families, i.e., BPh^{4-}, Br^{-}, I^{-} and Cl^{-} with melting points ranging from −76

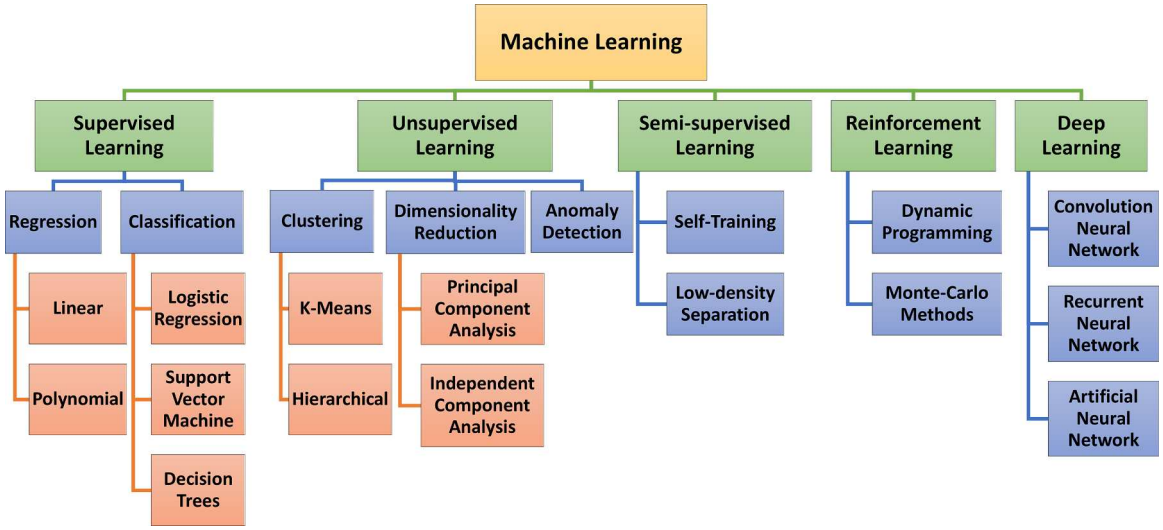

Fig. 3. Sub-classification of machine learning types and algorithms. Reproduced with permission, Copyright 2021, published by MDPI [21,22].

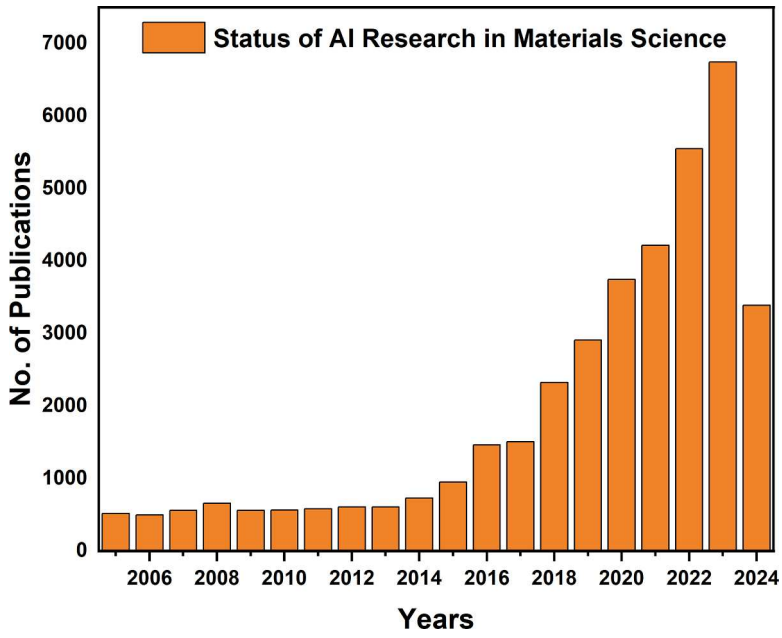

Fig. 4. Bibliometric analysis of publications related to use of AI in materials science field.

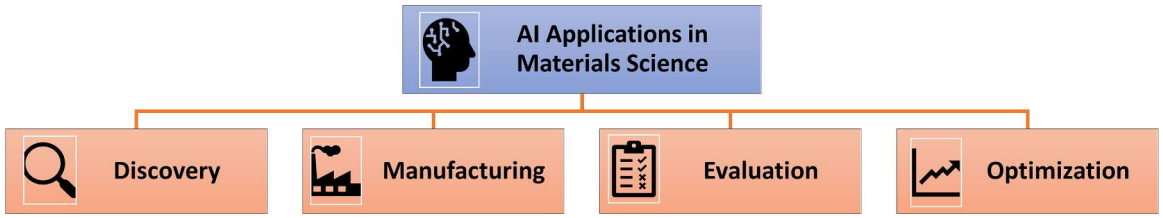

Fig. 5. Overview of different applications of AI in materials science.

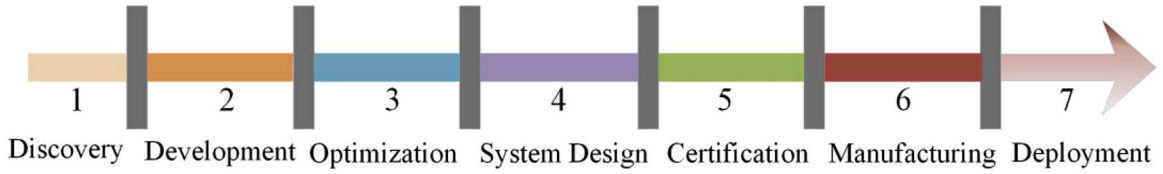

Fig. 6. Traditional process of materials discovery and deployment. Reprinted with permission, Copyright 2017, Published by Elsevier [82].

to 322 °C. The ML model was based on a counter-propagation neural network (CPG NN), which carries out a non-linear projection of molecular structures facilitating 2D visualization of cationic structural features and the anionic influence on melting point, giving a multi-dimensional output. The study claimed that the model aided in the discovery and prediction of six new salts, which were then experimentally synthesized and tested, confirming the accuracy of the model. Fig. 7 shows the overview of the working of the CPG NN in the stated study.

In a similar study, Farrusseng et al. [94] used ML-based ANNs with a genetic algorithm to predict new catalytic materials with improved characteristics. The model implemented the QSPR approach using the activity dataset comprising of unconverted to converted propane ratio after reaction completion, type of oxidation products at five different reaction temperatures for a large number of solid catalysts for the reaction of propylene (C_3H_6) oxidation to establish a relationship between their catalytic performance and structure, composition, and surface area. The study determined that the ML model could be successfully used as a screening tool for identifying potential catalytic materials before the actual synthesis and testing of a material by computing desirability factor based on formation of preferred partial oxidation products (e.g., acetone, propionaldehyde, acrolein, acrylic acid etc.). One such catalytic material with a high desirability factor (~294) the study predicted was a mixed oxide with 14% gallium and 16% niobium supported on an oxide support (either SiO_2, TiO_2 or MgO). In another study, Raccuglia et al. [95] discussed an ML-based approach consisting of SVM algorithms for predicting outcome reactions of inorganic-organic hybrid materials such as vanadium selenites from organic amines for the potential synthesis and prediction of new and better materials. The training dataset for the ML-based model was acquired from various unsuccessful and failed hydrothermal synthesis experiments. The study reported an 89% success rate with the ML approach of accurate prediction of conditions necessary for the development and synthesis of new inorganic-organic hybrid materials (e.g. $[C_3H_{12}N_2]$ $[V_3O_5(SeO_3)_3]\cdot H_2O$, $[C_6H_{22}N_4][VO(C_2O_4)(SeO_3)]_2\cdot 2H_2O$ etc.) far superior to any traditional approaches. An interesting study by Meredig et al. [96] discussed the implementation of a combined heuristic-ML framework on a large input dataset of calculations of density functional theory (DFT) for the successful prediction of 4500

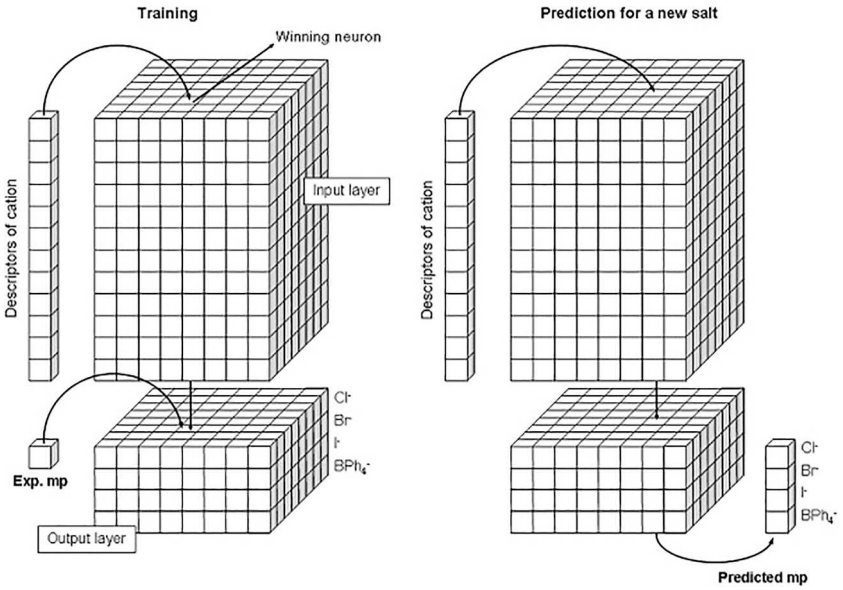

Fig.. 7. The mechanism of learning and prediction in a counter-propagation neural network (CPG NN) used for the discovery of new ionic liquids. Reprinted with permission, Copyright 2008, published by Elsevier [86].

thermally stable ternary compounds ($A_xB_yC_z$) out of 1.6 million different compositions using their formation energies as the criteria for discovery. A few examples of the ternary compound compositions, which the model predicted and later confirmed by the DFT database-search crystal structure prediction are given in Fig. 8.

2.2. Materials identification

ML models, usually with the help of classification and clustering algorithms analyzing data patterns, can also aid in identifying existing materials with the required properties and characteristics for a specific application.

One such research is reported by Philips et al. [97] where an ML-based hierarchical pattern and shape recognition method was utilized to automatically identify crystalline materials. The main inspiration behind the study was the capability of ML-based models to process complex and large datasets comprising visual molecular simulations of 2-D and 3-D Lennard-Jones-Gauss (LJG) systems and perform classification of structural trends based on a small number of training data as opposed to the limitations faced by computational and experimental methods in crystal structure prediction. The study concluded that the automated pattern analysis based on the analysis of peaks in radial function detected structural trends with more accuracy than visual comparison. ML has also been successfully employed to identify another important group of materials i.e., thermoelectric materials. Thermoelectric materials have gained attention since they allow direct

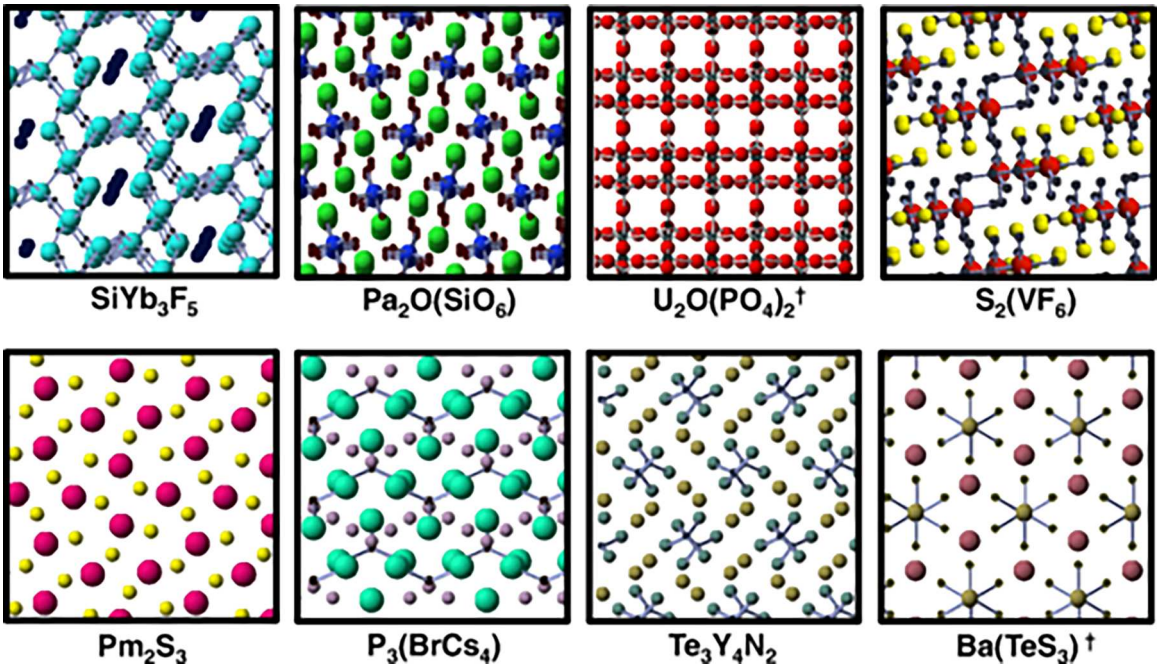

Fig. 8. A few examples of thermodynamically stable ternary compounds as identified by a novel ML-based model. Reprinted with permission, Copyright 2014, published by APS [96].

conversion of thermal energy into electricity and can be implemented in many heating and cooling applications [98]. A study by Parse et al. [99] utilized a regression model to identify the best doping elements for BiCuSeO compounds based on optimal Figure-of-Merit (ZT), a dimensionless metric based on its thermal and electrical conductivity, operating temperature and voltage generated by a temperature difference as shown in Fig. 9. The authors found the feature with highest importance was the total number of unfilled electrons in electronic shells indicating Si as best candidate because of its improved carrier mobility from decreased carrier scattering.

Apart from thermoelectric materials, ML was successfully employed to identify natural porous materials which are used as low-cost, green adsorbents and catalysts. A study by Dico et al. [101] used extremely randomized trees regressor algorithm to identify the best candidate for acid catalysis from a dataset consisting of surface activity and morphological properties of 9 different clay materials with different grades of purity. The model achieved a validation accuracy of 0.943 in terms of R^2, thereby facilitating the identification of optimal materials for this application [101].

Similarly, using ML-based material identification and prediction techniques, certain materials with properties of interest among fuel cells and electrolyzer systems, such as electronic or ionic conductivity, catalyst stability, catalytic activity, electrolytic compositions, etc., could be identified or predicted, which could pave the way towards better performing electrochemical systems, as discussed later in more details.

ML has also found numerous applications in the manufacturing of different materials, especially for additive manufacturing (AM) of metals. AM has gained enormous attention due to its applicability in the fulfilling the emerging industrial demands and involves the layer by layer three-dimensional (3D) deposition of metal to form parts for a variety of different industries such as healthcare, automotive, marine, aerospace, etc. [102]. Metal AM offers the advantage of producing user-specific products with intricate structures, special features, and optimized properties [102,103]. For an in-depth study of the various types of additive manufacturing and their associated processes, readers are directed to the detailed study by Raja et al. [103].

However, careful control of certain parameters related to the metals (and metal alloys) AM process, such as the type of the printing process, process variables (e.g., beam power, feed rate, heat treatment temperature, scanning speed, etc.), is essential to prevent damage and variability in the properties and structure of the final part, increasing the complexity of the whole process [104,105]. It is projected that the challenges faced by metal AM can be addressed effectively by using up-to-date mechanical models and ML. ML models, along with the knowledge of metallurgy, can be employed to design, process, monitor, and control the AM technique to yield the required results [106]. Some applications of ML-based metal AM are discussed below [102].

2.3. Design control

ML models have been successfully applied for AM where design control is of utmost importance to the serviceability of the product, such as in the fabrication of single crystal parts for metallic superalloys where a proper control of melting and solidification procedure parameters is necessary for achieving directional solidification and high-temperature creep resistance. Accordingly, Weber et al. [107] introduced a multi-scale modeling process based on ML to develop a parametrically homogenized crystal plasticity model (PHCPM) for Ni-based super-alloys. ML-based techniques such as support vector regression, k-means clustering, symbolic regression, and ANNs were applied at each development stage of the PHCPM model development linking morphology and mechanism of intragranular γ - γ' microstructures to crystal plasticity coefficients enabling efficient and precise image-based polycrystalline microstructural simulations. In another study, Liu et al. [108] used an ML-based divide-and-conquer self-adaptive (DCSA) model for successful prediction of creep life of 266 different Ni-based single crystal superalloy samples keeping into consideration their composition, and heat treatment process involved, stress and temperature testing. The DCSA model was based on the automatic separation of alloys with different creep mechanisms followed by a self-adaptive selection of the optimal model as shown in Fig. 10.

ML-based models have also been used to manufacture metal AM parts with site-specific properties (also referred to as functionally graded materials (FGMs)) such as in the case of crankshafts and gearboxes which require hard exteriors with soft internal cores. ML-based manufacturing of site-specific AM metal parts is particularly useful as it can help avoid defects and the formation of unwanted brittle phases which can lead to mechanical failure. Such a type of ML-based model was introduced and employed by Eliseeva et al. [109] involving multi-dimensional mapping of compositions of unwanted phases in the composition-temperature space followed by a robotics planning algorithm predicting an appropriate compositional gradient path minimizing the formation of unwanted brittle phases in additive manufacturing of samples with the functional gradient of 316 L stainless steel to pure chromium [109]. In a similar study, Rankouhi et al. [110] implemented a multivariate Gaussian process-based ML algorithm for effective estimation of optimal process parameters i.e. laser power, laser speed and laser hatch spacing for AM of a 316L-Cu part with compositional gradients using part density and surface roughness as input parameters.

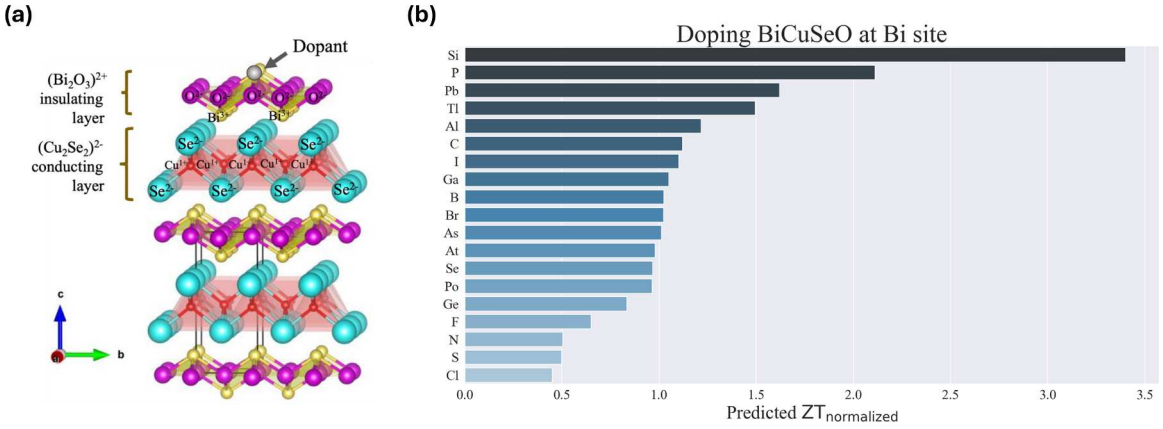

Fig. 9. (a) Crystal structure of BiCuSeO consisting of conducting $(Cu_2Se_2)^{2-}$ layer, insulating $(Bi_2O_3)^{2+}$ layer and the dopant substituted at the Bi site. (b) Predicted $ZT_{normalized}$ values for the selected $Bi_{0.98}A_{0.02}CuSeO$ compounds, where A represents dopants shown on y-axis. Reprinted with permission, Copyright 2022, published by MDPI [100].

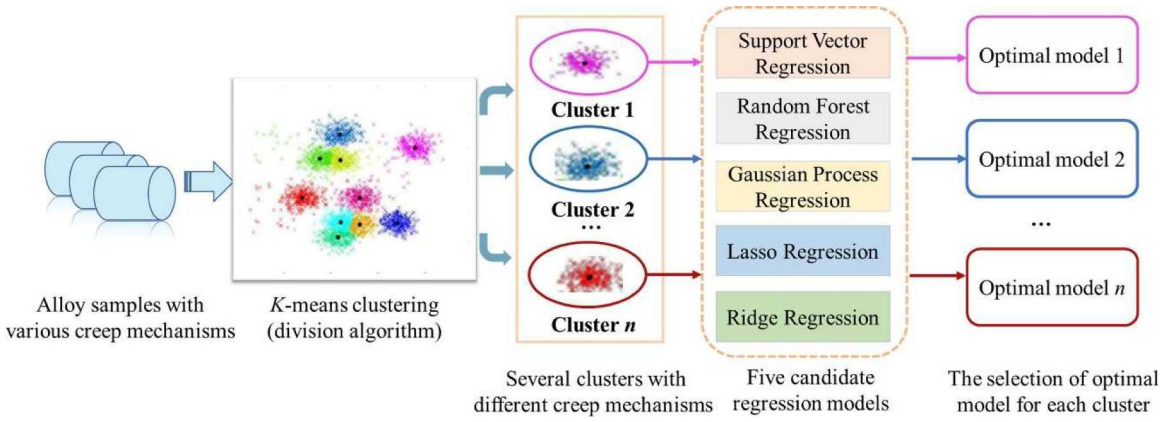

Fig. 10. ML-based creep life prediction model for Ni-based single crystal superalloys. Reprinted with permission, Copyright 2020, Published by Elsevier [108].

2.4. Process monitoring

ML has also been employed to help with in-process monitoring of manufacturing of high-performance components not only limited to metal AM [93]. For example, in a study by Denkana et al. [111], the authors aimed to enhance the end quality of the machined workpieces of friction-welded shaft materials (i.e., hybrid materials) by adaptation of changing process parameters via in-process material identification during the machining process. The reason for the continual alteration in process parameters is due the change in material properties and chemical compositions during machining leading to deviation of cutting edge from the programmed tool path, changes in surface topography or cutting-edge displacement due to edges build-up. The study assessed the material monitoring quality of four different ML algorithms i.e., neural networks, k-nearest neighbor (kNN) algorithm, SVM, and decision trees by first training the algorithms on the dataset of signals measured for tool turret vibration, cutting force, feed force and passive force, spindle torque and motor current for each different composition of material followed by experimental validation. The results showed that the kNN algorithm showed the best performance for in-process material identification.

Another application of ML is in materials processing (e.g., welding) optimization through ML-aided data analysis, as described next. Nb-bearing nickel-based superalloys such as Inconel 625, due to their excellent anti-corrosive properties, have been widely implemented as a weld overlay for carbon steel pipes used for offshore oil and gas transport [112]. However, during the welding process, micro-segregation and precipitation of secondary phases can lead to solidification cracking, which reduces the alloy's resistance to corrosion. Therefore, optimal control of welding conditions during phase transformations is necessary [113]. To analyze the phase transformations in such materials, ultrasound testing is usually employed, which involves processing and analysis of a large dataset of backscattered ultrasound signals captured by direct contact techniques. To tackle this problem, Vejdannik et al. [114] used an independent component analysis (ICA) to reduce statistical redundancy and a probabilistic neural network (PNN, a type of ANN) for the classification of selected features from the backscattered ultrasound signal data for successful automated in-process characterization of phase transformations kinetics. The study employed a bees algorithm (a population-based search algorithm to find best solution to an optimization problem) by selecting the smoothing parameters of pattern neurons for computing the probability distributions of training data for PNN. They concluded that, ICA components of cumulant coefficients of ultrasound signals with the optimized PNN yielded highest average accuracy of 97% and 83.5% for thermally aged as-welded Nb base alloy at 650 and 950 °C, respectively.

2.5. Quality control

ML can also be employed for checking for quality assurance and control of the final part during the manufacturing step [115]. For instance, Kwon et al. [116] reported the use of a neural network-based classification model to investigate the effect of six different laser powers in metal AM upon crack and pore formation in melt-pool images with a classification failure rate of 1.1% for over 13,200 test images. The study also concluded that the introduced model could also be effectively used to locate deformation for non-destructive separation of defective products.

It has been reported that the use of the laser power bed fusion (LPBF) method during the AM of high-strength metals can induce defects such as anisotropy and pores in the final part, which could be potentially avoided by the use of ML-based algorithms. For example, Zhang et al. [117] introduced two different ML-based approaches i.e., spatial-temporal sparse dictionary learning (STSDL) and spatial-temporal blind source separation (STBSS) to investigate the defects in LPBF manufacturing of stainless steel 316 L and Inconel 718 using their thermography images as data input. Flash thermography is commonly used for quality control of such parts but is prone to non-consistent sample illumination and experimental and imaging thermal noise which causes blurring of hot spots indicating defects. The STBSS method involved de-noising of wavelet transform followed by data decomposition using PCA and later defect separation by ICA. The STSDL method involved denoising of wavelet transform followed by data decomposition with sparse dictionary learning (SDL) method. The methods were evaluated using a test accuracy indicator called F-score and runtime of the execution and concluded that the STBSS method is better suited for the detection of smaller defects while the STSDL method is more suitable for finding larger defects and increased accuracy for both methods is achievable through an increase in runtime [117]. In another study, Wu et al. [118] successfully used a random forest-based ML prediction model for determining the surface roughness with high accuracy of the products manufactured by the fused deposition modeling (FDM) manufacturing method [118].

ML algorithms have not only been successfully implemented for the discovery and manufacturing of materials but also for evaluating the performance and properties of developed materials [119]. Besides, in situations or experiments where exact operating and experimental conditions could not be anticipated beforehand, a detailed study of diagnostics and characterization data after being subjected to the actual conditions becomes the best option to optimize the performance of the material [120].

2.6. Performance assessment

Materials performance analysis via ML methods is being carried out

for a wide range of applications these days. For example, it has been recognized that the design of battery materials and their selection greatly impact the performance of lithium-ion (Li-ion) batteries, but owing to the complexity of design variables, the performance of batteries is not easy to assess. Therefore, the use of the ML model based on association rule mining (ARM) was proposed by Kilic et al. [121] to study the effect of charging/discharging cycles and current on the performance of lithium-sulfur batteries (Li-S) batteries. The study involved the accumulation of performance data from 1660 different cells which was processed by the ML-based ARM approach. The ARM method was used to investigate the associations of numerous performance variables with individual factors within the input dataset (including but not limited to discharge current density, material of encapsulation, anode, electrolyte, binder, type of current collector, separator, interlayer, electrolyte to sulfur (E/S) ratio, etc.) and identify factors resulting in high peak discharge capacity and superior cycle life ultimately leading to improved battery performance. The study concluded that solid-state carbon-based encapsulated cathodes with encapsulation material over 40% as well as binder and conductive-free encapsulated cathodes, electrolyte materials with low electrolyte to sulfur (E/S) ratio, carbon interlayers, and carbon current collectors all contribute towards enhanced battery performance [121].

Metal-organic frameworks (MOFs) due to their inherent high interstitial porosity are considered promising candidates for gas storage and separation applications [122]. With the development and implementation of robust computational methods, a large amount of simulated performance data for MOFs is easily available. However, the large dataset of simulated data requires speedy interpretation and analysis with high accuracy which can be facilitated by the application of ML algorithms. Different types of input descriptors can be used for ML-based performance prediction of MOFs as shown in Fig. 11 [123].

This strategy was used by Fernandez et al. [124] to successfully predict the methane storage capacity of MOFs using ML algorithms of multilinear regression, decision trees, and non-linear SVMs based on geometric descriptors data for MOFs.

Another important application of ML is the determination of the thermoelectric performance of layered IV-V-VI semiconductors. Gan et al. [125] utilized deep neural networks to predict the energy conversion efficiency and optimum doping type (p or n-type) for a family of layered IV-V-VI semiconductors at different temperatures from an input dataset containing information about number of atoms, atomic and covalent radii, valence electronic configurations, electronegativities, lattice constants average atomic mass, interatomic bond lengths, lattice constants etc., for 40 different compounds investigated at different temperatures (from 100 to 650 K). The study also compared the output values predicted by the introduced ML method with the DFT calculated values finding a ML prediction accuracy above 90%.

2.7. Characterization data analysis

Study of materials usually involves the use of a wide range of advanced characterization techniques which results in a large dataset of information that typically requires further processing for extracting useful information [126]. ML models have been productively utilized to analyze such materials characterization data and can help researchers to correlate different microstructural descriptors and interactions to material behaviors and properties [127].

An example of such an application is in the analysis of the weld heat-

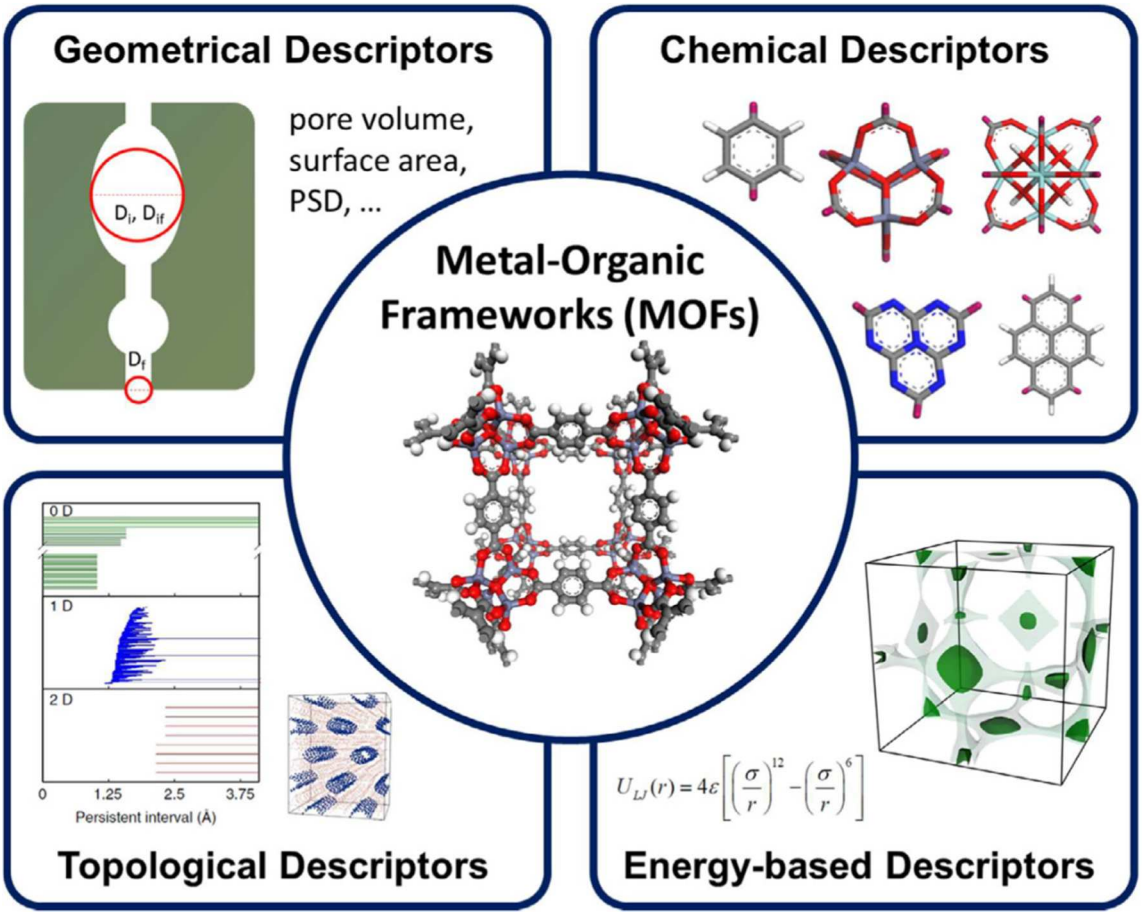

Fig. 11. Different types of descriptors that can be used in machine learning models for performance evaluation of MOFs. Reprinted with permission, Copyright 2020, Published by Elsevier [123].

affected zone (HAZ), which plays an important role in determining the quality of the welding procedure in metallurgy. HAZ is defined as the area of the welded metal which does not melt but undergoes a significant microstructural change due to high-temperature exposure [128]. Welding of austenitic steel also involves the formation of HAZ with different microstructures due to formation of different phases, such as ferrite, pearlite, bainite, and martensite, depending on different cooling rates as well as cementite precipitation. The quantification of dimensions, morphology, and volume fraction of these phases is important in predicting the mechanical properties of austenitic steel, but it is a long and laborious process if done manually. Therefore, Bulgarevich et al. [129] introduced an automated pattern recognition ML method via the implementation of random forest algorithms for automated segmentation of different types of austenitic steel microstructures in a large set of optical microscopy data. The study concluded that the developed framework, in combination with appropriate image processing methods, could be used as an accurate. In another study by Rettenburger et al. [130], DL-based instance segmentation of particles was carried out to predict particle sizes of powdered $LiCoO_2$ was trained on a dataset of 90 images and compared to segmentation results from a U-Net model trained on the same dataset. The performance of the models was evaluated using Aggregated Jaccard Index (AJI+) which takes into account the segmentation quality as well as localized segmentation accuracy. The authors reported that the R-CNN model significantly outperformed the U-net model by AJI+ of 0.81 vs. 0.55 for low magnification and AJI of 0.51 vs. 0.34 at high magnifications, respectively (Fig. 12).

Another important application of ML is in the construction sector, particularly in the research of supplementary cementitious materials which can be used in conjunction with Portland cement (OPC) to enhance the properties of concrete contributing to low-carbon footprint and promoting sustainability [131,132]. Sui et al. [133] reported using DL based approach to investigate the pore morphology of one of such materials i.e. calcined limestone clay (LC^3) using a dataset of scanning electron microscopy (SEM) and micro-computed tomography (micro-CT) images. The approach based on deep neural network (DNN) architecture helped compare the connectivity of pores and solid particles, identify stress concentration regions and quantify packing fraction in cured LC^3 compared to OPC sample which is vital for future material design considerations. The authors reported that the increased physical size of the images led to an increase in CNN classification accuracy reaching ~ 74% and 96% for the micro-CT and SEM images, respectively for images of 81.12 × 81.12 μm.

2.8. Degradation studies

Machine learning has also been employed to study the effects of materials degradation to better predict and understand failure mechanisms and potentially avoid them in the future. Understanding materials degradation mechanisms are, among others, particularly important for research and development in clean energy applications such as fuel cells, batteries, solar cells, etc. [134–136].

An example of application of ML in degradation studies in Li-ion batteries is described below. While characterized as key energy storage technology, Li-ion batteries suffer from a progressive loss in performance due to the battery aging process. Accumulation of a large quantity of aging data, vital for understanding involved material degradation mechanisms, is also a challenging process because of the long and extensive experimental procedures involved [137,138]. To tackle these issues, Tang et al. [139] presented a unique approach of combining accelerated aging test data with an industrial aging dataset via a migration-based ML approach facilitating the acquisition of a high-quality aging dataset that can be further employed for the

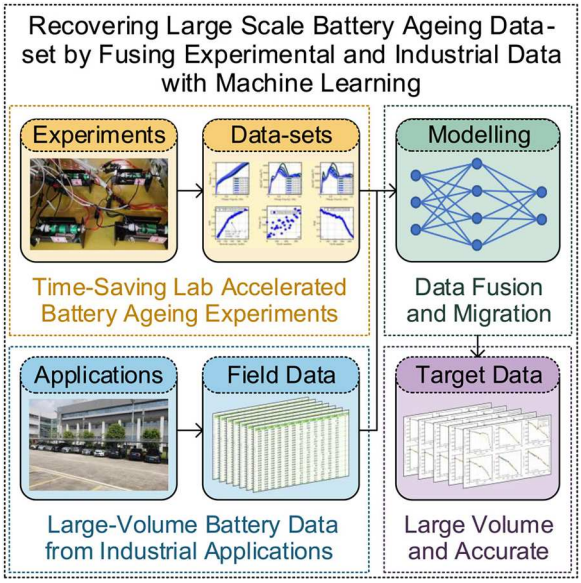

Fig. 13. Overview of a unique method to recover large-scale battery aging dataset with the help of ML. Reprinted with permission, Copyright 2021, Published by Elsevier [139].

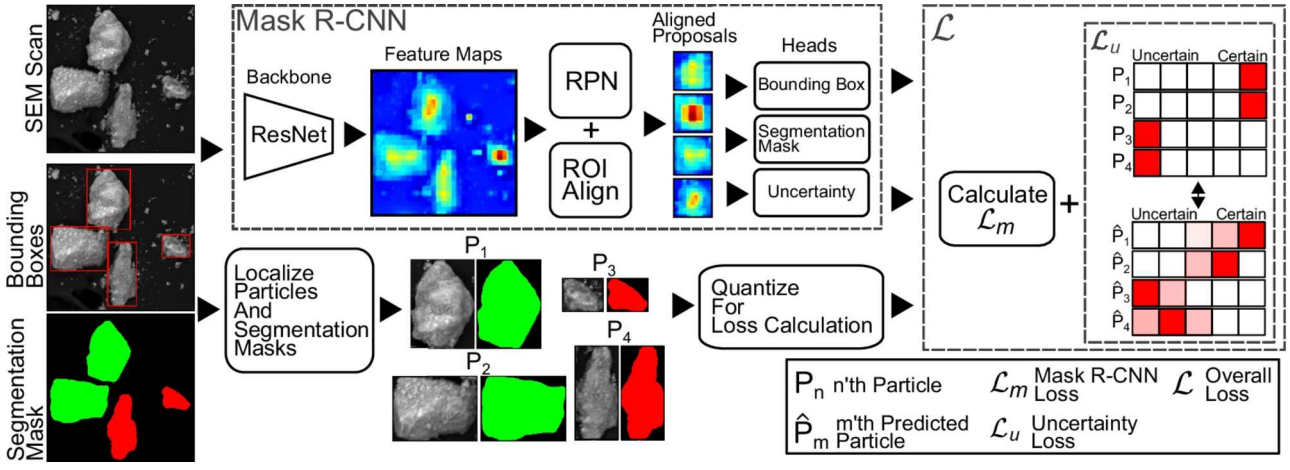

Fig. 12. Flowchart depicting the R-CNN architecture based on ResNet-50 backbone to extract feature maps from SEM images. Reprinted with permission, Copyright 2024, Published by Springer Nature [130].

degradation assessment of Li-ion batteries. The graphical overview of the whole process is given in Fig. 13.

Another example focuses on perovskite solar cells degradation. These cells have been explored due to their high performance and low-cost solar energy generation. However, they consist of halide perovskite materials that suffer from environmental instability preventing their widespread commercialization. It is suggested that significant development in perovskite-based technology can be made possible through the examination of perovskite degradation data [140]. To address this problem, Naik et al. [141] introduced a scientific ML approach combining differential equation modeling with a sparse regression model to correctly identify equations controlling the degradation of methylammonium lead iodide perovskite (MAPI) with an error percentage of only 6%.

Since the ultimate aim of research in the field of materials science and engineering is motivated by the development of novel materials which can outperform conventional materials, ML-based models can also assist with materials design optimization and experiment selection at each stage of the materials development and implementation process [142]. Similarly, since lifetime stability is a significant concern for all types of fuel cells and electrolyzer technologies, necessitating thorough microstructure and performance evaluations, ML could be particularly useful in addressing these challenges, as discussed later.

2.9. Materials optimization

In the past, the process of material optimization was solely dependent on a combination of materials physical and chemical properties data and trial-and-error experimental procedures. However, with the development of ML approaches and high-performance computational techniques, the optimized designing of innovative materials has become easier and more efficient. On this basis, a study is reported by Xie et al. [143] which involved the development of a crystal graph CNN framework possessing the ability to learn properties of materials from the atomic configuration of atoms in the crystal structure. The study stated that the developed model provided DFT calculated properties for eight different crystalline properties for inorganic crystalline materials of various structures and compositions with high accuracy and can serve as a basis for advanced materials design.

Simulations of molecular dynamics can also be used for the computational designing of new materials by providing a speculative perception of the microstructure of condensed-phase materials. However, these atomistic simulations are difficult to achieve because of the complexity of thermodynamic and kinetic phenomena in materials. To address this issue, Wang et al. [144] introduced ML-based methods for optimization of coarse-grained molecular modeling representation followed by deep neural networks-based fitting of coarse-grained potentials acquired from atomistic simulations to aid in the effective designing of materials.

2.10. Experiment selection

Progress in materials science had been led by experimental studies in the past which were usually time-taking and required the use of specialized equipment and numerous resources. Machine learning combined with the design of experiments (DoE) approach can help with the selection of experiments to facilitate materials optimization efficiently as illustrated in Fig. 14 [145,146].

Particularly for research related to organic photovoltaic devices, which involve numerous complex components and processing conditions, experiment selection can be extremely helpful. One such study has been reported by Kirkey et al. [147] that collectively employed DoE and machine learning models for optimization of bulk heterojunction (BHJ) layer in organic photovoltaic devices. The study involved the implementation of the DoE method on donor and acceptor ink solution concentrations and the temperature and duration of annealing used for the synthesis of films followed by the use of SVM algorithms to identify the optimal experimental parameters to ensure the development of high-efficiency organic photovoltaics.

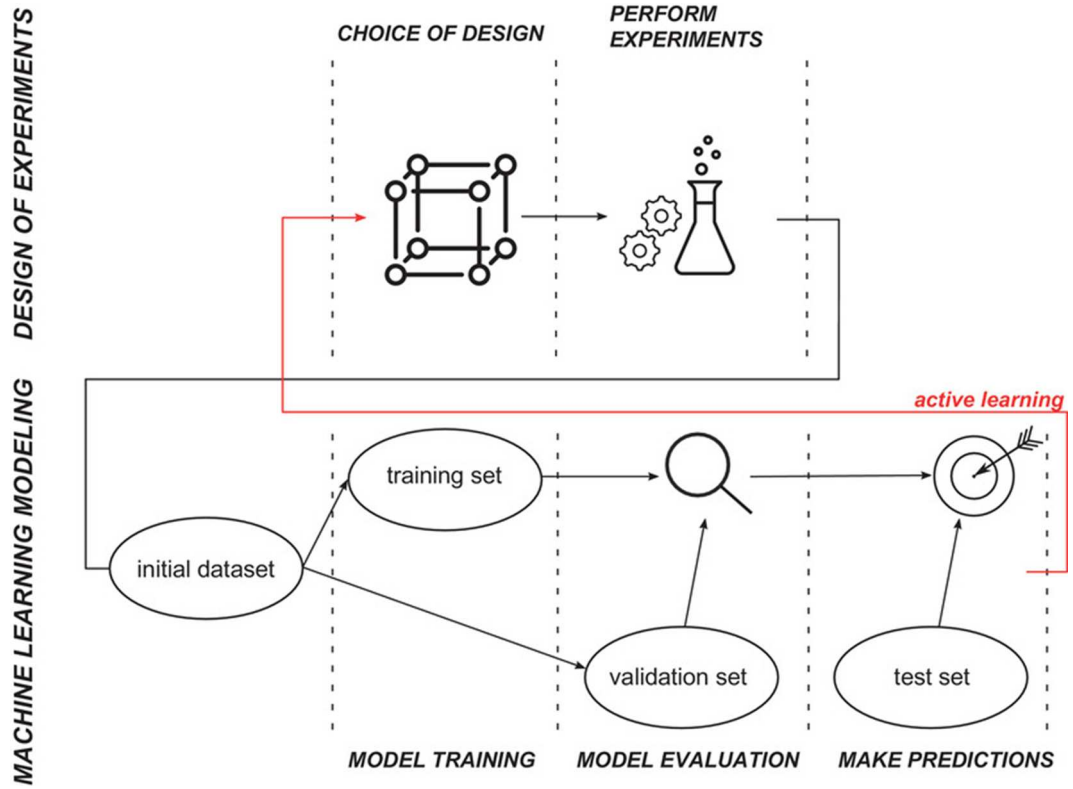

Fig. 14. . The representation of the design of experiments (DoE) approach combined with the ML-based approach. Reprinted with permission, Copyright 2022, Published by Wiley [146].

Electrical discharge machining (EDM) is an advanced material removal process for generating complex contours with high accuracy. EDM is a complex thermal process that can induce different microstructural changes and thermal stresses in the machined material affecting the durability of the processed part. To prevent this problem, Markopoulos et al. [148] employed an ANN model with a back-propagation algorithm trained on a series of EDM experiments on various steel grades using the pulse current, processed material, and pulse duration as input parameters to predict surface roughness with high precision, aiding the efficient selection of experiments.

Similarly to other systems discussed above, fuel cells and electrolyzers are currently the focus of intensive research to improve performance and durability through the synthesis of new catalytic materials, optimization of electrode composition and microstructure, and control of the operating conditions. Traditional methods, such as design modifications, trial-and-error synthesis, and prolonged durability testing, can be both costly and resource-intensive. In this context, ML-based approaches offer a valuable alternative, potentially reducing the time, material, and energy required for effective research and development.

Below, we will focus specifically on application of ML in fuel cells and electrolyzers, two systems of our interest. As these devices share common characteristics in their design and operations, the application of ML to these devices can enhance performance prediction, service life expectation, fault detection and design optimization. ML algorithms can efficiently handle non-linear problems, as in the case of current-voltage performance curves, thereby leading to improved accuracy in predicting outcomes and optimizing design and operational parameters of these devices.

3. Application of Machine Learning in fuel cells and electrolyzers

Fuel cells and electrolyzers are clean energy, hydrogen-based, electrochemical devices that have the potential to contribute to the reduction of carbon emission globally [149–151]. Electrolyzers are devices that use electricity to electrochemically split water, generating hydrogen [152,153]. Fuel cells, on the other hand, convert chemical energy of hydrogen through electrochemical oxidation on the anode, and oxygen reduction on the cathode, producing useful electrical energy and only water (vapor) as a by-product [154,155]. If the energy supplied to the electrolyzer comes from renewable systems, like solar [156,157], hydro or wind [158,159], the produced hydrogen is considered green, while produced energy in the fuel cell clean and renewable.

There are a number of different types of fuel cells and electrolyzers, depending on the type of electrolyte used and operating conditions [160,161]. Our main focus in this review will be proton exchange membrane (PEM) fuel cells (FCs) and water electrolyzers (WEs), although other types will be discussed as well. Both fuel cells and electrolyzers are crucial for advancing sustainable energy solutions, sharing many underlying principles and challenges.

Despite these similarities, a clear discrepancy exists in the literature: while numerous reviews focus on the application of AI in fuel cells, there is a noticeable lack of similar studies on electrolyzers], [162–167]. Moreover, there is an absence of comprehensive reviews that address both technologies simultaneously. One reason for this disparity could be that electrolyzer research is still in its early stages, whereas research on fuel cells has been relatively consistent over the past decade. To better understand this, a thorough literature survey was conducted using Scopus to assess the overall status of research in fuel cells and electrolyzers over the past 20 years, with a specific focus on the use of AI, including ML and DL in these technologies over the past 4 years. The bibliometric data, presented in Fig. 15, reveals that AI applications in both fuel cells and electrolyzers account for only a small fraction (approximately 2%) of the total publications in these technologies. Moreover, within this subset, AI-related research on electrolyzers constitutes merely about 5% of the total AI-focused publications in the combined fields of fuel cells and electrolyzers. This highlights the current state of AI-related research within these domains and underscores the need for a more integrated approach to reviewing AI applications across both technologies. This paper aims to address this gap by providing a comprehensive examination of AI's role in both fuel cells and electrolyzers, offering insights into the current research landscape and identifying areas that warrant further investigation.

The electrochemical reaction in both PEMFCs and WEs happens in membrane electrode assemblies (MEA), consisted of a porous cathode catalyst layer (CL) (typically platinum (Pt) nano-catalyst supported on carbon nanoparticles, bonded by proton-conductive ionomer), porous anode CL (similar composition in PEMFC, while containing Ir-based catalyst in PEMWEs), bonded to a polymer electrolyte membrane. Both MEAs contain additional layers for water and heat management (gas diffusion layer (GDL), microporous layer (MPL) and porous transport layer (PTL). Fig. 16 represents the illustration of a PEMFC MEA. The major difference between the PEMWE and PEMFC MEA shown in Fig. 16 is the reverse electrochemical reaction that occurs both at the anode and cathode side of the electrochemical setup. Materials composition, microstructure and component distribution in MEAs, especially in the catalyst layers, significantly affect the performance and durability of these devices, having in mind that both PEM FCs and WEs are exposed to harsh operating conditions during their lifetime (e.g., high voltages, temperatures to 80–100 °C, corrosive environments).

Development of materials in these devices are in high need to meet the demand for clean and sustainable energy generation. In developing

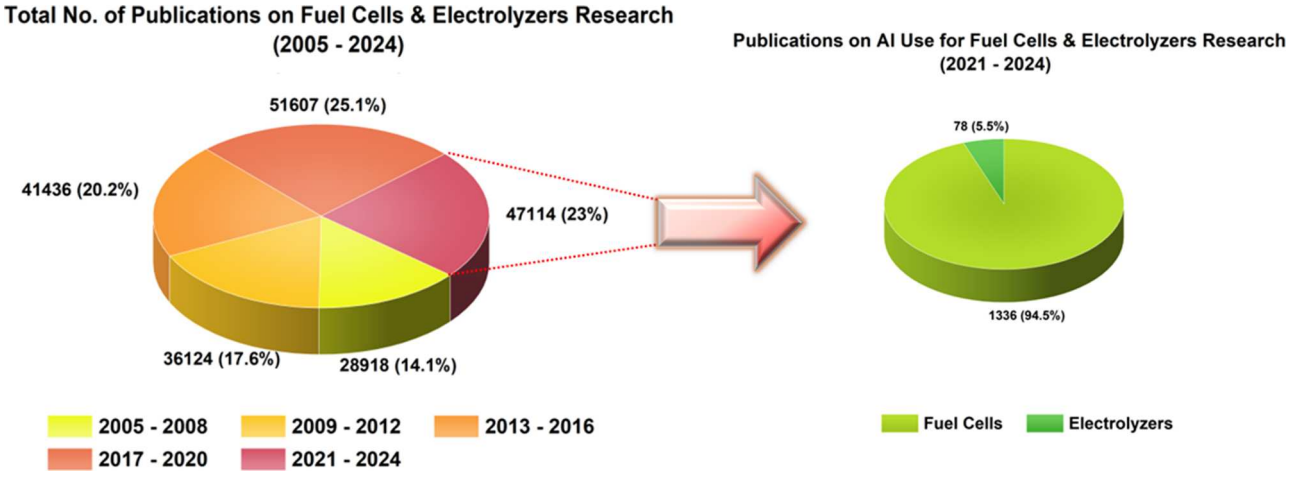

Fig. 15. Bibliometric analysis of publications related to use of AI in fuel cells and electrolyzers.

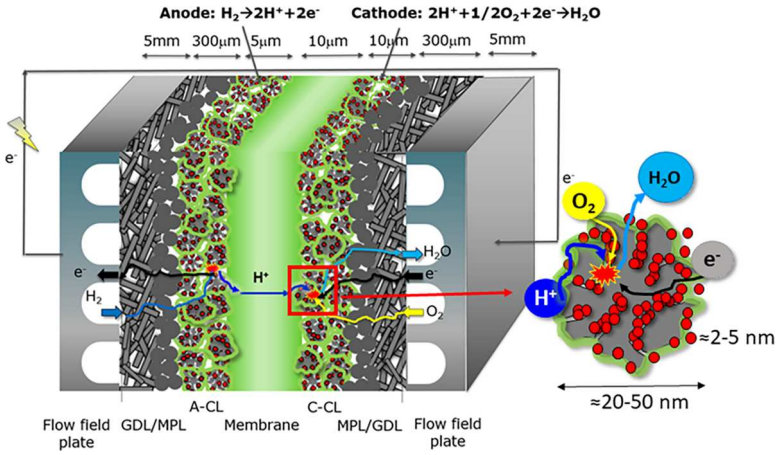

Fig. 16. Illustration of a PEMFC MEA. Reprinted with permission, Copyright 2019, Published by Cambridge University Press [168].

these materials, their structural properties are of paramount importance as they determine the device's activity and efficiency [169–171]. In a nutshell, current research focuses on enhancing catalyst materials, improving membrane performance, extending durability and scaling up production methods to make these technologies more commercially viable], [172–177]. However, challenges remain, including high costs of platinum-based catalysts, membrane degradation, and limited operational lifetime under varying conditions. Despite these challenges, PEMWEs and PEMFCs hold immense potential for applications in green hydrogen production, clean transportation, aerospace, underwater applications and grid energy storage, offering pathways to reduce carbon emissions and enhance energy security in the transition to a low-carbon economy [178]. Several decades ago, multilevel computational methods such as equivalent circuit, physics based, pseudo two-dimensional, computational chemistry, quantum mechanics, molecular dynamics, and many more, have been employed to understand materials either as a standalone or composite systems for various application processes in battery management systems, fuel cells and supercapacitors [179]. Widely used equivalent circuit models include Rint, Randles, Thevenin and hysteresis models while physics-based models are based on electrode theory, such as Bulter-Volmer equation [180–183]. However, many of these methods are too idealistic and complex. Furthermore, the cost of computing is high, limiting the scale-up of these approaches to larger material volumes. As a result, it is imperative to find alternative methods for understanding and developing efficient materials without spending an inordinate amount of time developing them. During fuel cell and electrolyzer operations, there exist sensors that collect data per time based on several operating parameters such as humidity, pressure, temperature, flow rates of reaction gases etc. The application of artificial intelligence is crucial to monitoring and controlling these operating conditions with the aim of achieving optimal performance. This is achieved when an artificial intelligent system measures input data from a sensor unit, generates a model for predicting and controlling performance of the fuel cell/electrolyzers through the learning and analysis of the collected data, compares the generated model with the data measured in real time and diagnoses a state of the fuel cell/electrolyzer stack, and generates a control signal for changing an operation condition of the fuel cell stack; and a control unit which changes the operation condition of the fuel cell stack according to the generated control signal. Examples of these artificial intelligent systems include neural networks, fuzzy logic and neural fuzzy [184,185]. AI and ML can help in this sense, by employing the use of historical data in training, learning, identifying patterns and predicting futuristic properties, problems and/or possibilities of concepts/processes, which can significantly speed up the process of understanding and development of fuel cells and electrolyzers [186–188].

3.1. *Application of ML algorithms for MEA and performance optimization*

The structural makeup of MEAs in fuel cells and electrolyzers poses a lot of challenges due to their design complexity and heterogeneous nature. The right design of MEAs taking into account the electrode catalyst loadings, ink formulation techniques, catalyst-electrolyte interface, anode-membrane-cathode proton transport, transport of reactants in the electrodes, GDL, PTL and current flow between the electrodes and current collectors, are of great importance in determining the performance of fuel cells and electrolyzers [189]. ML algorithms, such as ANN, extreme gradient boost (XGBoost), KNN, random forest (RF), support vector machine/regressor (SVM/SVR), logistic regression (LR) and elastic net (EN), to mention just a few, can be used to predict and optimize the performance of fuel cells and electrolyzers based on compositional and structural parameters, and other MEA/system descriptors. ML models combined with optimization algorithms, such as genetic algorithm (GA), can further optimize the design and operating parameters to achieve multiple optimization goals with high accuracy and efficiency [190–194].

For example, Khajeh-Hosseini et al. [191] applied ANN to investigate the influence of different CL structural parameters on the performance of CL in PEMFCs. The authors developed an agglomerate model (see Fig. 17a) based on laws governed by Fick's law of diffusion and electrochemical reaction equations to generate nine structural parameters that are responsible for influencing the performance of CL. The structural parameters which include CL liquid saturation, ionomer film thickness, catalyst agglomerate radius, Pt and carbon loading, membrane composition, extent of GDL penetration into the CL, and CL thickness were used as input parameters for the neural network to predict the activation overpotential associated with the electrochemical cell. The researchers encountered challenges in establishing a direct correlation between each independent physical property and output parameter using ANN. To address these challenges, they applied a linear superimposition approximation statical model to find these correlations, revealing that increase in ionomer thickness, increase in Pt, and carbon mass loadings, and GDL penetration into the CL impedes oxygen diffusion into the CL due to less pores, thus increasing the activation potential. On the other hand, large agglomerate radius allows for larger pores and high oxygen diffusion coefficient which could ultimately reduce the activation potential and hence increase the overall performance of the cell. Despite these complexities, the neural network achieved a near-perfect correlation value of 0.8 with a mean square error of 0.0016, showcasing its effectiveness as a modeling tool, as shown in Fig. 17c.

In another study by Wang et al. [195], the authors optimized the CL composition of a PEMFC with ANN based on data generated from computational fluid dynamics (CFD) agglomerate model. These

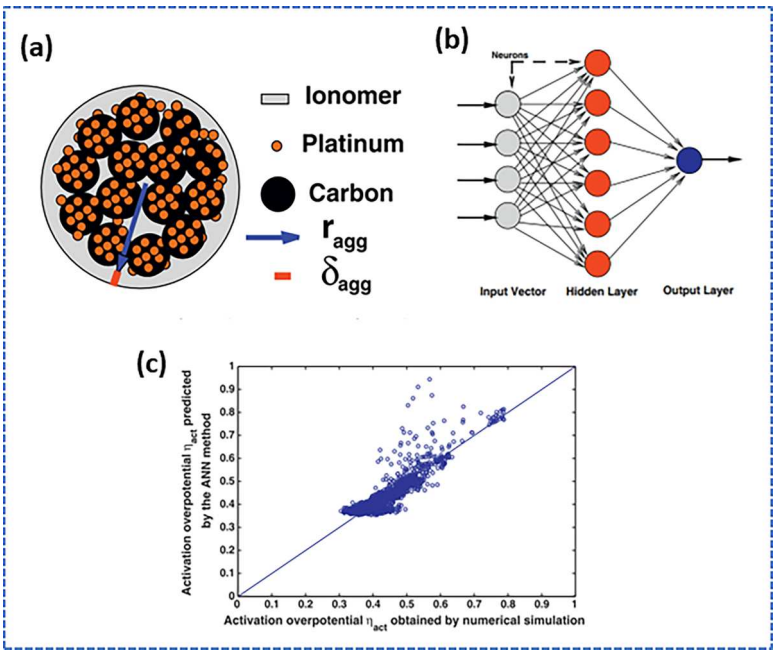

Fig. 17. (a) Agglomerate model design (b) schematic representation of ANN (c) Predicted activation overpotential versus actual activation potential from numerical simulation. Reprinted with permission, Copyright 2011, Published by Elsevier [191].

composition parameters include Pt loading, Pt weight percentage, ionomer to carbon weight ratio (I/C), electrolyte volume of carbon, and Pt and ionomer volume fraction, and porosity. Current density was used as the output parameter. In their study, ANN model achieved a high accuracy with correlation coefficient (R^2) greater than 95% for both training and validation data. With GA, the current density was optimized from 2.1379 A/cm^2 to 2.1729 A/cm^2. The researchers went further to optimize for the maximum current density using similar input parameters but explored SVM coupled with GA for optimization purposes. The R^2 for both the training and test data was found to be about 99% with an increase in power density after optimization from the starting values of 1.2647 and 1.2473 W/cm^2.

Zhang et al. [196] studied the influence of porous structure CL of MEA on the cell performance of a high temperature (HT) PEMFC using Monte Carlo method combined with Deep Neural Networks (DNN) and gaussian regression model. The accuracy metrics explored for this study were R^2 and root mean square error (RMSE). In their investigation, they employed the Monte Carlo approach in combination with DNN and Gaussian Process Regression (GPR) model to analyze the cell performance based on 11 structural parameters. With the Monte Carlo method approach, 11 porous structural layers were generated. These parameters include the thickness of the anode and cathode GDL, the porosity of the anode and cathode GDL, the thickness of the anode and cathode CL, porosity of anode and cathode, the electrolyte volume fraction, and the Pt content of the anode and cathode. These structural parameters were used as input parameters to train the neural networks regression model, which aimed to determine the optimal power density at different Pt loadings. The R^2 performance of the DNN and GPR models was found to be 0.9993 and 0.995, respectively. Their study revealed that as the Pt loading is increased, the optimal GDL thickness and CL porosity decrease. Furthermore, cathode MEA parameters have a greater impact on cell performance than anode parameters. With bi-objective GA, these parameters were optimized to achieve maximum power densities at 0.4 V and 0.6 V for platinum loadings of 0.3 mg/cm^2 and 0.5 mg/cm^2 respectively.

Jienkulsawad et al. [190] applied ANN to determine the optimal polyvinyl alcohol (PVA)/Pt compositional weights that would be required as an additive to the cathode-side catalyst layer component of a PEMFC. PVA is an additive that is added to membrane or catalyst layer of PEMFCs to enhance hydrophilicity in low humid environments during operation. In their study, they predicted the PVC/Pt ratio that is sufficient for the design of PEMFC catalyst layer using cell voltage (V), current density (I), relative humidity (RH), and power density (P), I/V, I/RH, V/RH, P/RH, PI, PV, IRH, VRH, and PRH as input parameters. ANN based on Levenberge-Marquardt algorithm with first, second and third hidden layers of 9, 8 and 9 nodes respectively was used for the model development with root mean square error (RMSE) as an accuracy metric to determine how good is the model. The researchers found that ANN was able to predict the best PVA/Pt ratio in the CL with minimal RMSE of 0.1293 and 0.031 for the predictions of Pt and PVA respectively, even with the use of the hidden layers. Indeed, when applying ANN to any ML task, the choice in the number of hidden layers used for such task plays a significant role in achieving high accuracy. Too many hidden layers in a neural network can slow down the training process. However, this approach can improve accuracy if time complexity is not a major concern. Furthermore, too many hidden layers in a neural network model can result in overfitting of the training data causing the model to struggle with effective generalization on the test data. As a result, it is important that the training data is well analyzed to avoid model inaccuracy.

Mohamed et al. [197] investigated the prediction of hydrogen production rate and cell current density of PEMWE using ANN, PR, SVM, KNN, Decision Trees. The first step of their investigation was to construct a database consisting of 1203 experimental data (1086 assigned for training purposes and 117 for testing) and having fifteen input variables that includes anode and cathode support (porous titanium, titanium, porous carbon, 304 stainless steel and carbon plate), membrane type (Nafion 115, Nafion 117, Nafion 112, and Nafion 110), anode/cathode catalyst (e.g. Pt, Ir, Ru), anolyte/catholyte composition, cell structure, electrode area, anode/cathode flow path area, voltage, number of cells, power, water flow rate, and cell temperature. Secondly, they used box and whisker plots as data analysis tools to get insights on the distribution of some input parameters such as anode/cathode support type, membrane type, and anode/cathode catalysts that significantly contribute to high current density. Their results showed that configurations having —specifically, Nafion 115 and 117 membranes, porous titanium for anode/cathode support, platinum and ruthenium for anode catalyst, platinum for cathode catalyst, methanol for anolyte, and

deionized water for catholyte — played a substantial role in achieving high current density. Among the five ML algorithms studied, the ANN exhibited superior performance in predicting both hydrogen production rate and current density with the testing data mean squared error of 5.0006 and 0.04026 respectively.

To the best of our literature search, the use of box and whisker plots as data analysis tool before the application of ML model is not often reported in most publications of fuel cells and electrolyzers application. However, these data analysis tools offer crucial insights into the relationships between input and output parameters in data. Günay et al. [198] explored box and whisker plots prior to applying decision tree ML to model the performance of PEMWE. This comprehensive methodology not only deepens the understanding of the factors influencing PEMWE performance, but also underscores the importance of integrating traditional statistical methods with advanced ML techniques for more robust predictive modeling. In their study, 789 data points from 30 publications were collected and analyzed, revealing significant correlations between cathode/anode support, catalyst mole fraction on support surface, catalyst loading, operating temperature, and PEMWE performance. The box and whisker data analysis identified that the most significant elements contributing to high current densities for cathode and anode supports, and cathode surface were carbon, Ti, and pure Pt, respectively. This is attributed to the high electrochemical activity of pure Pt, the stability of the Ti support, and the high surface area and electrical conductivity of carbon. Following the statistical analysis, a decision tree was employed to evaluate the feature importance contributing to both current density and power density. The researchers found that the most influential factors for current density were the nickel (Ni) catalyst mole fraction on the cathode surface, the Ir mole fraction on the anode surface, and the potential for operating conditions. For power density, the most critical parameters were catalyst to support surface ratio, Cobalt (Co) mole fraction on anode surface and operating potential.

Another algorithm that has been used to study the influence of the structural components on the performance of fuel cells and electrolyzers is called the extreme gradient boost (XGBoost) algorithm. It is a powerful ML technique that has proven effective in both regression and classification tasks. This model combines the prediction of multiple models for decision making with capacity to handle high dimensional data [199]. For example, Uenishi and Imoto [200] investigated the correlation between the physical properties of PEMFC catalyst layer and generated voltage at low and high current density using XGBoost ML method, and optimized the output with GA. The input features that were used in training and testing the model were extracted from 99 MEAs with varying physical properties from the carbon support, catalyst and catalyst layer. The authors reported that the performance of the output voltage at low current depends largely on the features extracted from SEM cross-sectional image of the CL. These features include total pore volume, pore diameter and surface area of carbon in the CLs. The researchers found that the characteristics (e.g. image contrast representing pore volume) generated from the SEM cross-sectional image are correlated to the diffusion of oxygen in the CL. However, output voltage also depends on the catalyst loading. The authors observed, however, that the pore structure of the catalyst layer can be optimized for improved performance without necessary increasing catalyst loading, lowering the overall cost of production.

Zhang et al. [201] undertook a study utilizing ML, constructing a database comprising 58 MEAs and 16 input features related to the MEA fabrication (catalyst ink drying temperature, catalyst ink water content, ink flow rate when coating, MEA hot-pressing time, cathode compression rate, anode PTL porosity, and MEA configuration) with 11,025 data points. Employing regression tasks coupled with GA, they developed machine learning models to optimize output voltage, utilizing algorithms like ANN, XGBoost, AdaBoost, K-nearest neighbors, Random Forest, SVR, and Elastic Net. Among these algorithms, XGBoost had the highest R^2 value of 0.99926, leading to an optimized output voltage of 1.83107 V and achieving a 67.9% improvement in computation efficiency. XGBoost model is known to be a complex ML algorithm. Complex ML models are prone to overfitting when applied to simple problems and simple ML models are susceptible to underfitting in complex tasks. While simpler ML models like linear regression and ridge regression offer interpretability, complex ML models often function as black boxes, hindering interpretability. To address the lack of model interpretability in this work, the researchers applied the Shapley additive explanations (SHAP) method to rank features in order of their importance, revealing that operating temperature, anode ionomer content, anode catalyst loading, membrane thickness, and MEA hot pressing significantly influence output voltage. This underscores the importance of employing interpretable methodologies to gain insights into feature-output relationships, particularly in the optimization of electrolyzers performance.

SHAP method is an explainable AI method that provides qualitative insight into the interactions that exist between input features and predicted output feature(s). In Ding et al. [202] work, the SHAP method was used to deduce relationships between 21 input MEA parameters and performance (current density) of PEMWE. They explored 9 different ML algorithms to predict and optimize the performance in terms of current density and long-term durability of their fabricated MEAs. Of all the ML methods used, gradient boost regression model in conjunction with GA as an optimization tool was found to perform better with R^2 of 0.943. Even though a higher electrochemical activity results in high current density, based on the interpretable capabilities of SHAP, their results suggested that the catalyst loading for Ir and Pt values for anode and cathode should not exceed 1.5 mg/cm^2 and 0.2 mg/cm^2 respectively. For the I/C ratio, the results suggested that the optimal value should be within 0.2–0.25 to avoid the possibility of proton conduction and oxygen transfer resistances.

Using XGBoost algorithm, Lou et al. [193] investigated the structural and compositional parameters of cathode CL of PEMFC with Pt loading, Pt/C weight ratio, I/C weight ratio, Pt/C agglomerate size, Pt and carbon radii, pore diameters, cathode CL thickness, and surface tension of CL as input parameters. Their study utilizes a 2D, steady state physical model as data source for the XGBoost ML task. Their study showed that out of the 9 input features, the agglomerate radius greatly impacts the power density of PEMFC, having a feature importance greater than 0.4. The XGBoost algorithm was able to accurately predict the relationship between 9 input parameters and output power density parameter, with an MSE greater than 0.95 and RMSE error less than 0.05. Subsequently optimizing the Pt loading with GA, the researchers achieved 28% reduction in Pt loading without a decrease in performance of the PEMFC.

The application of SVM algorithm for predicting and optimizing structural components of fuel cells and electrolyzers cannot be overemphasized. SVM algorithm can be used for both regression and classification tasks. SVM works by finding the best hyperplane, or dividing line, in a high-dimensional space that either separates different classes of data or predicts values with minimal error. Although SVM is known as a complex model, it can give good results even when working with small datasets, thereby finding a good balance between complexity and sample size [203]. For example, Wang et al. [194] explored the support vector machine model to predict the optimal catalyst layer compositions capable of generating maximum power density in PEMFCs. In their work, as shown in Fig. 18, the authors simulated the current density of PEMFCs under different output voltages and catalyst layer compositions, such as the Pt loading, Pt/C and I/C ratios, using a 3D CFD based agglomerate model and subsequently applied GA to determine the optimal catalyst composition for the PEMFC. The data generated from the CFD model was used as an input parameter for the SVM model development, achieving an R^2 accuracy of 0.9908 with approximately 3% as the mean percentage error (MPE). After optimization with GA, it was found that percentage error between the SVM prediction and the 3D CFD simulation of the maximum power densities under the optimal CL

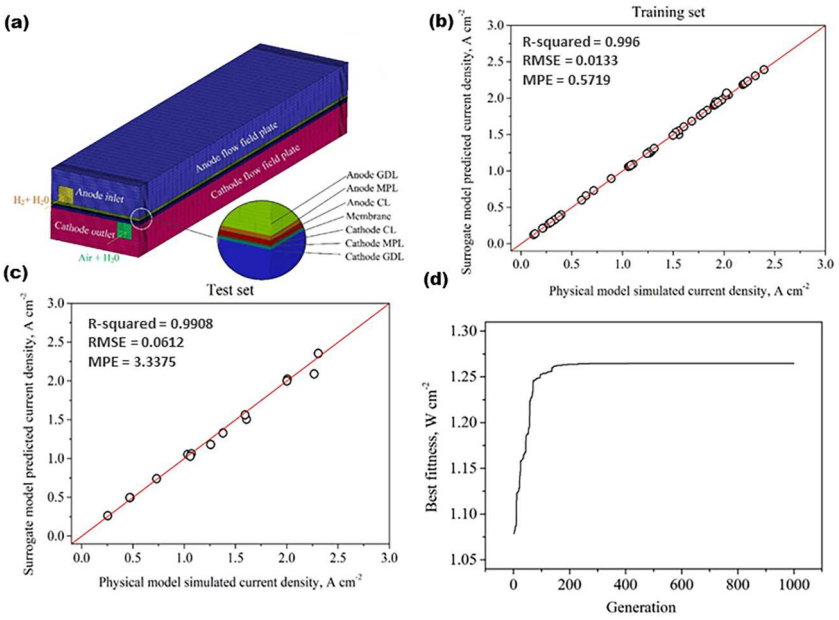

Fig. 18. (a) CFD model design used for PEMFC performance simulation. SVM predicted and simulated current density of (b) training set and (c) test set. (d) Optimization result of the maximum power density by GA. Reprinted with permission, Copyright 2020, Published by Elsevier [194].

composition was only 1.3950 % indicating that SVM could potentially predict and optimize CL composition and structural parameters of PEMFC and by extension to electrolyzers.

Arjmandi et al. [204] studied the parameters that affect the anode side catalyst of a PEMWE using linear regression, decision tree, and SVM. The researchers used two different data named Data1 and Data2 for this study. Data1 consists of current density, water feed rate, catalyst loadings and high frequency resistance of the anode, while Data2 focused on the characteristics of the PTL that includes the average pore diameter, average grain diameter, area surface porosity, average porosity and permeability. The combination of these data was used to make informed decisions on appropriate PTL types based on their characteristics and experimental performances. From their study, they deduced that performance of the linear regression model declines upon the addition of more data points, suggesting the non-flexibility of the model albeit a simple model. Moreover, the SVM exhibited higher accuracy with increasing data points, indicating its ability to handle more complex relationships within the dataset compared to linear regression. For decision tree model, different hyperparameter tuning of maximum depths 1, 2, 3 and 4 for modeling the algorithm were used. The maximum depth corresponds to the level of complexity and intricacy of the decision tree model, with higher depths allowing for more detailed splits in the data to capture finer patterns and relationships. It was found that an accuracy of 100% was achieved with a maximum depth of 4, showcasing the model's capability to capture intricate patterns within the dataset. Additionally, the decision tree model demonstrated robustness against overfitting, as evidenced by consistent performance across different depths during hyperparameter tuning.

Ali et al. [205] also focused on the anode side catalyst in PEMWE, specifically predicting the performance and durability of PEMWE using SVR, SVR-GA and ANN. The influencing parameters such as operating temperature, PTL pore diameters, and catalyst loading of three anode catalysts (Ir-black, IrO2 and Ir0.7 Ru0.3Ox) were derived from experimental studies of existing literatures [206] [207], [208], [209],. For the three catalysts datasets, temperature ranging between 30 and 90 °C and current density were used as the input features, and cell potential as the output feature. Their results indicated that the ANN has the capacity to predict the PEMWE behavior of Ir-black and IrO2 with R2 of 0.999228 and 0.998646 respectively. On the other hand, SVR-GA showed effectiveness in modelling the PEMWE behavior of Ir0.7 Ru0.3Ox when its hyperparameters are tuned. This highlights the importance of fine-tuning model parameters to optimize predictive accuracy when modeling PEMWE behavior. The researchers noted that the performance of ANN on catalyst Ir-black and IrO2 could be attributed to the large sample size of data collected as compared with smaller sample size of data used to model Ir0.7 Ru0.3Ox. This suggests that increasing the size of the dataset could potentially enhance the predictive capabilities of the ANN models for various catalyst materials. However, SVR/SVR-GA models are quite flexible in handling nonlinear relationships and may offer an alternative approach for modeling PEMWE behavior, especially when dealing with smaller datasets.

In concluding this session, the application of ML is a useful approach in predicting the performance and optimizing structural parameters of fuel cell and electrolyzers. Several key takeaways can be concluded: (i) The choice of model depends on the data complexity; (ii) Complex data requires complex models for generalization; (iii) When complex models are used, interpretability of the model is important and can be achieved with sensitivity analysis such as Pearson correlation. Other interpretability methods include SHAP and PDP.

3.2. Application of ML algorithms in image segmentation for analysis of fuel cells and electrolyzers

Structural analysis of the materials and different layers in the PEM FCs, WEs (e.g. catalysts, CL, GDL, PTL, etc.), and solid oxide fuel cells (SOFCs) are of crucial importance in understanding their effect on performance and durability. While significant attention has been given to PEMFCs and PEMWEs in previous sessions, it is noteworthy to emphasize the importance of SOFCs in this session. Like PEMFCs and PEMWEs, SOFC is composed of complex porous anode and cathode electrode structure which determines its electrochemical performance. The anode, cathode and electrolyte structures often made of ceramic-metal composite, mixed oxides and stabilized zirconia respectfully require optimal design for a highly efficient performance especially when operated at elevated temperatures (600–1000 °C) [210]. Over the years, researchers have relied on the use of manual approach to extract information from microstructure of these electrochemical devices. Usually, this process is laborious, time-consuming, and prone to human inconsistency. The application of DL, a subset of ML that applies algorithms which mimic the structure and function of the human brain to learn and make

predictions based on data supplied, can be used to automate this process. The success of DL in image processing could be attributed to its ability to identify, learn, and extract complex features from images using CNN, DNN, and RNN [211]. A DL approach that helps to analyze, understand, and recognize patterns in images is known as computer vision [212]. In fuel cells and electrolyzers, DL has been applied to identify and segment microstructural images captured from transmission electron microscope (TEM), focused ion beam-scanning electron microscopy (FIB-SEM) and X-ray computed tomography (XCT) images. This section will discuss various applications of deep learning for image segmentation of fuel cells and electrolyzers.

Phase segmentation. Phase segmentation is the process of dividing an image into distinct regions of similar morphological properties. Traditional methods such as Watershed and Weka segmentation methods have been used to extract valuable information from materials microstructure [213]. As stated earlier, DL algorithms are suitable to achieve phase segmentation of components of fuel cells and electrolyzers. For example, Liu et al. [192] demonstrated the application of Deeplab DL architecture to distinctly segment FIB images containing pore and carbon black phases in the CL of PEMFC. The Deeplab architecture works by extracting dense features of an image and uses characteristics of the image to improve segmentation accuracy. Subsequently, they applied a deep convolutional generative adversarial network (DCGAN) DL algorithm to generate artificial 2D microstructures from the originally segmented 600 images and reconstruct them into 3D form as shown in Fig. 19. The DCGAN algorithm comprises of the generator and discriminator models. It works by generating artificial images during training process and subsequently deceives the discriminator model that the image generated is real while making the discriminator model get better at classifying artificial and real images. From 3D reconstructed images, the researchers found that the porosity significantly affects the diffusion of oxygen within the CL and that applying spherical linear interpolation of DCGAN, better 3D images were produced with good diffusion coefficients as compared to linear interpolation.

In another study, Hwang et al. [214], applied Deeplabv3+ DL algorithm in combination with stereological analytical approach to semantically segment and quantify a 3-phase microstructure consisting of Gd2O3-doped CeO2 (GDC), La0.6Sr0.4CoO3-δ (LSC) and pores in a cathode composite material of a SOFC. Deeplabv3+ algorithm is an algorithm built on the Deeplab architecture that utilizes CNN in conjunction with atrous spatial pyramid pooling to classify each pixel of an image into a category and distinctly segment objects within the image while the stereological analysis allows for the quantification of volume, shape and surface area of complex 2D images without necessarily undergoing 3D reconstruction. In their work, they quantified the area of catalyst agglomerates occupied, compared to the total area, mean intercept length, and interconnectivity of the 3 phases. A total of 49 FIB-SEM images were explored for this segmentation study with 40 of the images trained as the ground truth and 9 images used for testing. Although the dataset was small for a deep learning task, the authors accurately segmented the 3-phase microstructure with the blue area as GDC, green as LSC and red as the pores shown in Fig. 20b and c. Comparing their prediction with the ground truth obtained from image processing, they achieved a high mean Intersection over Union (mIoU) accuracy of 0.7 suggesting the potential applications of this algorithm to automatically segment different microstructural composition of a 2D image and more importantly its application in fuel cells and electrolyzers.

The authors went further to explore the utilization of the same Deeplabv3+ algorithm to segment the microstructural components of Ni/Y_2O_3-stabilized ZrO_2 (Ni/YSZ) anodes of a SOFC using 120 image datasets from FIB-SEM. The segmentation of these phases assisted in quantifying the intercept lengths, volume fractions, and interconnectivity of constituent phases. In their result, they achieved an mIoU accuracy of 0.87, an accuracy scores greater than their previous study. This better performance could be attributed to 120 images used in this study as compared to their previous work as this provides the algorithm to opportunity to learn on a large and diverse dataset. Further validation of their segmentation with pixel-based matching method, a

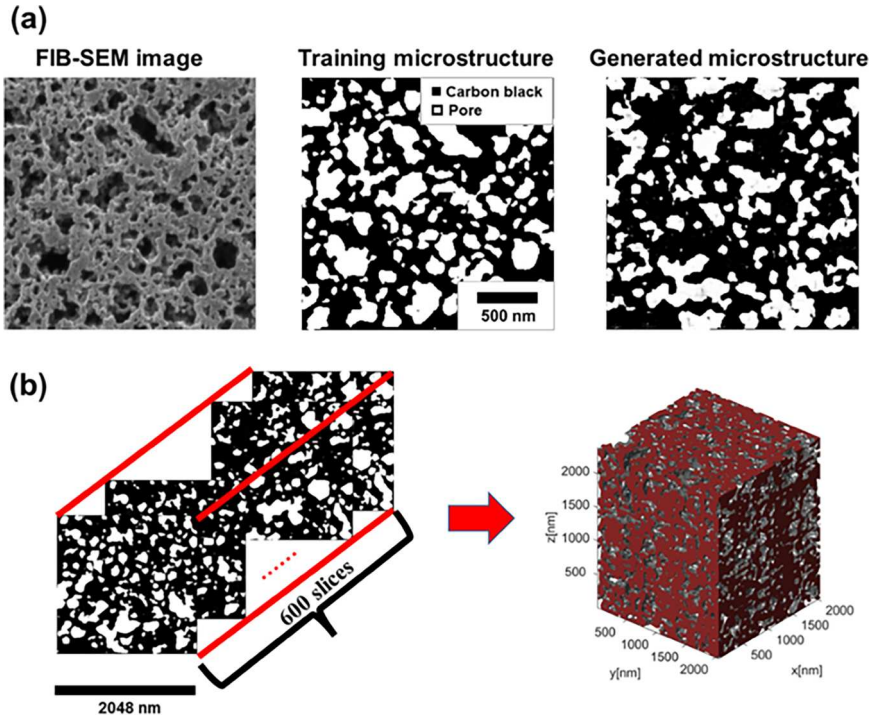

Fig. 19. (a) 2D FIB-SEM image (left), segmented image with Deeplab (middle) and generated microstructure by DCGAN (right) wherein the black phases represent carbon black and the white indicate pores; (b) 3D reconstruction from 2D continuous sectional slice images. Reprinted with permission, Copyright 2022, Published by Elsevier [192].

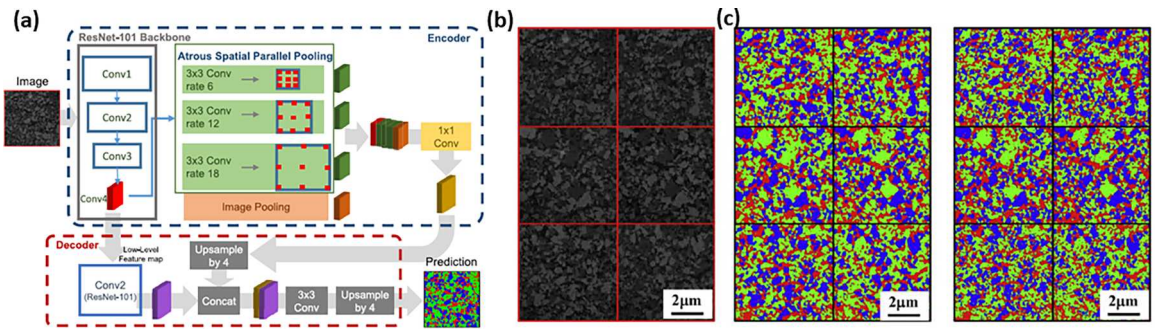

Fig. 20. (a) DL-assisted flow process for semantic segmentation of solid oxide fuel cells (b) Test images for validating the deep learning method and, (c) Obtained deep learning images (left) and ground truth obtained from image processing (right). Blue areas are GDC, green areas are LSC, and red areas are pores. Reprinted with permission, Copyright 2020, Published by Elsevier [214].

process that quantifies the degree of accuracy between the predicted segmented images and ground truth, yielded accuracies ranging between 0.919 to 0.957. The authors noted that factors such as undesired artifacts, unavoidable curtain effects, charging effects, and unclear interphase boundaries from FIB-SEM could negatively impact the prediction performance of the algorithm. This implies that if the ground truths (training images) are not well prepared, incorrect identification and classification of microstructural phases is bound to occur [215].

Another DL algorithm that has been widely used for semantic segmentation tasks is UNet architecture. The UNet architecture is a type of CNN that was initially designed for segmentation of biomedical images but has now gained prominence in segmentation of microstructural components of metals, rock, fuel cells, and electrolyzers. The architecture consists of a downsampling and upsampling path as shown in Fig. 21. The downsampling path reduces spatial dimensions of the images captured but increases the depth of the feature maps. On the other hand, the upsampling path ensures the recovery of the reduced spatial dimensions of image by increasing the resolution of features maps to enable precise localization, which implies accurate segmentation.

For instance, Rena et al. [217] applied the conventional encoder-decoder and UNet algorithms to segment Ni and YSZ phases in SOFCs from low resolution laser microscope images capture in an operando situation. With these algorithms, they calculated the phase fractions and triple phase boundary (TPB) of the phases. In their work, it was observed that the two algorithms were able to segment these phases. However, tiny microstructural details of each phase were lost due to the low resolution of the laser microscope as seen Fig. 22. To improve the resolution, pix2pix GAN architecture was explored to convert low resolution laser microscope images to an SEM-like images with high resolution. It was deduced that the segmentation of low-resolution images can be attained through the utilization of UNet architecture, yielding outcomes that closely approximate the ground truth. However, for a more accurate prediction and analysis of the phases, it was necessary to enhance the image resolution using the pix2pix GAN DL algorithm, with the performances of the conventional encoder-decoder, UNet, and pix2pix architectures as 0.867, 0.889, and 0.897 respectively.

It is widely known that the performance of fuel cells and electrolyzers rely strongly on the microstructural properties of GDLs and PTLs respectively. These properties include pore size, tortuosity, GDL thickness, fiber diameter, porosity, etc. [218]. Previous studies have shown that the increased porosity of GDLs and PTLs results in better performance of these electrochemical devices [219,220]. The ability to quantitively measure these physical properties can give insight to the mass transport properties or diffusion behavior as the reactant species (hydrogen and oxygen) pass through the GDL/PTL to the catalyst layers. Mehdi et al. [221] investigated the fluid flow mechanism that occurs in a GDL having varying percentages (5, 20, 40, and 60 wt%) of coated hydrophobic polytetrafluoroethylene (PTFE). In order to study these mechanisms, they utilized 2D and 3D UNet DL algorithms to segment the water, air, and PTFE coated fiber phases of the GDL component from X-ray computed tomography (XCT) images. The outcomes obtained from the DL algorithms were compared to the traditional Watershed and

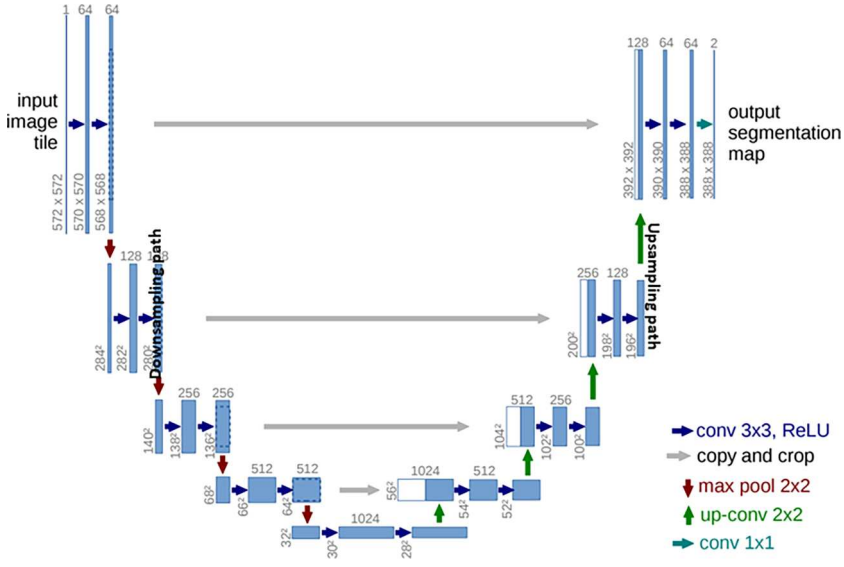

Fig. 21. Representation of a UNet architecture. Reprinted with permission, Copyright 2021, Published by Elsevier [216].

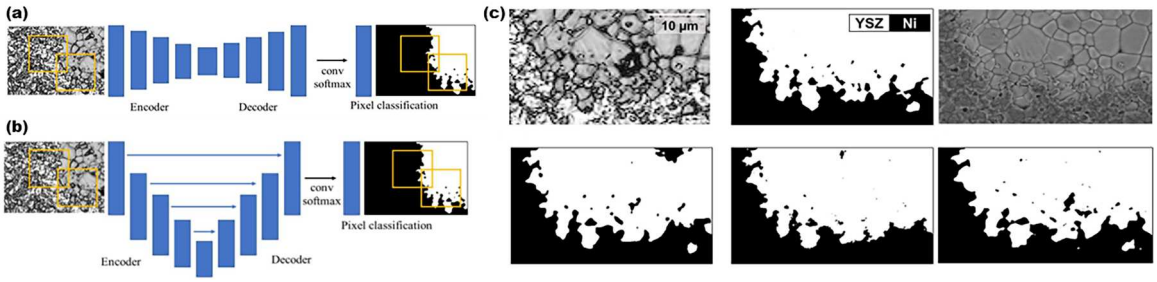

Fig. 22. (a) Conventional encoder-decoder network (b) U-net with encoder-decoder network (c) Low resolution laser image (top-left), ground truth segmented image (top-middle), segmented images with conventional encoder-decoder network (bottom-left) and segmented images with UNet with encoder-decoder (bottom-middle), high resolution SEM image (top-right), pix2pix GAN output (bottom-right). Reprinted with permission, Copyright 2021, Published by IOP Publishing [217].

Weka segmentation process, which is commonly employed for phase segmentation. The results indicated that both DL algorithms effectively classified the three phases, with the 3D UNet algorithm demonstrating superior performance compared to the 2D UNet, Watershed and Weka segmentation methods. This distinction can be observed in Fig. 23c, which visually represents the discrepancies captured by each segmentation process. The 3D model's performance is reflected in higher Intersection over Union (IoU) values and F1-scores when compared to the 2D model, indicating a more precise segmentation of the different phases within the GDLs. While UNet algorithm has the capability to capture intricate information from XCT images, it has been found that the performance of U-Net model degrades when the network is too deep [222].

In order to mitigate this challenge, the U-ResNet model that combines the long skip feature connection of the U-Net architecture and the short residual bock of the RestNet architecture that preserve shallow domain information in images has been developed for efficient segmentation of materials which offers better performance than each of the standalone models. For instance, Tang et al. [223] classified specific features such as carbon fibers, void, MPL, CL, membrane, and binder phases of a PEMFC GDL using grayscale, manual and U-ResNet segmentation methods. 19 XCT high quality slices cropped of 128 by 128 pixels were used for the study. The training data used 70% of the data (slices) and the rest were used for assessing the performance of the model. In their study, the U-ResNet architecture could detect and classify different phases of the GDL structure. However, the grayscale method inaccurately classified the phases due to differences in pixel intensity while the manual segmentation method over-segmented the GDL due to the variation in contrast of MPL, CL and membrane layers as a function of material density (see Fig. 24).

The advantage of the U-RestNet model is its ability to segment interfaces bordering the fuel cell MPL, CL and membrane layers, which is an enormous task with manual segmentation. This could be attributed to the additional residual connections which help in addressing the vanishing gradient problem, allowing for the training of deeper networks by enabling the flow of gradients through the network more effectively. As previously discussed, improving the resolution of images captured from XCT, SEM, TEM, and other microscopy techniques enhances the accurate segmentation of phases. With low resolution images, critical components of a MPL and GDL will be inaccurately segmented leading to inaccurate physical representation of phases. Wang et al. [224] employed the dual enhanced deep super-resolution (DualEDSR) DL algorithm to improve the resolution of their XCT images (see Fig. 25b) and then subsequently apply the U-ResNet DL architecture to segment voids, fibers with different orientation (parallel or perpendicular), CL, MPL and membrane as seen in Fig. 25c. This high segmentation accuracy,

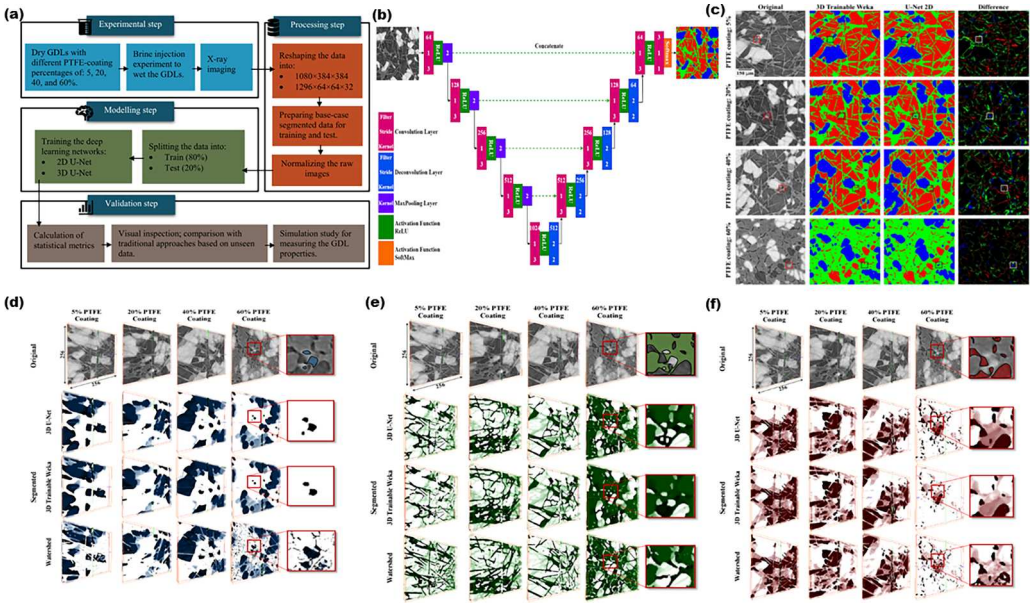

Fig. 23. (a) Process flow for DL development (b) 2D UNet architecture (c) Comparison between trainable Weka and the U-Net 2D network performance with blue, red, and green colours representing water, air, and fibre phases respectively. Color back in column four depicts zero differences. Comparison between U-Net 3D network, trainable Weka, and watershed segmentation for identification of (d) water (e) fibres and (f) air in the GDL images. Reprinted with permission, Copyright 2023, Published by Elsevier [221].

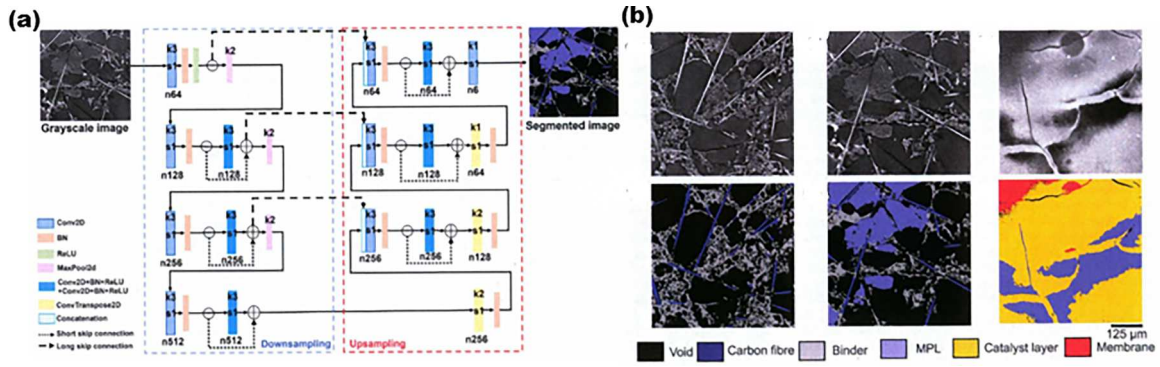

Fig. 24. (a) U-ResNet architecture (b) manual grey scale image segmentation (top-left to top-right) and U-ResNet image segmentation (bottom-left to bottom-right). Reprinted with permission, Copyright 2022, Published by Elsevier [223].

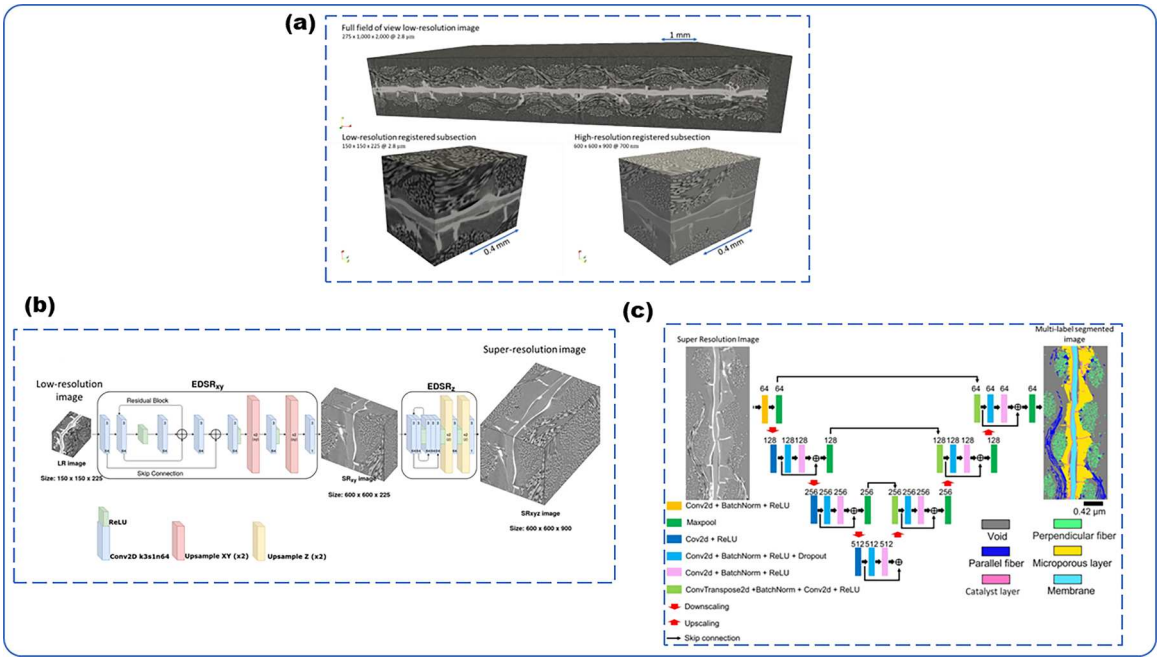

Fig. 25. PEMFC images acquired from a micro-CT (a) full field low-resolution image @ 2.8 µm (top), subsection of low resolution (bottom-left), subsection of high resolution from DualEDSR algorithm (botto-right), (b) process flow of DualEDSR algorithm and (c) U-ResNet architecture with parallel fiber, perpendicular fiber, void, microporous layer, catalyst layer, and membrane segmented as blue, green, grey, yellow, pick and pale blue colors respectively. Reprinted with permission, Copyright 2023, Published by Springer Nature [224].

quantified at 93% for most phases and 86% for the membrane, was crucial for the subsequent heterogeneity analysis and flow simulation.

In their subsequent study, they classified CL ink images using two different CNN architectures. The first CNN architecture was built from scratch as a custom network while mini-VGG, a pre-trained model was explored as the second CNN architecture for their study. The first CNN architecture was observed to be shallow and could only achieve a low validation score of 0.25. The low validation suggested the simplicity of the model as it was built having limited convolution layers. In order to improve on this accuracy, min-VGG architecture was explored to extract features from the images, which were then used to train a logistic regression model for classification task and thereby achieving an accuracy of approximately 0.98.

Particle segmentation. The accurate quantification of the catalyst particle sizes in fuel cells and electrolyzers is crucial in understanding the catalytic activity and stability of a CL which impacts the efficiency of the system. For instance, Colliard-Granero et al. [225] applied DL to segment, identify, and automate the particle size distribution of the Pt catalyst nanoparticles within the CL of PEMFCs. They employed U-Net architecture combined with StarDist, an algorithm that identifies densely packed and overlapped objects for the particle segmentation process. The DL pipeline involves the annotation of TEM images of the CL containing Pt nanoparticles, segmentation of the TEM images into different phases, diameter measurement of segmented particles and statistical visualization of particulate distribution within the catalyst layers. 40 images with varying diameters (10 nm, 20 nm, 50 nm and 100 nm) were employed in the training process to achieve robust model development. Their method yielded a high accuracy of 86% compared to manual measurements, with the ability to classify, detect and automatically measure the particle size distribution of Pt particles (see Fig. 26). Saaim et al. [226] compared the performance of U-Net, with R2U-Net, Attention U-Net, BDC U-Net, U-Net++, U-Net 3+, Attention W-Net, and K-means clustering models to determine Pt particle sizes of a PEMFC using 150 bright field TEM images containing approximately 3629 Pt particles. They found that U-Net, R2U-Net, and U-Net++ demonstrated similar performance, while BDC U-Net showed reduced effectiveness, particularly in handling larger nanoparticles due to its Bi-ConvLSTM layer. Attention U-Net, despite its design to enhance

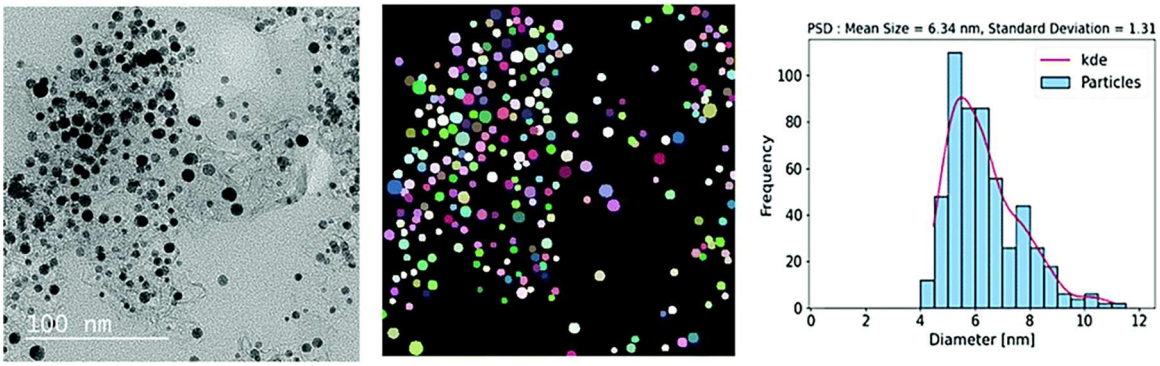

Fig. 26. DL assisted Pt particles segmentation and particle size distribution analysis in TEM images of the catalyst layers in PEMFCs. Left: raw TEM image; Middle: Annotated image using DL; Right: Particle size distribution results. Reprinted with permission, Copyright 2022, Published by RSC Publishing [225].

feature mixing, fell short of U-Net's results. In unsupervised segmentation, Attention W-Net underperformed, missing many nanoparticles, whereas K-means clustering was generally more reliable. U-Net 3+ outperformed all other methods, including traditional algorithms and earlier U-Net variations, in terms of IoU, showcasing its superior architecture for segmenting bright field TEM Pt nanoparticles. Table 1 shows the summary of all the accuracies of models explored in their study.

Another application of DL for phase segmentation is the screening of catalyst layer inks for PEMFC. Eslamibidgoli et al. [227] were the first to use a DL architecture called ConVNets to automatically segment and quantify the agglomerate size distribution in catalyst inks. The inks used for their study were based on commercial Tanaka EA50, F50, and V50 catalysts with Nafion and Aquivion supports. These inks were imaged with high resolution TEM and were used for training the ConVNets model. Their first task was to annotate the imaged inks, and subsequently apply region-based object detection algorithm that could effectively identify regions of the inks and enhance detection accuracy. With the ConVNets architecture, features such as edges and other spatial details were extracted from the images and fed into the convolution as input parameters. A transfer learning approach using pre-trained model was then implemented to fine-tune the ConVNets specifically for detecting the unique characteristics of the catalyst inks, resulting in a significant improvement in detection performance. Gradient-weighted Class Activation Mapping (Grad-CAM) was then to visualize segmented regions containing ink agglomerates. Based on the findings, the ConVNets succesful segmented the catalyst ink having a F1-score of not less than 99% for all the inks. They also observed that the V50 has the largest agglomerates followed by the EA50 and F50.

Image-based defect detection of fuel cells and electrolyzers with DL. In energy devices, the life cycle prediction needs to be evaluated to avoid failure in service [228]. In fuel cells and electrolyzers, failure arises from the inability of the system to adjust to electrical, temperature and gas-delivering -time variation during operation. The inability for fuel cell system to adjust under these conditions can lead to thermal shock, the overrun of system temperature, or insufficient supply of fuel [229, 230]. As a result, the need to predict the state of health of a fuel cell system using various ML algorithms is paramount to avoiding a catastrophic failure [231]. ML models have also aided the diagnosis of internal defects such as cracks, pin holes, and catalyst contamination. It has also been explored for the diagnosis of external defects which includes failure of heating units, fuel, and air supply [232]. Defects are characterized as a form of imperfections and abysmal pattern observed in the CL or any part of a fuel cell/electrolyzers that can potentially reduce the overall efficiency of the system. They can occur in interfaces of materials used for electrode fabrication leading to cracks, agglomerates, scratches, debris, scuffs, and delaminated surface [233–235], defects in structural components [236], and pin holes in membranes [237]. Several approaches have been used to detect and evaluate forms of defects that exist in fuel cells and electrolyzers. One of the main traditional methods that have been used to detect defects in these systems is the application of infrared thermography [238–242]. Infrared thermography is a non-destructive technique approach for quality assurance or in-line inspection of fabricated products in most industries. In fuel cells and electrolyzers industry, it is used to detect anomalies by applying a wide range of electromagnetic rays ranging from visible light to microwave (750 nm – 1 mm) on a material. Irregularities that cannot be visually observed on material surfaces are scanned with the infrared camera and documented. Other diagnostic methods explored in defect detections of electrode materials in fuel cells and electrolyzers include optical inspection, X-ray, and microscopy techniques. The optical techniques include the use of optical cameras for visual defect detection, X-ray fluorescence for catalyst loading and chemical compositions measurements, while the microscopy techniques include the use of SEM to visualize defects on film surfaces [243]. While these traditional methods are good in detecting defects, they are compounded with the limitation to acquire defects at a faster rate, ability to detect defects during in-service roll to roll process, and the ability to cover large surface area of materials. The use of object detection, also known as computer vision, is a DL technique that helps identify localized information in objects and videos. It goes beyond simple object classification and helps provide a better understanding of the object in question. With object detection, the images are first classified into different classes called labels using image annotation tools and subsequently subjected to training using DL algorithms. It is imperative to state that the adoption of object detection in defect detection is promising and more importantly, it is a cost effective, and reliable technique [244].

Lu et al. [245] applied the use of computer vision in defect recognition of ceramic chips used in high temperature solid oxide fuel cells. Generally, object detection requires copious amounts of data for training. Since there was limited amount of data of ceramic chips containing defects, the researchers developed a system to physically acquire these images containing defects (as shown in Fig. 27) for training and

Table 1
Summary of models with 45 testing images [226].

Model	Accuracy	Precision	Recall	TPR	IoU	Dice coefficient
U-Net	99.26	96.65	96.22	93.11	92.96	96.43
R2U-Net	99.27	96.42	96.56	93.20	92.92	96.48
Attention U-Net	99.16	97.41	94.47	92.14	91.95	95.91
BDC U-Net	99.00	96.79	93.71	90.84	90.96	95.18
UNet++	99.24	97.65	94.94	92.82	92.86	96.27
UNet 3+	99.42	97.30	97.09	94.54	94.45	97.19
Attention W-Net	95.19	97.68	59.31	58.38	58.38	72.99
K-means clustering	96.95	87.42	82.65	73.87	80.66	84.97

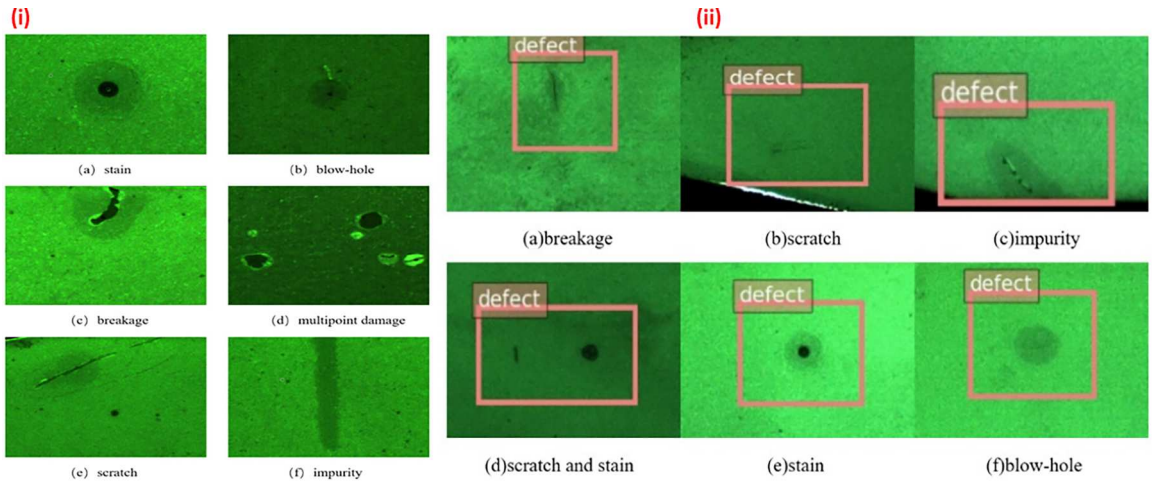

Fig. 27. (i) Various surface defects of acquired ceramic chips (ii) detected defects. Reprinted with permission, Copyright 2022, IEEE [245].

test purposes. Firstly, features from these ceramic chips were extracted using feature extraction networks such as VGG-16, VGG-16+ FPN, ResNet-50, ResNet-101. These networks are known for their ability to extract high-level semantic information from small objects. Images extracted from these networks were used as training data for the SSD, YOLOv5, Faster R-CNN and improved Faster R-CNN DL models. In their study, an optimized version of the Faster R-CNN (improved Faster R-CNN) model based on the VGG-16 feature extraction had better performance of 89.39% than other models used in detecting breakage, scratch, impurity, stains, and blow hole. The performance of the improved Faster R-CNN was ascribed to the enhancement of the algorithm through region of interest (ROI) pooling and, feature pyramid networks (FPN). The utilization of ROI pooling presents the opportunity to achieve accurate localization of objects across a wide range of image scales. In addition, FPN detects objects of different sizes more accurately by creating pyramids of feature maps. The selection of algorithms for computer vision applications depends upon two competing factors. These factors include the computational time and the pursuit of achieving a high of model accuracy. For instance, when opting for algorithms with the objective of achieving high accuracy, Faster R-CNN and SDD present themselves as a great choice. On the other hand, YOLO is excellent for achieving faster computational speed.

Yan et al. [246] investigated two DL techniques in identifying in-line defect in PEMFC catalyst coated membrane (CCM) layers. The two algorithms explored in this research are patch distribution modelling (PaDiM) and Faster R-CNN DL algorithms, which focused on defects such as scratches, scuffs, and pinholes. Faster RCNN and PaDiM are supervised and unsupervised algorithms respectively that are used for object detection and with capabilities of achieving high accuracy. In their research optical images were used for labeling of defects while model performances were evaluated using the leave-one-out cross--validation (LOOCV). For PaDiM, the model performs better in identifying pin holes than scratches and scuffs with more possibility of detecting contaminations. However, Faster R-CNN could not detect faint defects as PaDiM does. However, it classified defects into different types. In the electrolyzers industry, the application of object detection in detecting faults has not been explored to its full potential. Based on literature search, the first research group that explored this technique for identifying faults in electrolyzers is Zhu et al's group [242]. They applied the use of Mask R-CNN with ResNet-50 backbone network to investigate the detection of faults on infrared captured electrolyzers plates. A total of 2000 infrared images were used for the analysis of which 1280, 320 and 400 datasets were used for training, validation and testing, respectively. Three variations of Mask R-CNN were adopted for the study which includes original Mask R-CNN, original Mask R-CNN with bounding box (Mask R-CNN + G2-IoU) and improved Mask RCNN. The improved Mask RCNN had a better performance than the other Mask RCNN algorithms with precision of 86.8% (10% higher than the original Mask RCNN). The researchers demonstrated that the reason for the better performance is attributed to the introduction of a globally generalized intersection over union (G2-IoU) loss function. The G2-IoU loss function improves object detection by accurately characterizing the position and scale relationship between the predicted bounding box and the target bounding box. It considers the coincidence rate, distance, and scale relationship between the two boxes, leading to better detection accuracy.

3.3. Application of ML algorithms in degradation studies

Widespread commercialization of electrochemical devices such as fuel cells and electrolyzers are limited by their durability issues which require extensive analysis of aging and degradation mechanisms now possible through ML models [247]. With recurrent neural network (RNN) machine learning algorithm, we can predict the performance evolution also referred to as the remaining use life (RUL) and voltage degradation of these devices based on the operating time and system conditions without any dependence on complex modelling from physical laws and electrochemical equations [248–250]. A RNN is a form of artificial neural network that processes input data recurrently and allows output from one step to be fed back as input to the network at the next time step thereby capturing dynamic relationships between input and output data [251]. In a simpler term, it means that the input features fed into system A produces output features and the output features from system A now serves as an input feature into system B with the goal of capturing dynamic relationships between the sequential input features and final output. An example of RNN is echo state network (ESN), a reservoir computing neural network known for its unique architecture that randomly generate a reservoir with static internal weights and replaces the hidden layer found in traditional neural networks, making it computational cost-effective for degradation prediction as shown in Fig. 28. The advantage of ESN is that the output layer of the network is optimized by multiple linear regression [252].

A study by Vichard et al. [254] involved executing a 5000-hour durability test on a PEMFC system to understand the performance evolution, concluding that lower ambient temperature leads to better humidification, ultimately resulting in lower voltage degradation rates. While this PEMFC application was designed as a postal delivery vehicle, the operation of fuel cells under ambient temperature is beneficial for aerospace application [255]. In their study, the researchers segmented the operating time for the durability test into 6 stages at different operating time and temperatures for each stage. The operating ambient temperatures for stages 1–6 are 20 °C, 30 °C, 20 °C, 7 °C, 20 °C and 10 °C

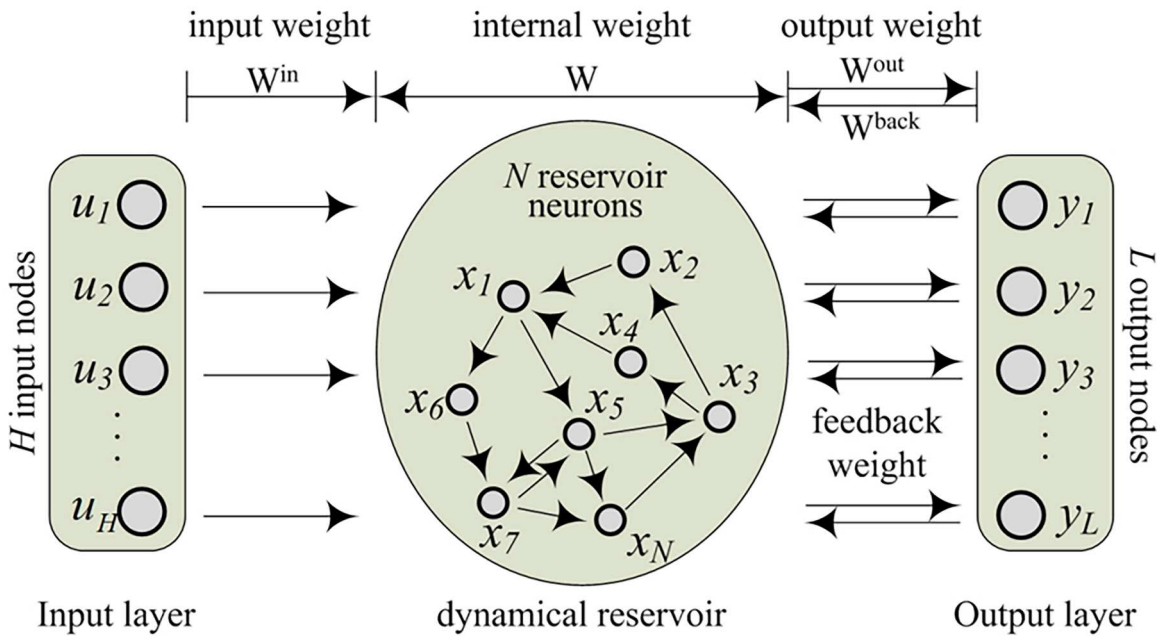

Fig. 28. The architecture of standard Echo State Network (ESN). Reprinted with permission, Copyright 2015, Published by MDPI [253].

respectively. For stage 1, the input parameter for the ESN network was operating time and ambient temperature while the output parameter was the initial degraded output voltage. Based on the working principles of ESN model and its capabilities to predict non-linear relationships, the output parameter of the initial step will serve as an input parameter for other steps. In this case, the model has three input parameters that are the output voltage of the previous step combined with the operating time and ambient temperature current step serves as an input parameter for subsequent steps. This data was then used as training in an ESN model for output voltage degradation prediction. The study reported that the developed degradation model showed promising results with a low normalized RMSE value of 0.098 and computing time of 2 s. The authors also addressed the significance of learning rate as a hyper-parameter tuning in ESN for the prediction of voltage degradation. They observed that the application of 33% and 60% learning rates resulted in the prediction of the end of life of the PEMFC system to be about 3000 h and 6000 h respectively. Morando et al. [256] developed an ageing algorithm based on the combination of signal filtering and prognostic analysis using ESN algorithm to predict the voltage degradation of PEMFC. Firstly, the authors conducted an experiment to evaluate the mean cell voltage of a PEMFC based on current density (constant load), absolute pressure of air and H_2, operating temperature and cathode and anode relative humidity parameters over a period of 1700 h. The output signal (mean cell voltage) from these experiments was then filtered with wavelet transform and preprocess with Hurst coefficient to ensure temporal dependencies (relationship between data points) before used as an input parameter into the ESN algorithm to forecast what the output voltage of PEMFC will be at a given period. In their study, they achieved good accuracy with a mean average percentage error (MAPE of less than 5% and also showing that the first 340 h of the data acquired under constant load is sufficient to predict the degradation of fuel cells (remaining use life) for at least 1000 h (6 weeks). Mezzi et al. [257] proposed multi-reservoir ESN (MR-ESN) and classical ESN algorithm to predict the cell voltage degradation of 5-cell PEMFC stack based on temperature, stoichiometry and relative humidity operated continuously over a duration of 1700 h under constant load condition. While the MAPE accuracy errors for both algorithms were less than 10%, the MR-ESN performed better than the classical ESN as its prediction matches closely with the real RUL. A study by Zhang et al. [258] improved on the MR-ESN architecture by incorporating a mini-reservoir into main MR-ESN architecture to enhance the network's ability to process and predict degradation of 5-single cell PEMFC stack based having an active surface area of 100 cm^2 and power density of 0.7 A/cm^2 under static and dynamic test conditions. Their study sought to also understand how the length of training set affects the accuracy prediction made by MR-ESN using the first 350 h, 450 h, 550 h, and 650 h of data respectively for training, and tested the model's predictions against the remaining data within the first 1000 h. In order to improve the quality of data fed into the neural network, Savitzky-Golay (SG) filter was used for data preprocessing. The pre-processing step using the Savitzky-Golay filter helped to smooth out noise and artifacts in the raw data, ensuring a cleaner input for the algorithm to work effectively on predicting performance degradation accurately. Furthermore, the effect of main reservoir and main reservoir neurons were evaluated and optimized using particle swarm optimization algorithm (PSO). Their findings showed that the shorter training set of 350 h had the highest prediction accuracy for the static test condition. In addition, the optimal main reservoir and main reservoir neurons achieved by PSO was 20,550 and 10,800 for static and dynamic test conditions respectively. Compared to other forms of recurrent neural networks such as Long Short-Term Memory (LSTM) and Bidirectional Long Short-Term Memory (Bi-LSTM) used for this study, MRM performed better for both test conditions.

Another algorithm that has gained wide prominence in investigating the degradation of fuel cells and electrolyzers is LSTM. The LSTM model, a form of RNN, was developed in Hochreiter and Schmidhuber in 1997 [259]. The model captures patterns and relationships in a time series sequential data. It is designed to address the problem of vanishing gradient associated with traditional RNN by introducing complex gates (input, forget, and output gates) to regulate information flow thereby maintaining long term dependencies in data processed. For instance, Liu et al. [260] developed an LSTM framework to predict the durability of a vehicle PEMFC based on 1155 h experimental data (see Fig. 29a and b). In designing their framework, they utilized regular interval sampling and locally weighted scatterplot smoothing (LOESS) for data reconstruction and data smoothing in order to preserve the integrity of the original data. Their study demonstrates the capability of this algorithm to forecast the RUL of PEMFC having achieved a high accuracy of 99.23% as compared to the traditional back propagation neural network (BPNN) of 70.77% accuracy. Furthermore, the LSTM model predicted

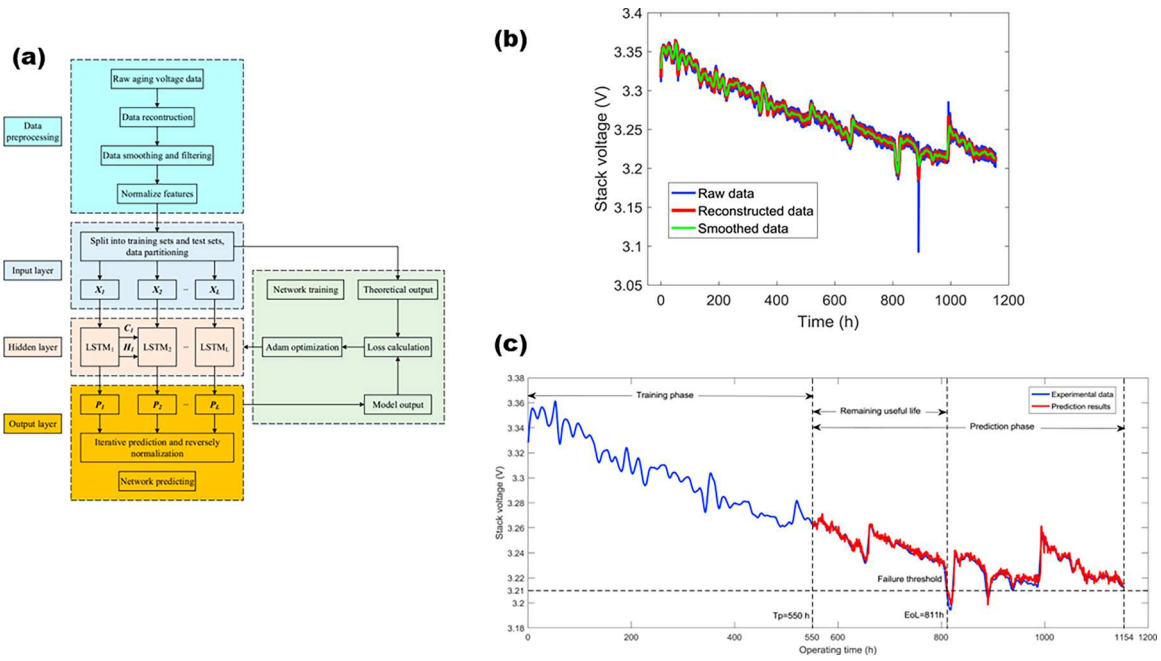

Fig. 29. (a) RUL prognostic framework based on LSTM RNN (b) Degradation data of PEMFC stack (c) Prognostic results of LSTM RNN. Reprinted with permission, Copyright 2019, Published by Elsevier [260].

the RUL of the PEMFC stack to be 260 h which was close to the actual end of life estimated as 261 h using 511 h as the testing starting point.

Xu et al. [261] applied CNN-LSTM algorithm to predict the voltage degradation of PEM WE from data carried out experimentally under constant and start-stop load operating conditions (current densities). The constant load condition was operated for 1140 hr (900 h for training and 240 h for testing) while the start-stop-stop load condition was conducted for 660 hr (528 h for training and 132 h for testing) to evaluate the algorithm's performance. From the experimental study, the output voltage was recorded every minute and 1.5 min for constant and start-stop load conditions. The measured output voltages from these two experimental conditions are now used as input parameters for the CNN-LSTM algorithm. The CNN-LSTM combines CNN and LSTM algorithms. In this case, CNN extracts input feature (measured output voltages at intervals) from the raw data, while the LSTM processes the sequential information to predict the performance degradation of the PEM water electrolyzers accurately over time. Before the application of these combined algorithms, the raw data was pre-processed using the Savitzky-Golay filter method. From their findings, the authors observed an initial decline followed by an increase in output voltage over the operating time both load condition which is consistent with the behaviour exhibited from the experimental study carried out. The authors attributed this behavior to IrO2 exhibiting an initial redox cycle which increases its active surface area and improves performance. Their findings revealed that the CNN-LSTM achieved an average absolute error of 0.39 mV and 2.1 $\times$ 10^{-2} mV for constant and start-stop load conditions respectively. Furthermore, the researchers compared the performance of the algorithm with traditional LSTM models and GRU, showing that the CNN-LSTM outperformed these models in terms of prediction accuracy and generalization capability across different load conditions.

Wang et al. [262], proposed a bi-directional long short-term memory recurrent neural network couple with an attention mechanism (BILSTM-AT) model to predict the voltage degradation of the PEMFC stack under static and dynamic load conditions. Out of 24 input parameters measured experimentally, random forest was used to rank important features that significantly contribute to the voltage degradation of the PEMFC system. These important features include ageing time, 5-cell voltages, outlet temperature of H_2 gas, inlet and outlet temperatures of air, outlet temperatures of cooling water, outlet flow rate of H_2 and Inlet flow rate of air. The output voltage profile is then used to predict the voltage degradation based on the operating time. The authors observed that the RUL of the PEMFC with dynamic test condition was less than that of static test conditions. With respect to the performance of the model, the BILSTM-AT outperforms other models with relative errors for both testing conditions ranging between 0.09% to 0.29%.

Other forms of ML algorithms that have been reported in the investigation of degradation studies of fuel cells include support vector machine (SVM), relevance machine vector (RVM) [263,264], and least square support vector machine (LS-SVM) [265]. RVM is a Bayesian approach to machine learning that offers the ability to produce sparse models, which means it relies on fewer data points (relevance vectors) without compromising the prediction accuracy. It has shown superior performance in predicting the RUL of lithium-ion batteries [266,267], demonstrating its effectiveness in online battery prognostics and practical applications.

Integration of ML algorithms can also help to handle complex, nonlinear patterns found in these energy systems. Lee et al. [268] applied a data driven approach as a prognostic and health management system for voltage predictions of alkaline water electrolyzers (AEM) using SVM and GPR. In their work, an in-house experiment was conducted for 480 h at an operating temperature of 80 °C and flow rate of 330 ccm. The researchers monitored measured parameters such as time, current, and power density as input parameters and measured voltage as output performance. After the analysis of the measured parameters using SVM and GPR, they achieved a performance of 1.28 $\times$ 10^{-3} and 8.03 $\times$ 10^{-6} respectively. While the algorithm performed excellently well based on the input data, they observed that an introduction of an input data with large deviation from the original data could result in an inaccurate prediction. To address this limitation, it is expedient that researchers implement these algorithms on wide range of input parameters that can predict voltage degradation in an AEM system.

To the best of our literature search, ML focus on the degradation or aging performance of PEM FC and especially WE are still limited and needs further extensive investigation for better understanding of the short and long-term durability and efficiency of these systems. Table 2

Table 2
Summary of literatures of machine learning for degradation studies of PEMFC and electrolyzers with their respective references.

Case study	Energy device	Cell configuration	Data source/Test duration	Data filtering method	ML method	Model accuracy	Findings
Vichard et al. [254]	PEMFC	Fuel cell stack composed of 28 cells with open air cathode cooling	Experimental, 5000 h`	Nil	ESN	RMSE: 0.098	Lower temperatures lead to better humidification conditions thereby reducing rate of degradation.
Morando et al. [256]	PEMFC	5-cell PEMFC stack	Experimental, 1700 h	Wavelet transform & Hurst coefficient.	ESN	MAPE: <5%	20% of the data was sufficient to accurately predict the RUL of PEMFC. ESN can capture the complex dynamics of PEMFC degradation which is not fully understood or modelled yet.
Mezzi et al. [257]	PEMFC	5-cell PEMFC stack	Experimental, 1700 h	Nil	Classical ESN & MR-ESN	Both MAPEs are < 10 %	The integration of multi-reservoirs in the ESN architecture improves the predictive capability of the model as compared to single reservoir in a classical ESN network.
Zhang et al. [258]	PEMFC	5-cell PEMFC stack	Experimental	Savitzky-Golay	MR-ESN + mini-reservoir	For static test condition data RMSE:1.412e^{-4} MAPE: 3.065e^{-3} For dynamic test condition data RMSE: 1.298e^{-4} MAPE – 1.824e^{-3}	The multi-reservoir component architecture of the ESN algorithm coupled with a mini-reservoir architecture enhanced the predictive capability of the algorithm.
Liu et al. [260]	PEMFC	5-cell PEMFC stack with water cooling system	Experimental, 1155 h	Locally weighted scatterplot smoothing	LSTM BPNN	RMSE: 0.003 MAE: 0.026 Accuracy: 99.23% RMSE: 0.0203 MAE: 0.0234 Accuracy: 70.77%	The use of regular interval sampling and (LOESS) for data reconstruction and smoothing ensures that the primary trend of the original data is preserved while effectively removing noise and spikes, which is crucial for maintaining the reliability of PEMFC systems in practical applications.
Wang et al. [262] [87]	PEMFC	5-cell PEMFC stack	Experimental	Nil	BILSTM-AT & Random Forest for feature selection	RMSE < 0.0029	The inclusion of an attention mechanism to the BILSTM algorithms contributed to the model's predictive capability by focusing on the most relevant features of the data, thus enhancing the accuracy of the degradation predictions.
Zuo et al. [269]	PEMFC	Single cell	Experimental	Moving average smoothing method.	LSTM, gated recurrent unit (GRU), attention-based LSTM and attention-based GRU.	RSME for attention-based LSTM, attention-based GRU, LSTM and GRU models are 0.016409, 0.015518, 0.017637 and 0.018206, respectively.	Attention-based LSTM RNN model achieves higher prediction accuracy, making it particularly suitable for fuel cell performance degradation prognosis.
Wang et al. [270]	PEMFC	5-cell PEMFC stack	Experimental, >1000 h	Singular Spectrum Analysis (SSA)	LSTM, Gaussian process regression (GPR) and LSTM-GPR	**LSTM** RMSE: 0.0066 MAPE: 0.0016 MAE: 0.0053 **GPR** RMSE: 0.0072 MAPE: 0.0018 MAE: 0.0058 **LSTM+GPR** RMSE: 0.0049 MAPE: 0.0011 MAE: 0.0036	LSTM-GPR showed excellent performance over other models by accurately predicting the voltage degradation of the system. The deep structure displayed by this model enhances its learning capabilities for non-linear patterns of PEMFC degradation trends.
Wu et al. [263]	PEMFC	1.2 kW PEMFC stack	Experimental, 400 h	Data down-sampling	RVM and SVM	**RVM** RMSE: 0.1751 MAPE: 0.0044 R^2: 0.9153 **SVM** RMSE: 0.2022 MAPE: 0.0054 R^2: 0.8896	The RVM algorithm can accurately predict the ageing of a PEMFC when fed with limited training data and with relatively fewer input vectors (features).
Zhong et al. [265]	PEMFC	36 cells fuel cell stack	Experimental data from Ref. [271,272]	Nil	LS-SVM	MAE: 0.0002 R^2: 98.98%	The model displayed higher predictive accuracy. Higher current densities lead to increased voltage degradation.

(*continued on next page*)

Table 2 (*continued*)

Case study	Energy device	Cell configuration	Data source/Test duration	Data filtering method	ML method	Model accuracy	Findings
Xu et al. [261]	PEMWE	-	Experimental	Savitzky-Golay	CNN-LSTM	Average absolute error Constant – 0.39 mV Start–stop – 2.1 × 10^{-2}	The model performed better than GRU and LSTM with predicted RUL for constant and start-stop condition of 2550 h and 11,736 h respectively.
Lee et al. [80,268]	AWE	AWE stack with are 34.56 cm^2	Experimental data, 480 h	Nil	SVM and GPR	RMSE for SVM and GPR is 1.28 × 10^{-3} and 8.03 × 10^{-6} respectively	Better performance of both models. However, the prediction capability on new data is low.

provides a concise overview of ML algorithms for performance and degradation evaluation studies of PEM FCs and WEs. Even though studies are evolving, more focus on correlating the changes of the structural and compositional parameters in the MEAs of these systems to their performance, as they degrade is needed.

4. Current challenges and future aspects

Apart from numerous advantages, there are so some roadblocks to the successful implementation of AI technology in materials and especially in the energy industry. A few of the critical issues are listed below [273–276]:

AI-based methods typically require the collection of large amounts of data to accurately predict reliable outcomes while the acquisition of materials data, such as various forms of materials characterization, is itself a quite expensive process and sometimes the tradeoff between time and cost is not achieved. Another challenge faced in using AI-based methods is the under-representation of high complexity data by simpler models or the overestimation of trivial data by high-capacity models. AI-based approaches are also typically very sensitive to small variations in the system, environment, or parameters and a little offset can significantly the quality of output.

The operation and interpretation mechanism of AI-based models cannot be easily understood and is frequently referred to as a black box, limiting users from successfully identifying weaknesses of the model. The application of SHAP method is a new method in the interpretation of black box models. However, it has not been widely explored in ML for fuel cells and electrolyzers applications.

Despite the current challenges, AI has shown immense progress over the last few years and continues to excite researchers with its unique capabilities. Moreover, since ML is intrinsically a data-driven approach, therefore, we can state with absolute certainty that the surfeit of knowledge and data continually being extracted from advanced data mining techniques will undoubtedly benefit AI-based models in materials science to meet and even exceed performance demands. Furthermore, AI-based models, which are highly efficiently trained on smaller datasets, are being introduced, which can eliminate the need for the collection of larger input datasets altogether, especially for applications where data collection is a long, difficult, and exhaustive process. Furthermore, by combining AI-based models with high-performance computational approaches, efficient screening methods, and evolutionary algorithms, we can perceive significant advancement in materials research in the near future [277–279].

In conclusion, the advancement of ML algorithms in fuel cells and electrolyzers is currently evolving, presenting numerous research opportunities, particularly in exploring data-driven degradation mechanisms with focus on internal interactions between MEA parameters and RUL, as well as the study of defect detection, phase segmentation.

5. Conclusions

The presented paper offers a comprehensive discussion on the introduction and application of AI, particularly ML and DL, within material science and engineering, with a special focus on energy systems like fuel cells and electrolyzers. The advancement of ML algorithms in fuel cells and electrolyzers is evolving rapidly, presenting numerous research opportunities, particularly in exploring data-driven degradation mechanisms with a focus on internal interactions between MEA parameters and durability, as well as the study of defect detection and phase segmentation. The need for processing large, complex datasets efficiently and automating experimental selection processes is a central challenge for researchers in these fields and an area where AI, ML, and DL can offer a significant contribution. Hence, the paper discusses how innovative AI-based algorithms predict and optimize material behavior in these high-demand applications. It highlights how AI techniques like support vector machines, gradient-boosting, and recurrent neural networks help improve the accuracy and efficiency of predicting material degradation and lifespan. Additionally, model interpretability offers insights into critical parameters affecting material performance. The application of AI, especially ML models, has shown immense potential in expediting the materials discovery process and optimizing designs for specific needs in these PEM-based systems. For example, algorithms like XGBoost and CNN-LSTM demonstrated high accuracy in predicting fuel cell and electrolyzer degradation with mean absolute errors (MAE) as low as 0.0002 and improved decision-making in material selection. These advancements allow for more efficient material design and enhanced performance predictions, crucial for energy sustainability. The future research scope includes developing AI models that require smaller datasets, making AI accessible for resource-limited applications. Integrating AI with advanced computational techniques, such as evolutionary algorithms, is expected to further revolutionize materials research by offering faster, more accurate predictions. Thus, collectively, these advancements mark significant strides in materials science and clean energy technologies' progression.

Declaration of generative AI and AI-assisted technologies in the writing process

During the preparation of this work the authors used ChatGPT 4.0 to improve language and readability. After using this tool/service, the authors reviewed and edited the content as needed and take full responsibility for the content of the publication.

CRediT authorship contribution statement

Mariah Batool: Writing – review & editing, Writing – original draft, Visualization, Investigation, Formal analysis, Conceptualization. **Oluwafemi Sanumi:** Writing – review & editing, Writing – original draft, Visualization, Investigation, Formal analysis, Conceptualization. **Jasna Jankovic:** Writing – review & editing, Writing – original draft, Supervision, Project administration, Funding acquisition, Conceptualization.

Declaration of competing interest

The authors declare that they have no known competing financial interests or personal relationships that could have appeared to influence the work reported in this paper.

Acknowledgments

This work is supported by the U.S. National Science Foundation (NSF) under The Faculty Early Career Development (CAREER) Program (Grant # 2046060).

Supplementary materials

Supplementary material associated with this article can be found, in the online version, at doi:10.1016/j.egyai.2024.100424.

References

[1] Lu Y. Artificial intelligence: a survey on evolution, models, applications and future trends. J Manag Analytics 2019;6(1):1–29. https://doi.org/10.1080/23270012.2019.1570365.
[2] Majumdar B, Sarode SC, Sarode GS, Patil S. Technology: artificial intelligence. Br Dent J 2018;224(12):916. https://doi.org/10.1038/sj.bdj.2018.485.
[3] D.T. Pham and P.T.N. Pham, "Artificial intelligence in engineering," vol. 39, pp. 937–49, 1999.
[4] B. Sharma, "Processing of data and analysis," vol. 1, pp. 3–5, 2018, doi: 10.30881/beij.00003.
[5] Ott LR, Longnecker M. An introduction to statistical methods and data analysis. Sixth 2010.
[6] Z. Saleh, "Artificial intelligence definition, ethics and standards," 2019.
[7] D. Dobrev, "A definition of artificial intelligence," pp. 1–7, 2004.
[8] M. Haenlein and A. Kaplan, "A brief history of artificial intelligence:," pp. 5–14, 2019, 10.1177/0008125619864925.
[9] Aizawa K. Connectionism and artificial intelligence: history and philosophical interpretation. J Exp Theoret Artif Intell 1992;4(4):295–313. https://doi.org/10.1080/09528139208953753.
[10] M. Negnevitsky, "The history of artificial intelligence or from the " Dark Ages " to the knowledge-based systems," vol. 19, 1997.
[11] Frana PL, Klein MJ. Encyclopedia of artificial intelligence: the past, present, and future of AI. ABC-CLIO; 2021.
[12] Lele A. Artificial Intelligence (AI). Disruptive technologies for the militaries and security. 2019. p. 139–54. https://doi.org/10.1007/978-981-13-3384-2.
[13] Hassani H, Silva ES, Unger S, TajMazinani M, Feely SMac. Artificial Intelligence (AI) or Intelligence Augmentation (IA): what is the future? Ai 2020;1(2):143–55. https://doi.org/10.3390/ai1020008.
[14] H. Khan, "Types of AI | different types of artificial intelligence systems," no. October 2021.
[15] Campesato O. Artificial intelligence, machine learning, and deep learning. Mercury Learning \& Information; 2020.
[16] H. Wehle, "Machine learning, deep learning, and AI: what's the difference?," 2017.
[17] Latif J, Xiao C, Imran A, Tu S. Medical imaging using machine learning and deep learning algorithms: a review. In: 2019 2nd International Conference on Computing, Mathematics and Engineering Technologies, iCoMET 2019; 2019. p. 4–8. https://doi.org/10.1109/ICOMET.2019.8673502.
[18] Hu Y, et al. Artificial intelligence approaches. Geogr Inf Sci Technol Body Knowl 2019;2019(Q3). https://doi.org/10.22224/gistbok/2019.3.4.
[19] J. Vrana and R. Singh, "NDE 4.0 from design thinking to strategy," no. March, pp. 0–27, 2020, doi: 10.1007/s10921-020-00735-9.
[20] Kaluarachchi T, Reis A, Nanayakkara S. A review of recent deep learning approaches in human-centered machine learning. Sensors 2021;21(7):1–29. https://doi.org/10.3390/s21072514.
[21] Moubayed A, Injadat M, Nassif AB, Lutfiyya H, Shami A. E-learning: challenges and research opportunities using machine learning data analytics. IEEE Access 2018;6(July):39117–38. https://doi.org/10.1109/ACCESS.2018.2851790.
[22] Aldahiri A, Alrashed B, Hussain W. Trends in using IoT with machine learning in health prediction system. Forecasting 2021;3(1):181–206. https://doi.org/10.3390/forecast3010012.
[23] Nassif AB, Shahin I, Attili I, Azzeh M, Shaalan K. Speech recognition using deep neural networks: a systematic review. IEEE Access 2019;7:19143–65. https://doi.org/10.1109/ACCESS.2019.2896880.
[24] Maglogiannis IG. Emerging artificial intelligence applications in computer engineering: real word ai systems with applications in EHealth, HCI, information retrieval and pervasive technologies. in frontiers in artificial intelligence and applications. IOS Press; 2007.
[25] Nasteski V. An overview of the supervised machine learning methods. Horizons B 2017;4(December 2017):51–62. https://doi.org/10.20544/horizons.b.04.1.17.p05.
[26] J.K. Mandal and D. Bhattacharya, *Emerging technology in modelling and graphics*, vol. 937. 2018. doi: 10.1007/978-981-13-7403-6_26.
[27] Dreiseitl S, Ohno-Machado L. Logistic regression and artificial neural network classification models: a methodology review. J Biomed Inform 2002;35(5–6):352–9. https://doi.org/10.1016/S1532-0464(03)00034-0.
[28] M. Awad and R. Khana, *Efficient learning machines*. 2015.
[29] Rokach L, Maimon O. Decision trees,". In: Maimon O, Rokach L, editors. Data mining and knowledge discovery handbook. Boston, MA: Springer US; 2005. p. 165–92. https://doi.org/10.1007/0-387-25465-X_9.
[30] Pal M. Random forest classifier for remote sensing classification. Int J Remote Sens 2005;26(1):217–22. https://doi.org/10.1080/01431160412331269698.
[31] Caruana R, Niculescu-Mizil A. An empirical comparison of supervised learning algorithms. In: ACM International Conference Proceeding Series. 148; 2006. p. 161–8. https://doi.org/10.1145/1143844.1143865.
[32] Hastie T, Tibshirani R, Friedman J. Overview of Supervised Learning. In: Hastie T, Tibshirani R, Friedman J, editors. The elements of statistical learning. New York, NY: Springer New York; 2009. p. 9–41. https://doi.org/10.1007/978-0-387-84858-7_2.
[33] Ong HC, Leong CH, Tai SH. A functional approximation comparison between neural networks and polynomial regression. WSEAS Trans Math 2008;7(6):353–63.
[34] Gentleman R, Carey VJ. Unsupervised Machine Learning. Bioconductor case studies. New York, NY: Springer New York; 2008. p. 137–57. https://doi.org/10.1007/978-0-387-77240-0_10.
[35] Syarif I, Prugel-Bennett A, Wills G. Data mining approaches for network intrusion detection: from dimensionality reduction to misuse and anomaly detection. J Inf Technol Rev 2012;3(2):70–83.
[36] Caron M, Bojanowski P, Joulin A, Douze M. Deep clustering for unsupervised learning of visual features. Lecture Notes in Computer Science (including subseries Lecture Notes in Artificial Intelligence and Lecture Notes in Bioinformatics 2018;11218 LNCS:139–56. https://doi.org/10.1007/978-3-030-01264-9_9.
[37] Mathur B, Ant P, Kaushik M, Mathur MB. Comparative study of K-means and hierarchical clustering techniques related papers K-mean evaluation in weka tool and modifying it using standard score method international. J IJRIT CC K-Attractors 2014.
[38] Sinaga KP, Yang MS. Unsupervised K-means clustering algorithm. IEEE Access 2020;8:80716–27. https://doi.org/10.1109/ACCESS.2020.2988796.
[39] Talavera L. Feature selection as a preprocessing step for hierarchical clustering. In: Proceedings of the 25th international conference on Machine learning; 1999. p. 389–97.
[40] Peña JM, Lozano JA, Larrañaga P, Inza I. Dimensionality reduction in unsupervised learning of conditional Gaussian networks. IEEE Trans Pattern Anal Mach Intell 2001;23(6):590–603. https://doi.org/10.1109/34.927460.
[41] Abdi H, Williams LJ. Principal component analysis. Wiley Interdiscip Rev Comput Stat 2010;2(4):433–59. https://doi.org/10.1002/wics.101.
[42] T. Howley, M.G. Madden, M.-L. O'Connell, and A.G. Ryder, "The effect of principal component analysis on machine learning accuracy with high dimensional spectral data BT - applications and innovations in intelligent systems XIII," A. Macintosh, R. Ellis, and T. Allen, editors, London: Springer London, 2006, pp. 209–22.
[43] A. Hyvärinen, "Independent component analysis: recent advances," Feb. 13, 2013, Royal Society. doi: 10.1098/rsta.2011.0534.
[44] Omar S, Ngadi A, Jebur HH. Machine learning techniques for anomaly detection: an overview. Int J Comput Appl 2013;79(2):33–41. https://doi.org/10.5120/13715-1478.
[45] X. Goldberg, *Introduction to semi-supervised learning*, vol. 6. 2009. doi: 10.2200/S00196ED1V01Y200906AIM006.
[46] Batta M. Machine learning algorithms - a review. Int J Sci Res (IJ 2020;9(1):381. https://doi.org/10.21275/ART20203995. -undefined.
[47] M. C.B.B, *Deep low-density separation for semi-supervised classification*, vol. 1. Springer International Publishing, 2020. doi: 10.1007/978-3-030-50420-5.
[48] Bernstein AV, Burnaev EV. Reinforcement learning in computer vision. In: Verikas A, Radeva P, Nikolaev D, Zhou J, editors. Tenth International Conference on Machine Vision (ICMV 2017). SPIE; 2018. p. 458–64. https://doi.org/10.1117/12.2309945.
[49] Busoniu L, Babuska R, Schutter D, Ernst D. Reinforcement learning and dynamic programming using function approximators. Automation and control engineering. CRC Press; 2017.
[50] Wang Y, Won KS, Hsu D, Lee WS. Monte Carlo Bayesian reinforcement learning. In: Proceedings of the 29th International Conference on Machine Learning, ICML 2012. 2; 2012. p. 1135–42.
[51] Lecun Y, Bengio Y, Hinton G. Deep learning. Nature 2015;521(7553):436–44. https://doi.org/10.1038/nature14539.
[52] Kang M, Jameson NJ. Machine learning: fundamentals. Prognostics and health management of electronics, 4. John Wiley & Sons, Ltd; 2018. p. 85–109. https://doi.org/10.1002/9781119515326.ch4. ch.
[53] I.H. Sarker, "Deep learning: a comprehensive overview on techniques, taxonomy, applications and research directions," Nov. 01, 2021, Springer. doi: 10.1007/s42979-021-00815-1.
[54] Ardabili S, Mosavi A, Mahmoudi A, Gundoshmian TM, Nosratabadi S, Várkonyi-Kóczy AR. List of deep learning models. Eng Sustainable Future 2020;101:33–45. https://doi.org/10.1007/978-3-030-36841-8_3.
[55] Liao SH, Wen CH. Artificial neural networks classification and clustering of methodologies and applications - literature analysis from 1995 to 2005. Expert Syst Appl 2007;32(1):1–11. https://doi.org/10.1016/j.eswa.2005.11.014.
[56] L.B. Luckin, Rose; Holmes, Wayne; Griffiths, Mark and Forcier, *Intelligence unleashed : an argument for AI in education*. 2016.
[57] Alajrami E, Tabash H, Singer Y, Astal MTE. On using AI-based human identification in improving surveillance system efficiency. In: Proceedings - 2019 International Conference on Promising Electronic Technologies, ICPET 2019; 2019. p. 91–5. https://doi.org/10.1109/ICPET.2019.00024.
[58] Eli-Chukwu NC. Applications of artificial intelligence in agriculture: a review. Eng Technol Appl Sci Res 2019;9(4):4377–83. https://doi.org/10.48084/etasr.2756.

[59] Rajan K, Saffiotti A. Towards a science of integrated AI and Robotics. Artif Intell 2017;247:1–9. https://doi.org/10.1016/j.artint.2017.03.003.

[60] Lee YL, Tsung PK, Wu M. Technology trend of edge AI. Proc Int Symp Comput Archit 2017;Part F1286:1–12. https://doi.org/10.1145/3079856.3080246.

[61] Rastgarpour M, Shanbehzadeh J. Application of AI techniques in medical image segmentation and novel categorization of available methods and tools. In: IMECS 2011 - International MultiConference of Engineers and Computer Scientists 2011. 1; 2011. p. 519–23.

[62] Tyagi S, Sengupta S. Role of AI in Gaming and Simulation. In: Pandian AP, Palanisamy R, Ntalianis K, editors. Proceeding of the International Conference on Computer Networks, Big Data and IoT (ICCBI - 2019). Cham: Springer International Publishing; 2020. p. 259–66.

[63] Cihon P. Standards for AI governance: international standards to enable global coordination in AI research & development," *Future of Humanity Institute*. Univ Oxford 2019;(April):1–41.

[64] Candy DW, Herrod RA. Industry Applications of Artificial Intelligence. In: IEEE Region 5 Conference; 1985. p. 25–30.

[65] Gao XZ, Kumar R, Srivastava S, Soni BP. In: Applications of Artificial Intelligence in Engineering: Proceedings of First Global Conference on Artificial Intelligence and Applications (GCAIA 2020). Singapore: Springer; 2021. Algorithms for Intelligent Systems.

[66] Callister WD, Rethwisch DG. Fundamentals of materials science and engineering: an integrated approach. Wiley; 2020.

[67] Sha W, et al. Artificial intelligence to power the future of materials science and engineering. Adv Intell Syst 2020;2(4):1900143. https://doi.org/10.1002/aisy.201900143.

[68] Kalidindi SR, De Graef M. Materials data science: current status and future outlook. Annu Rev Mater Res 2015;45:171–93. https://doi.org/10.1146/annurev-matsci-070214-020844.

[69] Schleder GR, Padilha ACM, Acosta CM, Costa M, Fazzio A. From DFT to machine learning: recent approaches to materials science - a review. J Phys Mater 2019;2(3). https://doi.org/10.1088/2515-7639/ab084b.

[70] Agrawal A, Choudhary A. Perspective: materials informatics and big data: realization of the 'fourth paradigm' of science in materials science. APL Mater 2016;4(5). https://doi.org/10.1063/1.4946894.

[71] Duan Y, Edwards JS, Dwivedi YK. Artificial intelligence for decision making in the era of Big Data – evolution, challenges and research agenda. Int J Inf Manage 2019;48(January):63–71. https://doi.org/10.1016/j.ijinfomgt.2019.01.021.

[72] Q. Ai, P. Weaver, and M. Azarpeyvand, "Design optimization of a morphing flap device using variable stiffness materials," in *24th AIAA/AHS Adaptive Structures Conference*. doi: 10.2514/6.2016-0816.

[73] Wang AYT, et al. Machine learning for materials scientists: an introductory guide toward best practices. Chem Mater 2020;32(12):4954–65. https://doi.org/10.1021/acs.chemmater.0c01907.

[74] Sorkun MC, Astruc S, Koelman JMVA, Er S. An artificial intelligence-aided virtual screening recipe for two-dimensional materials discovery. NPJ Comput Mater 2020;6(1):1–10. https://doi.org/10.1038/s41524-020-00375-7.

[75] Schmidt J, Marques MRG, Botti S, Marques MAL. Recent advances and applications of machine learning in solid-state materials science. NPJ Comput Mater 2019;5(1). https://doi.org/10.1038/s41524-019-0221-0.

[76] K. Choudhary et al., "Recent advances and applications of deep learning methods in materials science," 2021, doi: 10.1038/s41524-022-00734-6.

[77] Lee JY, An J, Chua CK. Fundamentals and applications of 3D printing for novel materials. Appl Mater Today 2017;7:120–33. https://doi.org/10.1016/j.apmt.2017.02.004.

[78] Krohns S, et al. The route to resource-efficient novel materials. Nat Mater 2011;10(12):899–901. https://doi.org/10.1038/nmat3180.

[79] Cannillo V, et al. Microscale computational simulation and experimental measurement of thermal residual stresses in glass-alumina functionally graded materials. J Eur Ceram Soc 2006;26(8):1411–9. https://doi.org/10.1016/j.jeurceramsoc.2005.02.012.

[80] Thomas JM. Design, synthesis, and in situ characterization of new solid catalysts. Angew Chem Int Ed Engl 1999;38:3588–628.

[81] Liu Y, Zhao T, Ju W, Shi S, Shi S, Shi S. Materials discovery and design using machine learning. J Materiomics 2017;3(3):159–77. https://doi.org/10.1016/j.jmat.2017.08.002.

[82] Liu Y, Zhao T, Ju W, Shi S, Shi S, Shi S. Materials discovery and design using machine learning. J Materiomics 2017;3(3):159–77. https://doi.org/10.1016/j.jmat.2017.08.002.

[83] Tan C, Wu H, Yang L, Wang Z. Cutting edge high-throughput synthesis and characterization techniques in combinatorial materials science. Adv Mater Technol 2024;2302038:1–23. https://doi.org/10.1002/admt.202302038.

[84] Deng T, et al. High-throughput strategies in the discovery of thermoelectric materials. Adv Mater 2024;36(13):1–26. https://doi.org/10.1002/adma.202311278.

[85] Lu Z, et al. Materials genome strategy for metallic glasses. J Mater Sci Technol 2023;166:173–99. https://doi.org/10.1016/j.jmst.2023.04.074.

[86] Yang Y, et al. Implement the materials genome initiative: machine learning assisted fluorescent probe design for cellular substructure staining. Adv Mater Technol 2023;8(17):1–10. https://doi.org/10.1002/admt.202300427.

[87] Yan Q, Kar S, Chowdhury S, Bansil A. The case for a defect genome initiative. Adv Mater 2024;36(11):1–17. https://doi.org/10.1002/adma.202303098.

[88] Singh AK, Gorelik R, Biswas T. Data-driven discovery of robust materials for photocatalytic energy conversion. Annu Rev Condens Matter Phys 2023;14:237–59. https://doi.org/10.1146/annurev-conmatphys-031620-100957.

[89] Nyshadham C, et al. Machine-learned multi-system surrogate models for materials prediction. NPJ Comput Mater 2019;5(1). https://doi.org/10.1038/s41524-019-0189-9. Dec.

[90] Balachandran PV, Theiler J, Rondinelli JM, Lookman T. Materials prediction via classification learning. Sci Rep 2015;5. https://doi.org/10.1038/srep13285. Aug.

[91] Juan Y, Dai Y, Yang Y, Zhang J. Accelerating materials discovery using machine learning. J Mater Sci Technol 2021;79:178–90. https://doi.org/10.1016/j.jmst.2020.12.010.

[92] Pyzer-Knapp EO, et al. Accelerating materials discovery using artificial intelligence, high performance computing and robotics. NPJ Comput Mater 2022;8(1). https://doi.org/10.1038/s41524-022-00765-z.

[93] Carrera GVSM, Branco LC, Aires-de-Sousa J, Afonso CAM. Exploration of quantitative structure-property relationships (QSPR) for the design of new guanidinium ionic liquids. Tetrahedron 2008;64(9):2216–24. https://doi.org/10.1016/j.tet.2007.12.021.

[94] Farrusseng D, Clerc F, Mirodatos C, Rakotomalala R. Virtual screening of materials using neuro-genetic approach: concepts and implementation. Comput Mater Sci 2009;45(1):52–9.

[95] Raccuglia P, et al. Machine-learning-assisted materials discovery using failed experiments. Nature 2016;533(7601):73–6.

[96] Meredig B, et al. Combinatorial screening for new materials in unconstrained composition space with machine learning. Phys Rev B Condens Matter Mater Phys 2014;89(9):1–7. https://doi.org/10.1103/PhysRevB.89.094104.

[97] Phillips CL, Voth GA. Discovering crystals using shape matching and machine learning. Soft Matter 2013;9(35):8552–68. https://doi.org/10.1039/c3sm51449h.

[98] Disalvo FJ. Thermoelectric cooling and power generation. Science (1979) 1999;285(5428):703–6. https://doi.org/10.1126/science.285.5428.703.

[99] Parse N, Pongkitivanichkul C, Pinitsoontorn S. Machine learning approach for maximizing thermoelectric properties of BiCuSeO and discovering new doping element. Energies (Basel) 2022;15(3):779.

[100] Parse N, Pongkitivanichkul C, Pinitsoontorn S. Machine learning approach for maximizing thermoelectric properties of BiCuSeO and discovering new doping element. Energies (Basel) 2022;15(3). https://doi.org/10.3390/en15030779.

[101] Lo Dico G, Nuñez ÁP, Carcelén V, Haranczyk M. Machine-learning-accelerated multimodal characterization and multiobjective design optimization of natural porous materials. Chem Sci 2021;12(27):9309–17. https://doi.org/10.1039/d1sc00816a.

[102] Wong KV, Hernandez A. A Review of Additive Manufacturing. ISRN Mech Eng 2012;2012:1–10. https://doi.org/10.5402/2012/208760.

[103] Raja S, et al. Selection of additive manufacturing machine using analytical hierarchy process. Sci Program 2022;2022. https://doi.org/10.1155/2022/1596590.

[104] Chua ZY, Ahn IH, Moon SK. Process monitoring and inspection systems in metal additive manufacturing: status and applications. Int J Precis Eng Manuf - Green Technol 2017;4(2):235–45. https://doi.org/10.1007/s40684-017-0029-7.

[105] Tapia G, Elwany A. A review on process monitoring and control in metal-based additive manufacturing. J Manuf Sci Eng Trans ASME 2014;136(6):1–10. https://doi.org/10.1115/1.4028540.

[106] Goh GD, Sing SL, Yeong WY. A review on machine learning in 3D printing: applications, potential, and challenges. Artif Intell Rev 2021;54(1):63–94. https://doi.org/10.1007/s10462-020-09876-9.

[107] Weber G, Pinz M, Ghosh S. Machine learning-aided parametrically homogenized crystal plasticity model (PHCPM) for single crystal Ni-based superalloys. Jom 2020;72(12):4404–19. https://doi.org/10.1007/s11837-020-04344-9.

[108] Liu Y, et al. Predicting creep rupture life of Ni-based single crystal superalloys using divide-and-conquer approach based machine learning. Acta Mater 2020;195:454–67. https://doi.org/10.1016/j.actamat.2020.05.001.

[109] Eliseeva OV, et al. Functionally graded materials through robotics-inspired path planning. Mater Des 2019;182:107975. https://doi.org/10.1016/j.matdes.2019.107975.

[110] Rankouhi B, Jahani S, Pfefferkorn FE, Thoma DJ. Compositional grading of a 316L-Cu multi-material part using machine learning for the determination of selective laser melting process parameters. Addit Manuf 2021;38(January):101836. https://doi.org/10.1016/j.addma.2021.101836.

[111] Denkena B, Bergmann B, Witt M. Material identification based on machine-learning algorithms for hybrid workpieces during cylindrical operations. J Intell Manuf 2019;30(6):2449–56. https://doi.org/10.1007/s10845-018-1404-0.

[112] Pollock TM, Tin S. Nickel-based superalloys for advanced turbine engines: chemistry, microstructure and properties. J Propuls Power 2006;22(2):361–74. https://doi.org/10.2514/1.18239.

[113] Bunaziv I, Olden V, Akselsen OM. Metallurgical aspects in the welding of clad pipelines-a global outlook. Appl Sci (Switzerland) 2019;9(15). https://doi.org/10.3390/app9153118.

[114] Vejdannik M, Sadr A. Automatic microstructural characterization and classification using probabilistic neural network on ultrasound signals. J Intell Manuf 2018;29(8):1923–40. https://doi.org/10.1007/s10845-016-1225-y.

[115] Escobar CA, Morales-Menendez R. Machine learning techniques for quality control in high conformance manufacturing environment. Adv Mech Eng 2018;10(2):1–16. https://doi.org/10.1177/1687814018755519.

[116] Kwon O, et al. A deep neural network for classification of melt-pool images in metal additive manufacturing. J Intell Manuf 2020;31(2):375–86. https://doi.org/10.1007/s10845-018-1451-6.

[117] Zhang X, Saniie J, Cleary W, Heifetz A. Quality control of additively manufactured metallic structures with machine learning of thermography images. Jom 2020;72(12):4682–94. https://doi.org/10.1007/s11837-020-04408-w.

[118] Wu D, Wei Y, Terpenny J. Surface roughness prediction in additive manufacturing using machine learning. In: International Manufacturing Science and Engineering Conference. 3; 2018. https://doi.org/10.1115/MSEC2018-6501.

[119] Moosavi SM, Jablonka KM, Smit B. The role of machine learning in the understanding and design of materials. J Am Chem Soc 2020;142(48):20273–87. https://doi.org/10.1021/jacs.0c09105.

[120] Stoll A, Benner P. Machine learning for material characterization with an application for predicting mechanical properties. GAMM Mitteilungen 2021;44 (1):1–21. https://doi.org/10.1002/gamm.202100003.

[121] Kilic A, Odabaşı Ç, Yildirim R, Eroglu D. Assessment of critical materials and cell design factors for high performance lithium-sulfur batteries using machine learning. Chem Eng J 2020;390(December 2019). https://doi.org/10.1016/j.cej.2020.124117.

[122] James SL. Metal-organic frameworks. Chem Soc Rev 2003;32(5):276–88. https://doi.org/10.1039/b200393g.

[123] Chong S, Lee S, Kim B, Kim J. Applications of machine learning in metal-organic frameworks. Coord Chem Rev 2020;423:213487. https://doi.org/10.1016/j.ccr.2020.213487.

[124] Fernandez M, Woo TK, Wilmer CE, Snurr RQ. Large-scale quantitative structure-property relationship (QSPR) analysis of methane storage in metal-organic frameworks. J Phys Chem C 2013;117(15):7681–9. https://doi.org/10.1021/jp4006422.

[125] Gan Y, Wang G, Zhou J, Sun Z. Prediction of thermoelectric performance for layered IV-V-VI semiconductors by high-throughput ab initio calculations and machine learning. NPJ Comput Mater 2021;7(1):1–10. https://doi.org/10.1038/s41524-021-00645-y.

[126] Leng Y. Materials characterization: introduction to microscopic and spectroscopic methods. Wiley; 2009.

[127] Misra S, Li H, He J. Machine learning for subsurface characterization. Elsevier Science; 2019.

[128] Lee CS, Chandel RS, Seow HP. Effect of welding parameters on the size of heat affected zone of submerged arc welding. Mater Manuf Process 2000;15(5):649–66. https://doi.org/10.1080/10426910008913011.

[129] Bulgarevich DS, Tsukamoto S, Kasuya T, Demura M, Watanabe M. Pattern recognition with machine learning on optical microscopy images of typical metallurgical microstructures. Sci Rep 2018;8(1):3–9. https://doi.org/10.1038/s41598-018-20438-6.

[130] Rettenberger L, et al. Uncertainty-aware particle segmentation for electron microscopy at varied length scales. NPJ Comput Mater 2024;10(1):1–9. https://doi.org/10.1038/s41524-024-01302-w.

[131] Guo M, Gong G, Yue Y, Xing F, Zhou Y, Hu B. Performance evaluation of recycled aggregate concrete incorporating limestone calcined clay cement (LC3). J Clean Prod 2022;366:132820. https://doi.org/10.1016/j.jclepro.2022.132820.

[132] Liang Z, et al. Improving recycled aggregate concrete by compression casting and nano-silica. Nanotechnol Rev 2022;11(1):1273–90. https://doi.org/10.1515/ntrev-2022-0065.

[133] Sui H, Wang W, Lin J, Tang ZQ, Yang DS, Duan W. Spatial correlation and pore morphology analysis of limestone calcined clay cement (LC3) via machine learning and image-based characterisation. Constr Build Mater 2023;401(May):132721. https://doi.org/10.1016/j.conbuildmat.2023.132721.

[134] A.G. Li, A.C. West, and M. Preindl, "Towards unified machine learning characterization of lithium-ion battery degradation across multiple levels : a critical review," vol. 316, no. March 2021.

[135] Ma R, Yang T, Breaz E, Li Z, Briois P, Gao F. Data-driven proton exchange membrane fuel cell degradation predication through deep learning method. Appl Energy 2018;231(March):102–15. https://doi.org/10.1016/j.apenergy.2018.09.111.

[136] Odabaşı Ç, Yıldırım R. Machine learning analysis on stability of perovskite solar cells. Solar Energy Mater Solar Cells 2020;205(August 2019). https://doi.org/10.1016/j.solmat.2019.110284.

[137] Stephan AK. The age of Li-ion batteries. Joule 2019;3(11):2583–4. https://doi.org/10.1016/j.joule.2019.11.004.

[138] He W, Williard N, Osterman M, Pecht M. Prognostics of lithium-ion batteries based on Dempster-Shafer theory and the Bayesian Monte Carlo method. J Power Sources 2011;196(23):10314–21. https://doi.org/10.1016/j.jpowsour.2011.08.040.

[139] Tang X, Liu K, Li K, Widanage WD, Kendrick E, Gao F. Recovering large-scale battery aging dataset with machine learning. Patterns 2021;2(8):100302. https://doi.org/10.1016/j.patter.2021.100302.

[140] Al-Mashhadani R, et al. Deep learning methods for solar fault detection and classification: a review. Inf Sci Lett 2021;10(2):323–31. https://doi.org/10.18576/isl/100213.

[141] Naik RR, Tiihonen A, Thapa J, Batali C, Sun S, Liu Z. Discovering the underlying equations governing perovskite solar-cell degradation using scientific machine learning. NeurIPS 2020:1–8.

[142] R. Battiti, Y.D. Sergeyev, and D.E. Kvasov, *Learning and intelligent optimization*, vol. 10556 LNCS. 2017. doi: 10.1007/978-3-319-69404-7_35.

[143] Xie T, Grossman JC. Crystal graph convolutional neural networks for an accurate and interpretable prediction of material properties. Phys Rev Lett 2018;120(14):145301. https://doi.org/10.1103/PhysRevLett.120.145301.

[144] Wang W, Gómez-Bombarelli R. Coarse-graining auto-encoders for molecular dynamics. NPJ Comput Mater 2019;5(1). https://doi.org/10.1038/s41524-019-0261-5.

[145] B.C. Olsen, A. Mar, and J.M. Buriak, "How to optimize materials and devices via design of experiments and machine learning: demonstration using organic photovoltaics," 2018, doi: 10.1021/acsnano.8b04726.

[146] Arboretti R, Ceccato R, Pegoraro L, Salmaso L. Design of Experiments and machine learning for product innovation: a systematic literature review. Qual Reliab Eng Int 2022;38(2):1131–56. https://doi.org/10.1002/qre.3025.

[147] Kirkey A, Luber EJ, Cao B, Olsen BC, Buriak JM. Optimization of the bulk heterojunction of all-small-molecule organic photovoltaics using design of experiment and machine learning approaches. ACS Appl Mater Interfaces 2020;12 (49):54596–607. https://doi.org/10.1021/acsami.0c14922.

[148] Markopoulos AP, Manolakos DE, Vaxevanidis NM. Artificial neural network models for the prediction of surface roughness in electrical discharge machining. J Intell Manuf 2008;19(3):283–92. https://doi.org/10.1007/s10845-008-0081-9.

[149] de Figueiredo JN, Guillén MF. Green power: perspectives on sustainable electricity generation. Taylor \& Francis; 2014 [Online]. Available: https://books.google.com/books?id=YMzMBQAAQBAJ.

[150] United States Department of State, "The long-term strategy of the United States: pathways to net-zero greenhouse gas emissions by 2050," 2021. [Online]. Available: https://www.whitehouse.gov/wp-content/uploads/2021/10/US-Long-Term-Strategy.pdf.

[151] de Sá MH. Electrochemical devices to power a sustainable energy transition—an overview of green hydrogen contribution. Appl Sci (Switzerland) 2024;14(5). https://doi.org/10.3390/app14052168.

[152] Newman J, Thomas-Alyea KE. Electrochemical Systems. The ecs series of texts and monographs. Wiley; 2012 [Online]. Available: https://books.google.com/books?id=eyj4MRa7vLAC.

[153] Smolinka T, Garche J. Electrochemical power sources: fundamentals, systems, and applications: hydrogen production by water electrolysis. Elsevier Science; 2021 [Online]. Available: https://books.google.com/books?id=hJ7gDwAAQBAJ.

[154] J. Larminie, A. Dicks, and M.S. McDonald, *Fuel cell systems explained*, vol. 2. J. Wiley Chichester, UK, 2003.

[155] Li X. Principles of fuel cells. CRC press; 2005.

[156] Gopinath M, Marimuthu R. A review on solar energy-based indirect water-splitting methods for hydrogen generation. Int J Hydrogen Energy 2022;47(89):37742–59.

[157] Hosseini SE, Wahid MA. Hydrogen from solar energy, a clean energy carrier from a sustainable source of energy. Int J Energy Res 2020;44(6):4110–31.

[158] Tarnay DS. Hydrogen production at hydro-power plants. Int J Hydrogen Energy 1985;10(9):577–84.

[159] Sarrias-Mena R, Fernández-Ramírez LM, García-Vázquez CA, Jurado F. Electrolyzer models for hydrogen production from wind energy systems. Int J Hydrogen Energy 2015;40(7):2927–38.

[160] Carrette L, Friedrich KA, Stimming U. Fuel cells: principles, types, fuels, and applications. ChemPhysChem 2000;1(4):162–93.

[161] Smolinka T, Ojong ET, Garche J. Hydrogen production from renewable energies—electrolyzer technologies. Electrochemical energy storage for renewable sources and grid balancing. Elsevier; 2015. p. 103–28.

[162] A. Bennagi, O. AlHousrya, D.T. Cotfas, and P.A. Cotfas, "Comprehensive study of the artificial intelligence applied in renewable energy," Jul. 01, 2024, Elsevier Ltd. doi: 10.1016/j.esr.2024.101446.

[163] Al-Othman A, et al. Artificial intelligence and numerical models in hybrid renewable energy systems with fuel cells: advances and prospects. Energy Convers Manag 2022;253:115154. https://doi.org/10.1016/j.enconman.2021.115154.

[164] Grigoriev SA, Fateev VN, Bessarabov DG, Millet P. Current status, research trends, and challenges in water electrolysis science and technology. Int J Hydrogen Energy 2020;45(49):26036–58. https://doi.org/10.1016/j.ijhydene.2020.03.109. Oct.

[165] Oladosu TL, Pasupuleti J, Kiong TS, Koh SPJ, Yusaf T. Energy management strategies, control systems, and artificial intelligence-based algorithms development for hydrogen fuel cell-powered vehicles: a review. Int J Hydrogen Energy 2024;61:1380–404. https://doi.org/10.1016/j.ijhydene.2024.02.284.

[166] Feng Z, Huang J, Jin S, Wang G, Chen Y. Artificial intelligence-based multi-objective optimisation for proton exchange membrane fuel cell: a literature review. J Power Sources 2022;520:230808. https://doi.org/10.1016/j.jpowsour.2021.230808.

[167] Feng Z, Huang J, Jin S, Wang G, Chen Y. Artificial intelligence-based multi-objective optimisation for proton exchange membrane fuel cell: a literature review. J Power Sources 2022;520:230808. https://doi.org/10.1016/j.jpowsour.2021.230808.

[168] Jankovic J, Zhang S, Putz A, Saha MS, Susac D. Multiscale imaging and transport modeling for fuel cell electrodes. J Mater Res 2019;34(4):579–91.

[169] Kittner N, Lill F, Kammen DM. Energy storage deployment and innovation for the clean energy transition. Nat Energy 2017;2(9):1–6.

[170] Chu S, Majumdar A. Opportunities and challenges for a sustainable energy future. Nature 2012;488(7411):294–303.

[171] Chu S, Cui Y, Liu N. The path towards sustainable energy. Nat Mater 2017;16(1):16–22.

[172] Pedapati PR, Dhanushkodi SR, Chidambaram RK, Taler D, Sobota T, Taler J. Design and manufacturing challenges in PEMFC flow fields—a review. Energies (Basel) 2024;17(14):3499. https://doi.org/10.3390/en17143499. Jul.

[173] Borup RL, et al. Recent developments in catalyst-related PEM fuel cell durability. Curr Opin Electrochem 2020;21:192–200. https://doi.org/10.1016/j.coelec.2020.02.007.

[174] Zhao J, Tu Z, Chan SH. Carbon corrosion mechanism and mitigation strategies in a proton exchange membrane fuel cell (PEMFC): a review. Elsevier B.V; 2021. https://doi.org/10.1016/j.jpowsour.2020.229434. Mar. 15,.

[175] S. Gamburzev and A.J. Appleby, "Recent progress in performance improvement of the proton exchange membrane fuel cell (PEMFC)".

[176] Cheng M, et al. Technical challenges and enhancement strategies for transitioning PEMFCs from H2-air to H2-O2. Energy Convers Manag 2024;311:118525. https://doi.org/10.1016/j.enconman.2024.118525.

[177] Borup RL, et al. Recent developments in catalyst-related PEM fuel cell durability. Curr Opin Electrochem 2020;21:192–200. https://doi.org/10.1016/j.coelec.2020.02.007.

[178] Pourrahmani H, Gay M, Van herle J. Electric vehicle charging station using fuel cell technology: two different scenarios and thermodynamic analysis. Energy Reports 2021;7:6955–72. https://doi.org/10.1016/j.egyr.2021.09.211. Nov.

[179] M.-F. Ng, J. Zhao, Q. Yan, G.J. Conduit, and Z.W. Seh, "Predicting the current and future state of batteries using data-driven machine learning".

[180] Johnson VH. Battery performance models in ADVISOR. J Power Sources 2002;110(2):321–9.

[181] Fairweather AJ, Foster MP, Stone DA. Modelling of VRLA batteries over operational temperature range using pseudo random binary sequences. J Power Sources 2012;207:56–9.

[182] Huria T, Ludovici G, Lutzemberger G. State of charge estimation of high power lithium iron phosphate cells. J Power Sources 2014;249:92–102.

[183] Gould CR, Bingham CM, Stone DA, Bentley P. New battery model and state-of-health determination through subspace parameter estimation and state-observer techniques. IEEE Trans Veh Technol 2009;58(8):3905–16.

[184] Fayyazi M, et al. Artificial intelligence/machine learning in energy management systems, control, and optimization of hydrogen fuel cell vehicles. Sustainability 2023;15(6):5249.

[185] Jayakumar A, Ramos M, Al-Jumaily A. A Novel fuzzy schema to control the temperature and humidification of PEM fuel cell system. In: International Conference on Fuel Cell Science, Engineering and Technology. American Society of Mechanical Engineers; 2015. V001T06A005.

[186] Butler KT, Davies DW, Cartwright H, Isayev O, Walsh A. Machine learning for molecular and materials science. Nature 2018;559(7715):547–55.

[187] Ramprasad R, Batra R, Pilania G, Mannodi-Kanakkithodi A, Kim C. Machine learning in materials informatics: recent applications and prospects. NPJ Comput Mater 2017;3(1):54.

[188] Abadi M, et al. Tensorflow: large-scale machine learning on heterogeneous distributed systems. arXiv preprint 2016. arXiv:1603.04467.

[189] Rajalakshmi N, Dhathathreyan KS. Catalyst layer in PEMFC electrodes—fabrication, characterisation and analysis. Chem Eng J 2007;129(1–3):31–40.

[190] Jienkulsawad P, Wiranarongkorn K, Chen YS, Arpornwichanop A. Identifying catalyst layer compositions of proton exchange membrane fuel cells through machine-learning-based approach. Int J Hydrogen Energy 2022;47(75):32303–14.

[191] Khajeh-Hosseini-Dalasm N, Ahadian S, Fushinobu K, Okazaki K, Kawazoe Y. Prediction and analysis of the cathode catalyst layer performance of proton exchange membrane fuel cells using artificial neural network and statistical methods. J Power Sources 2011;196(8):3750–6.

[192] Liu X, et al. 3D generation and reconstruction of the fuel cell catalyst layer using 2D images based on deep learning. J Power Sources Adv 2022;14:100084.

[193] Lou Y, Hao M, Li Y. Machine-learning-assisted insight into the cathode catalyst layer in proton exchange membrane fuel cells. J Power Sources 2022;543:231827.

[194] Wang B, Xie B, Xuan J, Jiao K. AI-based optimization of PEM fuel cell catalyst layers for maximum power density via data-driven surrogate modeling. Energy Convers Manag 2020;205:112460.

[195] Wang B, Xie B, Xuan J, Gu W, Zhao D, Jiao K. Deep optimization of catalyst layer composition via data-driven machine learning approach. SAE Technical Paper 2020.

[196] Zhang W, Jiang Z, Lu Y, He Z, Shao Z, Yu J. Optimization of porous layer structure of high-temperature proton exchange membrane fuel cell based on deep learning and Monte Carlo method. Int J Hydrogen Energy 2024;50:1004–19.

[197] Mohamed A, Ibrahem H, Yang R, Kim K. Optimization of proton exchange membrane electrolyzer cell design using machine learning. Energies (Basel) 2022;15(18):6657.

[198] Günay ME, Tapan NA, Akkoç G. Analysis and modeling of high-performance polymer electrolyte membrane electrolyzers by machine learning. Int J Hydrogen Energy 2022;47(4):2134–51.

[199] Chen T, Guestrin C. Xgboost: a scalable tree boosting system. In: Proceedings of the 22nd acm sigkdd international conference on knowledge discovery and data mining; 2016. p. 785–94.

[200] Uenishi T, Imoto R. Optimization of cathode catalyst layer of membrane electrode assembly for polymer electrolyte fuel cells using machine learning. J Power Sources 2023;573:233105.

[201] Zhang Y, et al. Data-driven optimization of high-dimensional variables in proton exchange membrane water electrolysis membrane electrode assembly assisted by machine learning. Ind Eng Chem Res 2024;63(3):1409–21.

[202] Ding R, et al. Guiding the optimization of membrane electrode assembly in a proton exchange membrane water electrolyzer by machine learning modeling and black-box interpretation. ACS Sustain Chem Eng 2022;10(14):4561–78.

[203] Chang C-C, Lin C-J. LIBSVM: a library for support vector machines. ACM Trans Intell Syst Technol (TIST) 2011;2(3):1–27.

[204] Arjmandi M, Fattahi M, Motevassel M, Rezaveisi H. Evaluating algorithms of decision tree, support vector machine and regression for anode side catalyst data in proton exchange membrane water electrolysis. Sci Rep 2023;13(1):20309.

[205] Hayatzadeh A, Fattahi M, Rezaveisi A. Machine learning algorithms for operating parameters predictions in proton exchange membrane water electrolyzers: anode side catalyst. Int J Hydrogen Energy 2024;56:302–14.

[206] Siracusano S, Baglio V, Grigoriev SA, Merlo L, Fateev VN, Aricò AS. The influence of iridium chemical oxidation state on the performance and durability of oxygen evolution catalysts in PEM electrolysis. J Power Sources 2017;366:105–14.

[207] Siracusano S, Van Dijk N, Payne-Johnson E, Baglio V, Aricò AS. Nanosized IrOx and IrRuOx electrocatalysts for the O2 evolution reaction in PEM water electrolysers. Appl Catal B 2015;164:488–95.

[208] Lopata J, Kang Z, Young J, Bender G, Weidner JW, Shimpalee S. Effects of the transport/catalyst layer interface and catalyst loading on mass and charge transport phenomena in polymer electrolyte membrane water electrolysis devices. J Electrochem Soc 2020;167(6):064507.

[209] Bahr M, Gusak A, Stypka S, Oberschachtsiek B. Artificial neural networks for aging simulation of electrolysis stacks. Chemie Ingenieur Technik 2020;92(10):1610–7.

[210] Kusnezoff M. Fuel cells – solid oxide fuel cell | membranes," in *reference module in chemistry*. Mol Sci Chem Eng 2024. https://doi.org/10.1016/B978-0-323-96022-9.00184-5.

[211] França RP, Monteiro ACB, Arthur R, Iano Y. An overview of deep learning in big data, image, and signal processing in the modern digital age. Trends Deep Learn Methodol 2021:63–87.

[212] O'Mahony N, et al. Deep learning vs. traditional computer vision. In: Advances in Computer Vision: Proceedings of the 2019 Computer Vision Conference (CVC). 1. Springer; 2020. p. 128–44. *1*.

[213] Banerjee S, Datta S, Paul B, Saha SK. Segmentation of three phase micrograph: an automated approach. In: Proceedings of the CUBE International Information Technology Conference; 2012. p. 1–4.

[214] Hwang H, et al. Integrated application of semantic segmentation-assisted deep learning to quantitative multi-phased microstructural analysis in composite materials: case study of cathode composite materials of solid oxide fuel cells. J Power Sources 2020;471:228458.

[215] Hwang H, et al. Deep learning-assisted microstructural analysis of Ni/YSZ anode composites for solid oxide fuel cells. Mater Charact 2021;172:110906.

[216] Ronneberger O, Fischer P, Brox T. U-net: convolutional networks for biomedical image segmentation. In: Medical image computing and computer-assisted intervention–MICCAI2015: 18th international conference, Munich, Germany, October 5-9, 2015, proceedings, part III 18. Springer; 2015. p. 234–41.

[217] Yamagishi R, Sciazko A, Ouyang Z, Komatsu Y, Katsuhiko N, Shikazono N. Super-resolved in-operando observation of SOFC pattern electrodes. ECS Trans 2021;103(1):2087.

[218] Athanasaki G, Jayakumar A, Kannan AM. Gas diffusion layers for PEM fuel cells: materials, properties and manufacturing–a review. Int J Hydrogen Energy 2023;48(6):2294–313.

[219] Turkmen AC, Celik C. The effect of different gas diffusion layer porosity on proton exchange membrane fuel cells. Fuel 2018;222:465–74.

[220] Han B, Mo J, Kang Z, Zhang F-Y. Effects of membrane electrode assembly properties on two-phase transport and performance in proton exchange membrane electrolyzer cells. Electrochim Acta 2016;188:317–26.

[221] Mahdaviara M, Shojaei MJ, Siavashi J, Sharifi M, Blunt MJ. Deep learning for multiphase segmentation of X-ray images of gas diffusion layers. Fuel 2023;345:128180.

[222] Cao X-Z, Luo S-Z, Li J-C, Pan J-H. An optimized automatic prediction of stage and grade in bladder cancer based on U-ResNet. J Intell Fuzzy Syst 2021;40(6):12139–50.

[223] Tang K, et al. Deep learning for full-feature X-ray microcomputed tomography segmentation of proton electron membrane fuel cells. Comput Chem Eng 2022;161:107768.

[224] Wang YDa, et al. Large-scale physically accurate modelling of real proton exchange membrane fuel cell with deep learning. Nat Commun 2023;14(1):745.

[225] Colliard-Granero A, et al. Deep learning for the automation of particle analysis in catalyst layers for polymer electrolyte fuel cells. Nanoscale 2022;14(1):10–8.

[226] Saaim KM, Afridi SK, Nisar M, Islam S. In search of best automated model: explaining nanoparticle TEM image segmentation. Ultramicroscopy 2022;233:113437.

[227] Eslamibidgoli MJ, Tipp FP, Jitsev J, Jankovic J, Eikerling MH, Malek K. Convolutional neural networks for high throughput screening of catalyst layer inks for polymer electrolyte fuel cells. RSC Adv 2021;11(51):32126–34.

[228] Ng M-F, Zhao J, Yan Q, Conduit GJ, Seh ZW. Predicting the state of charge and health of batteries using data-driven machine learning. Nat Mach Intell 2020;2(3):161–70.

[229] Samms SR, Wasmus S, Savinell RF. Thermal stability of proton conducting acid doped polybenzimidazole in simulated fuel cell environments. J Electrochem Soc 1996;143(4):1225.

[230] McDonald RC, Mittelsteadt CK, Thompson EL. Effects of deep temperature cycling on Nafion® 112 membranes and membrane electrode assemblies. Fuel Cells 2004;4(3):208–13.

[231] Wang J, et al. Comparison of state-of-the-art machine learning algorithms and data-driven optimization methods for mitigating nitrogen crossover in PEM fuel cells. Chem Eng J 2022;442:136064.

[232] Onanena R, Oukhellou L, Côme E, Candusso D, Hissel D, Aknin P. Fault-diagnosis of PEM fuel cells using electrochemical spectroscopy impedance. In: IFAC Proceedings Volumes. 45; 2012. p. 651–6.

[233] M.P. Arkhat, "Investigation and propagation of defects in the membrane electrode assembly of polymer electrolyte membrane fuel cells: quality control analysis," 2019.

[234] Sun Y, et al. Defects and interfaces on PtPb nanoplates boost fuel cell electrocatalysis. Small 2018;14(3):1702259.

[235] Kundu S, Fowler MW, Simon LC, Grot S. Morphological features (defects) in fuel cell membrane electrode assemblies. J Power Sources 2006;157(2):650–6.
[236] Alnegren P, Sattari M, Froitzheim J, Svensson JE. Degradation of ferritic stainless steels under conditions used for solid oxide fuel cells and electrolyzers at varying oxygen pressures. Corros Sci 2016;110:200–12.
[237] Reshetenko TV, Bender G, Bethune K, Rocheleau R. Application of a segmented cell setup to detect pinhole and catalyst loading defects in proton exchange membrane fuel cells. Electrochim Acta 2012;76:16–25.
[238] Das PK, et al. Rapid detection of defects in fuel-cell electrodes using infrared reactive-flow-through technique. J Power Sources 2014;261:401–11.
[239] Zenyuk IV, Englund N, Bender G, Weber AZ, Ulsh M. Reactive impinging-flow technique for polymer-electrolyte-fuel-cell electrode-defect detection. J Power Sources 2016;332:372–82.
[240] Ulsh M, Porter JM, Bittinat DC, Bender G. Defect detection in fuel cell gas diffusion electrodes using infrared thermography. Fuel Cells 2016;16(2):170–8.
[241] Aieta NV, et al. Applying infrared thermography as a quality-control tool for the rapid detection of polymer-electrolyte-membrane-fuel-cell catalyst-layer-thickness variations. J Power Sources 2012;211:4–11.
[242] Zhu H, Peng T, Dai Y, Zhou C, Sun B. Fault detection of electrolyzer plate based on improved Mask R-CNN and infrared images. Meas Sci Technol 2022;33(8):085405.
[243] Arcot MP, Zheng K, McGrory J, Fowler MW, Pritzker MD. Investigation of catalyst layer defects in catalyst-coated membrane for PEMFC application: non-destructive method. Int J Energy Res 2018;42(11):3615–32.
[244] Yang J, Li S, Wang Z, Dong H, Wang J, Tang S. Using deep learning to detect defects in manufacturing: a comprehensive survey and current challenges. Materials (Basel) 2020;13(24):5755.
[245] Lu J, et al. Research on defect recognition of ceramic chips for high temperature fuel cells based on improved faster R-CNN. In: 2022 International Conference on Machine Learning and Knowledge Engineering (MLKE). IEEE; 2022. p. 143–50.
[246] Yan A, Rupnowski P, Guba N, Nag A. Towards deep computer vision for in-line defect detection in polymer electrolyte membrane fuel cell materials. Int J Hydrogen Energy 2023;48(50):18978–95.
[247] Lü X, Qu Y, Wang Y, Qin C, Liu G. A comprehensive review on hybrid power system for PEMFC-HEV: issues and strategies. Energy Convers Manag 2018;171:1273–91.
[248] Zhang X, Yang D, Luo M, Dong Z. Load profile based empirical model for the lifetime prediction of an automotive PEM fuel cell. Int J Hydrogen Energy 2017;42(16):11868–78.
[249] Zhang X, Pisu P. An unscented kalman filter based approach for the healthmonitoring and prognostics of a polymer electrolyte membrane fuel cel. In: Annual Conference of the PHM Society; 2012.
[250] Bressel M, Hilairet M, Hissel D, Bouamama BO. Fuel cells remaining useful life estimation using an extended Kalman filter. In: IECON 2015-41st Annual Conference of the IEEE Industrial Electronics Society. IEEE; 2015. p. 469–74.
[251] Kaushik A, Singh J, Mahajan S. Recurrent neural network: a flexible tool of computational neuroscience research. In: Proceedings of the Third International Conference on Information Management and Machine Intelligence: ICIMMI 2021. Springer; 2022. p. 377–84.
[252] H. Jaeger, "The 'echo state' approach to analysing and training recurrent neural networks-with an erratum note," *Bonn, Germany: German National Research Center for Information Technology GMD Technical Report*, vol. 148, no. 34, p. 13, 2001.
[253] Li G, Li B-J, Yu X-G, Cheng C-T. Echo state network with Bayesian regularization for forecasting short-term power production of small hydropower plants. Energies (Basel) 2015;8(10):12228–41.
[254] Vichard L, Harel F, Ravey A, Venet P, Hissel D. Degradation prediction of PEM fuel cell based on artificial intelligence. Int J Hydrogen Energy 2020;45(29):14953–63.
[255] Donateo T. Simulation approaches and validation issues for open-cathode fuel cell systems in manned and unmanned aerial vehicles. Energies (Basel) 2024;17(4):900.
[256] Morando S, Jemei S, Hissel D, Gouriveau R, Zerhouni N. Proton exchange membrane fuel cell ageing forecasting algorithm based on Echo State Network. Int J Hydrogen Energy 2017;42(2):1472–80.
[257] Mezzi R, Morando S, Steiner NY, Péra MC, Hissel D, Larger L. Multi-reservoir echo state network for proton exchange membrane fuel cell remaining useful life prediction. In: IECON 2018-44th annual conference of the IEEE industrial electronics society. IEEE; 2018. p. 1872–7.
[258] Zhang S, Chen T, Xiao F, Zhang R. Degradation prediction model of PEMFC based on multi-reservoir echo state network with mini reservoir. Int J Hydrogen Energy 2022;47(94):40026–40.
[259] Hochreiter S, Schmidhuber J. Long short-term memory. Neural Comput 1997;9(8):1735–80.
[260] Liu J, Li Q, Chen W, Yan Y, Qiu Y, Cao T. Remaining useful life prediction of PEMFC based on long short-term memory recurrent neural networks. Int J Hydrogen Energy 2019;44(11):5470–80.
[261] B. Xu et al., "Degradation prediction of Pem water electrolyzer under constant and start-stop loads based on Cnn-Lstm," *Available at SSRN 4858254*.
[262] Wang F-K, Mamo T, Cheng X-B. Bi-directional long short-term memory recurrent neural network with attention for stack voltage degradation from proton exchange membrane fuel cells. J Power Sources 2020;461:228170.
[263] Wu Y, Breaz E, Gao F, Miraoui A. A modified relevance vector machine for PEM fuel-cell stack aging prediction. IEEE Trans Ind Appl 2016;52(3):2573–81.
[264] Wu Y, Breaz E, Gao F, Paire D, Miraoui A. Nonlinear performance degradation prediction of proton exchange membrane fuel cells using relevance vector machine. IEEE Trans Energy Convers 2016;31(4):1570–82.
[265] Zhong Z-D, Zhu X-J, Cao G-Y, Shi J-H. A hybrid multi-variable experimental model for a PEMFC. J Power Sources 2007;164(2):746–51.
[266] Li H, Pan D, Chen CLP. Intelligent prognostics for battery health monitoring using the mean entropy and relevance vector machine. IEEE Trans Syst Man Cybern Syst 2014;44(7):851–62.
[267] Zhou J, Liu D, Peng Y, Peng X. An optimized relevance vector machine with incremental learning strategy for lithium-ion battery remaining useful life estimation. In: 2013 IEEE International Instrumentation and Measurement Technology Conference (I2MTC). IEEE; 2013. p. 561–5.
[268] Lee H, Gu J, Lee B, Cho H-S, Lim H. Prognostics and health management of alkaline water electrolyzer: techno-economic analysis considering replacement moment. Energy AI 2023;13:100251.
[269] Zuo J, et al. Deep learning based prognostic framework towards proton exchange membrane fuel cell for automotive application. Appl Energy 2021;281:115937.
[270] Wang T, Zhou H, Zhu C. A short-term and long-term prognostic method for PEM fuel cells based on Gaussian process regression. Energies (Basel) 2022;15(13):4844.
[271] Laurencelle F, et al. Characterization of a ballard MK5-E proton exchange membrane fuel cell stack. Fuel Cells 2001;1(1):66–71.
[272] Carrera GVSM, Branco LC, Aires-de-Sousa J, Afonso CAM. Exploration of quantitative structure-property relationships (QSPR) for the design of new guanidinium ionic liquids. Tetrahedron 2008;64(9):2216–24. https://doi.org/10.1016/j.tet.2007.12.021.
[273] Penumuru DP, Muthuswamy S, Karumbu P. Identification and classification of materials using machine vision and machine learning in the context of industry 4.0. J Intell Manuf 2020;31(5):1229–41. https://doi.org/10.1007/s10845-019-01508-6.
[274] Morgan D, Jacobs R. Opportunities and challenges for machine learning in materials science. Annu Rev Mater Res 2020;50:71–103. https://doi.org/10.1146/annurev-matsci-070218-010015.
[275] Sutton C, Boley M, Ghiringhelli LM, Rupp M, Vreeken J, Scheffler M. Identifying domains of applicability of machine learning models for materials science. Nat Commun 2020;11(1):1–9. https://doi.org/10.1038/s41467-020-17112-9.
[276] Gao C, et al. Innovative materials science via machine learning. Adv Funct Mater 2022;32(1). https://doi.org/10.1002/adfm.202108044.
[277] Wang M, Wang T, Cai P, Chen X. Nanomaterials discovery and design through machine learning. Small Methods 2019;3(5). https://doi.org/10.1002/smtd.201900025.
[278] Rise of the machines. Nat Rev Mater 2021;6(8):641. https://doi.org/10.1038/s41578-021-00351-7.
[279] Wei J, et al. Machine learning in materials science. InfoMat 2019;1(3):338–58. https://doi.org/10.1002/inf2.12028.